

March 2019

Investigating Cationic Metal Centers for Hydroformylation

Ryan Alexander Johnson

Louisiana State University and Agricultural and Mechanical College

Follow this and additional works at: https://digitalcommons.lsu.edu/gradschool_dissertations



Part of the [Inorganic Chemistry Commons](#)

Recommended Citation

Johnson, Ryan Alexander, "Investigating Cationic Metal Centers for Hydroformylation" (2019). *LSU Doctoral Dissertations*. 4820.

https://digitalcommons.lsu.edu/gradschool_dissertations/4820

This Dissertation is brought to you for free and open access by the Graduate School at LSU Digital Commons. It has been accepted for inclusion in LSU Doctoral Dissertations by an authorized graduate school editor of LSU Digital Commons. For more information, please contact gradetd@lsu.edu.

INVESTIGATING CATIONIC METAL CENTERS FOR HYDROFORMYLATION

A Dissertation

Submitted to the Graduate Faculty of the
Louisiana State University and
Agricultural and Mechanical College
in partial fulfillment of the
requirements for the degree of
Doctor of Philosophy

in

The Department of Chemistry

by

Ryan Alexander Johnson
B.S., Langston University, 2015
May 2019

Acknowledgments

First, I must give thanks to God for His continued involvement and blessings in my life. He continue to give me strength and guidance through my life and I am constantly amazed by the direction He is taking me in my journey. I must thank Dr. George Stanley for accepting me into his research group. I will never forget his kindness and support for me through the years. I will remember the research and many life lessons I learned from him. I also want to thank him for introducing me to the ChemDemo program, a passion I grew to love being in his group.

To my wife Ashley, I know I could not made it through this journey without you. Thank you for all your sacrifices you made by being by my side. I am forever grateful that you are in my life and you continue to propel me into becoming a better husband, father, and man. I want to thank my mother and father. I am blessed that my mom pushed me to pursue this degree and to my father I know you would have been proud to see the man I have become. I thank all of my family and friends for their support and cheers. I want to specifically thank my LSU friends who helped me get through the many milestones with laughter through our journey to our PhD.

I would like to thank my doctoral committee members: Dr. Weiwei Xie, Dr. Gerald Schneider, and Dr. Hyun Jeon. I appreciate your time and support through my graduate career. I thank Dr. Thomas Weldegiorghis and Dr. Fengli Zhang for their time and support to help me run numerous and various NMR experiments. I would like to thank the previous Stanley research group members: Dr. Ciera Gasery, Dr. Ranelka Fernando, and Dr. Marshall Moulis. I would especially like to thank Drew Hood for his help in understanding this research and great conversations over the last couple years in being Dr. Stanley's last graduate students. I could have not done this without all of you.

Table of Contents

Acknowledgments.....	ii
List of Abbreviations	v
Abstract.....	vii
Chapter 1: Introduction to Hydroformylation.....	1
1.1 Fundamentals of Hydroformylation.....	1
1.2 Discovery of Hydroformylation.....	2
1.3 Rhodium Catalysts for Hydroformylation.....	6
1.4 Chelating Ligands	8
1.5 References	10
Chapter 2: Bimetallic Cooperativity: a Tetrphosphine Ligand Story	12
2.1 Bimetallic Catalyst	12
2.2 $\text{Rh}_2(\mu\text{-CO})(\text{CO})_3(\text{rac-et,ph-P4-Ph})(\text{BF}_4)_2$	22
2.3 Probing the Catalyst Precursor, $[\text{Rh}_2(\text{nbd})_2\text{-(et,ph-P4-Ph)}](\text{BF}_4)_2$	24
2.4 The Degradation of the New Ligand.....	29
2.5 References	33
Chapter 3: Optimization of the New Tetrphosphine Ligand (et,ph-P4-Ph)	35
3.1 Previous Results	35
3.2 Standard Hydroformylation Procedure	35
3.3 Cyclooctadiene precursor.....	38
3.4 Solvent-ligand Precursors	40
3.5 Norbornadiene Precursor	47
3.6 Racemic vs. Meso	50
3.7 Stability of the New ligand Catalyst	54
3.8 References	59
Chapter 4: Characterization of the New Ligand Catalyst	60
4.1 NMR Studies of the Dirrhodium Catalyst Based on et,ph-P4.....	60
4.2 NMR Studies on New et,ph-P4-Ph Dirrhodium Catalyst.....	65
4.3 FT-IR Studies on the Old P4-Based Dirrhodium Catalyst	72
4.4 High pressure FT-IR Reactor Design.....	76
4.5 FT-IR Studies on the New P4-Ph Dirrhodium Catalyst.	79
4.6 Hydroformylation Catalytic Cycle	84
4.7 Conclusion.....	89
4.8 References	89

Chapter 5: Cationic Cobalt(II) Hydroformylation	92
5.1 Introduction	92
5.2 Monometallic Cationic Cobalt(II) Hydroformylation Catalysts	95
5.3 Characterization of the Cationic Cobalt Catalyst	100
5.4 Proposed Catalytic Mechanism	103
5.5 References	105
Chapter 6: Experimental Procedures	107
6.1 General Considerations	107
6.2 General Hydroformylation Procedures	108
6.3 Synthesis of Phenylphosphine	108
6.4 Synthesis of Bridge (H-Bridge)	109
6.5 Synthesis of Cl-Bridge	109
6.6 Synthesis of Diethylchlorophosphine	110
6.7 Synthesis of Small Arm (I-Small Arm)	111
6.8 Synthesis of Br-Small Arm	112
6.9 Synthesis of “New Ligand” et,ph-P4-Ph via I-Small Arm	112
6.10 Synthesis of “New Ligand” et,ph-P4-Ph via Br-Small Arm	113
6.11 Synthesis of Vinyldiethylphosphine	114
6.12 Synthesis of “Old Ligand” et,ph-P4	114
6.13 Column Chromatography for the Removal of Impurities from et,ph-P4-Ph	115
6.14 Column Chromatography for the Separation of meso- and rac-et,ph-P4-Ph	115
6.15 Synthesis of Rh(nbd) ₂ BF ₄	115
6.16 Synthesis of rac/meso/mix-Rh(OL)(nbd) ₂ BF ₄ or rac/meso/mix-Rh(NL)(nbd) ₂ BF ₄	116
6.17 Synthesis of Small Arm (Phenyl substituted and Methyl external arms)	116
6.18 Synthesis of Rh(cod) ₂ BF ₄	117
6.19 Synthesis of meso/rac- [Rh ₂ (CO) ₄ (et,ph-P4-ph)]BF ₄	117
6.20 Synthesis of Rh(nbd) ₂ BARF and Rh(nbd) BF ₂₀	118
6.21 Synthesis of [Rh ₂ (acetonitrile) ₄ (et,ph-P4-ph)]BF ₄	118
6.22 Synthesis of [Rh ₂ (solvent) _x (et,ph-P4-ph)]BF ₄ / Solvent = dioxane, pyridine	118
6.23 Synthesis of [Co(acac)(dioxane) ₄](BF ₄)•(dioxane) _x (x ≈ 2-6)	118
6.24 Synthesis of [Co(acac)(bisphosphine)](BF ₄)	119
6.25 References	120
Vita	121

List of Abbreviations

bridge	H(Ph)PCH ₂ P(Ph)H
Br-small arm	1-(diethylphosphino)-2-bromobenzene
chlorobridge	Cl(Ph)PCH ₂ P(Ph)Cl
COSY	correction spectroscopy
DCM	dichloromethane
DFT	density functional theory
DMF	N,N-dimethylformamide
DMSO	dimethylsulfoxide
DEPE	1,2-bis(diethylphosphino)ethane
DEPBz	1,2-bis(diethylphosphino)benzene
DPPE	1,2-bis(diphenylphosphino)ethane
DPPBz	1,2-bis(diphenylphosphino)benzene
eq.	equivalents
et,ph-P4	Old Ligand
et,ph-P4-Ph	New Ligand
FT-IR	Fourier transform-inferred spectrometry
GC-MS	gas chromatography-mass spectrometry
¹ H NMR	proton NMR
hydro	hydrogenation
I-small arm	1-(diethylphosphino)-2-iodobenzene
iso	isomerization
L:B	linear:branched

min minute
meso *mesomeric*
 mL milliliters
 mM millimolar (mmol/L)
 mmol millimole
 nbd norbornadiene
 NMR nuclear magnetic resonance
 ORTEP Oak Ridge thermal ellipsoid plot program
³¹P NMR phosphorus NMR
³¹P {¹H} NMR phosphorus, proton decoupled, NMR
 ppm parts per million
 psi pounds per square inch
 psig pounds per square inch, gauge
rac *racemic*
 syn-gas synthesis gas (H₂/CO)
 t-glyme dimethoxytetraglyme
 THF..... tetrahydrofuran
 TOF turnover frequencies
 vol volume

Abstract

Bimetallic cooperativity can potentially increase activity of reactions. This concept is another way to increase reactivity besides simply focusing on the steric and electronic effects of a ligand. A binucleating tetrasphosphine ligand has been developed to showcase bimetallic cooperativity between two rhodium metal centers. Hydroformylation is a widely used industrial process to produce aldehydes from alkenes, H_2 , and CO. The dirhodium catalyst, $[Rh_2(\mu-CO)(CO)_3(rac\text{-}et,ph\text{-}P4\text{-}Ph)](BF_4)_2$, is highly active leading to favorable results when using a DMF/water solvent system, 1-hexene, 90 psi 1:1 H_2 /CO, and 90° C: initial turnover frequency of 35.4 min^{-1} , linear to branch ratio of 17.6:1, isomerization of 1.9% alkene isomerization, and hydrogenation of < 1%. Unfortunately, this complex was very difficult to make from our usual catalyst starting material, $[Rh_2(nbd)_2(rac\text{-}et,ph\text{-}P4\text{-}P4)](BF_4)_2$ (nbd = norbornadiene).

My research has focused on the synthesis and optimization of the new dirhodium-tetraphosphine catalyst precursors. New catalyst precursors with acetonitrile, pyridine, and cyclooctadiene ligands demonstrate high activity for hydroformylation in water/acetone solvent with results displaying high turnover numbers ranging from 700-800 aldehyde turnovers and low side reactions (alkene isomerization = 5% -7%, hydrogenation = >1%) point to an effective catalyst. The chelator effect of the phenyl linkage ultimately became an issue for stability of the catalyst. The new P4-Ph tetraphosphine ligand, however, has internal phosphines with two P-aryl bonds and only one alkyl group (the central methylene bridge). These are considerably more reactive towards P-aryl group cleavage reactions that leading to rhodium-induced P4-Ph fragmentation. *In-situ* FT-IR and NMR experiments were performed on the bimetallic catalyst to understand the active catalyst and mechanism for the catalytic cycle. *In-situ* FT-IR ran in

water/acetone illustrates terminal carbonyls at 2120, 2055, 2026, and 2030 cm^{-1} indicating the presence of the open-mode pentacarbonyl complex at lower temperatures and mostly a monocationic monohydride complex, $[\text{Rh}_2(-\text{H})(\text{CO})_x(\text{mixed-P4-Ph})]^+$, $x = 2-4$, formed via proton dissociation from the dicationic dihydride complex. The proposed mechanism for the dirhodium-P4-Ph catalyst in water/acetone system is a monocationic monohydride system similar to the previous old catalyst.

Work with the bimetallic cobalt system led to a very active cationic cobalt(II) bisphosphine hydrido-carbonyl catalyst. The cobalt(II) catalyst has a very high alkene isomerization rate that causes a low L:B selectivity for simple alkenes, however, due to the high isomerization rate it shows an exceptional high L:B selectivity to hydroformylate difficult internal branch alkenes. The cobalt(II) catalyst approaches rhodium activity and has a remarkably long lifetime with no signs showing cobalt-induced phosphine ligand degradation.

Chapter 1: Introduction to Hydroformylation

1.1 Fundamentals of Hydroformylation

Hydroformylation, or oxo synthesis, is the most widely used industrial catalytic processes for the production of aldehydes and related products. Companies like DOW Chemical and Shell use this process to produce over 15 billion pounds of aldehydes per year globally.¹ The aldehydes produced are typically converted into alcohols and carboxylic acids that are used to make fatty acids, plasticizers, detergents, surfactants, and solvents.^{2,3}

Ideal hydroformylation catalysts should have high selectivity, limited side reactions, long lifetimes, and high turnover rates, preferably under mild reaction conditions. The aldehydes produced usually has two forms: branched and linear. Industry generally prefers the linear aldehyde over the branched regioisomer.

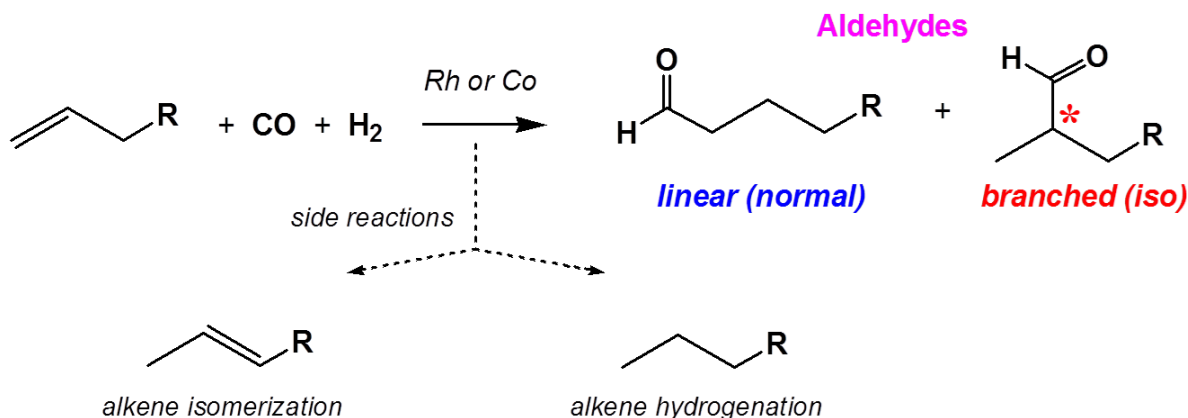


Figure 1.1. Hydroformylation, or oxo reaction.

The aldehyde linear to branched (L:B) selectivity depends on the catalyst. Industrial hydroformylation catalysts are based on cobalt or rhodium hydride carbonyl complexes, often involving phosphine ligands to increase the aldehyde L:B regioselectivity. During

hydroformylation there are two main side reactions: alkene isomerization and alkene hydrogenation.⁴ Alkene isomerization involves the catalyst moving the double bond to other available positions. Alkene hydrogenation occurs when hydrogen reacts with the alkene to form an alkane. These side reactions can be reversible, however, usually when the alkene turns into an alkane it is very difficult for it to revert back because that involves a C-H activation reaction. Alkene isomerization can be important when working with internal alkenes to move the double bond to a terminal position where hydroformylation is easier to occur and produce more linear aldehyde product. One typically wants to limit alkene isomerization when the reactant is a 1-alkene.

One also wants a good hydroformylation catalyst to have high turnovers (TOs) and an acceptable turnover frequency (TOF). A turnover refers to one loop through the catalyst cycle that converts one set of reactants to a product. Turnover frequency is another indicator of catalyst performance and is the number of turnovers per unit of time. Turnover number is the absolute number of passes through the cycle before the catalyst deactivates.

1.2 Discovery of Hydroformylation

Hydroformylation was discovered in 1938 by Otto Roelen, and the generally accepted mechanism for hydroformylation was proposed in 1961 by Heck and Breslow.⁵

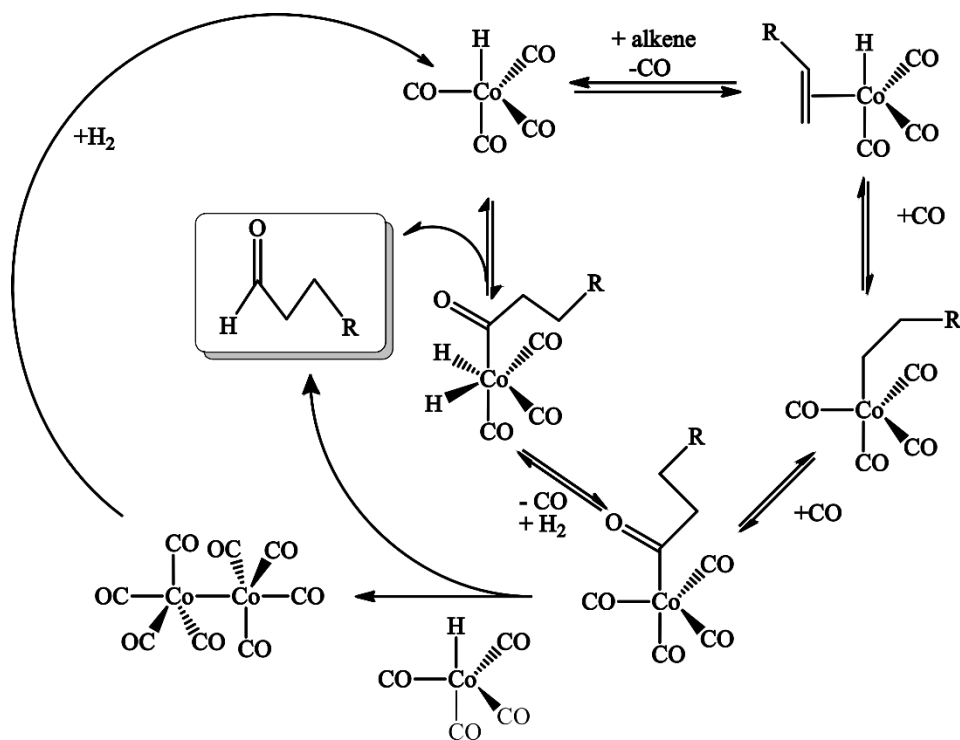


Figure 1.2. Heck and Brewslo's mechanism for Roelen's cobalt hydroformylation.

Heck and Brewslo used $\text{Co}_2(\text{CO})_8$ as the starting precursor, which is activated by oxidative addition of H_2 to the complex to form the monometallic active catalyst, $\text{HCo}(\text{CO})_4$. The cycle for hydroformylation begins with the 18 electron saturated $\text{HCo}(\text{CO})_4$ complex. In order to add the alkene a carbonyl ligand must dissociate to open up an empty coordination site for the alkene. Once the alkene is coordinated to the cobalt the next reaction step is a migratory insertion with the hydride to generate an alkyl ligand. This is the selectivity determining step where either a linear or branched alkyl is produced. Figure 1.2 shows the formation of a linear alkyl, but the sterically open $\text{HCo}(\text{alkene})(\text{CO})_3$ catalyst can also make the branched alkyl.

A new carbonyl ligand associates to fill the empty coordination site from the alkene-hydride migratory insertion. The alkyl ligand then undergoes a second migratory insertion with the carbonyl to form an acyl ligand. Another carbonyl coordinates to the complex to fill the empty site formed from the alkyl-CO migratory insertion. Once the acyl ligand is generated the

catalytic cycle can proceed in two different ways: monometallic or bimetallic reactions. The monometallic pathway involves a carbonyl dissociating and H_2 oxidatively adding to the complex to form a dihydride species. One of the hydrides then does a reductive elimination with the acyl group forming the final aldehyde product and regenerating the starting $\text{HCo}(\text{CO})_4$ catalyst after CO addition.

The bimetallic pathway involves a carbonyl dissociation and the intermolecular transfer of a hydride from $\text{HCo}(\text{CO})_4$ to reductively eliminate aldehyde. Once the aldehyde has been reductively eliminated a metal-metal bond forms the $\text{Co}_2(\text{CO})_8$ catalyst precursor, which is very reactive with H_2 to regenerate two $\text{HCo}(\text{CO})_4$ catalysts to start the hydroformylation cycle again. Although Heck and Breslow proposed the bimetallic pathway, they didn't favor it due to the low concentrations of $\text{Co}(\text{acyl})(\text{CO})_4$ and $\text{HCo}(\text{CO})_4$, combined with the need for CO dissociation, making the needed bimolecular reaction unlikely. Subsequent *in situ* spectroscopic studies strongly supported the monometallic mechanism.^{6,7}

The $\text{HCo}(\text{CO})_4$ process is referred to as the High Pressure Unmodified Cobalt Process because it involves high pressures (3000-4500 psig) and high temperatures (150-250 °C). The high pressure is needed to keep the catalyst stable as the temperature increases because the catalyst needs high CO partial pressures to keep $\text{HCo}(\text{CO})_4$ from decomposing to cobalt metal.⁸

In order to improve the High Pressure Unmodified Cobalt Process, a phosphine ligand was added to the catalyst to improve its stability. Slauch and Mullineaux at Shell demonstrated that the addition of a trialkylphosphine to generate a $\text{HCo}(\text{CO})_3(\text{PR}_3)$ catalyst dramatically improved its stability and increased the aldehyde L:B regioselectivity.⁹ Slauch and Mullineaux found that the electron-donating phosphine made the cobalt more electron-rich, which in turn increased the Co-CO π -backbonding and minimized decomposition to cobalt metal. The stronger

Co-CO bonds meant that the CO partial pressure could be substantially lower to stabilize the catalyst, but it did decrease the rate of hydroformylation, once again, due to the stronger Co-CO bonds. Dissociation of a carbonyl ligand is critically important in opening up an empty coordination site to allow alkene or H₂ to bind. The increased steric effects of coordinating a bulky alkylated phosphine ligand produced a cobalt-catalyst that was much more selective to linear aldehyde products. HCo(CO)₄, for example, typically produces low aldehyde L:B ratios of 1:1 to 2:1, while the phosphine-modified Shell catalyst produces aldehyde L:B ratios of 8:1.

Both the HCo(CO)₄ and phosphine-modified HCo(CO)₃(PR₃) catalysts are very active at alkene isomerization, which is highly desirable for the types of alkenes used by industry with these catalysts. ExxonMobil, for example, uses a complex mixture of internal branched alkenes in the C₆ to C₁₂ range that are very difficult to hydroformylate.¹⁰ The HCo(CO)₄ catalyst is very active and is sterically unencumbered enough to coordinate to these bulky internal alkenes. The isomerization activity of HCo(CO)₄ can move the double bond from an internal position to the 1-position and hydroformylate it to give an aldehyde L:B ratio of ~2:1. ExxonMobil hydrogenates this mixture of aldehydes to alcohols and blends them into motor oils to act as detergents and modifiers.

Shell uses the oligomerization of ethylene with a homogeneous nickel-phosphine catalyst via the Shell Higher Olefin Process (SHOP) to produce a C₄ to C₄₀ mixture of 1-alkenes.¹¹ The middle range of 1-alkenes (C₁₀-C₂₄) are separated and sold as α -olefins. The short and long chain 1-alkenes are then metathesized to produce internal alkenes in the C₁₀-C₁₆ range. These are then hydroformylated using the phosphine-modified HCo(CO)₃(PR₃) catalyst, which is very active at alkene isomerization. The isomerization generates 1-alkenes that are much more active with the Shell catalyst for hydroformylation to produce the 8:1 L:B ratio of aldehydes. The

phosphine ligand makes the Shell catalyst more active for hydrogenation of the aldehyde to alcohol, which is the desired final product. Unfortunately, it also increases the unwanted hydrogenation of alkene to alkane. This is a classic example of how modifying a catalyst can have both positive and negative effects.

1.3 Rhodium Catalysts for Hydroformylation

Hydroformylation had another major advancement when rhodium was discovered to be extremely active. Osborn, Young, and Wilkinson discovered a rhodium-PPh₃ based- catalyst in 1965 that showed high activity and high regioselectivity for hydroformylation.¹² Rhodium is usually claimed to be a 1000 times more reactive than cobalt for hydroformylation. This dramatically increased activity allowed it to function at much lower temperatures and pressures relative to cobalt-based catalysts.¹³ Originally, Wilkinson's catalyst, RhCl(PPh)₃, was used, but it was quickly discovered that halides inhibit hydroformylation. HRh(CO)(PPh₃)₂ could be isolated and found to be immediately active for hydroformylation under mild conditions. The current accepted mechanism involving the rhodium-PPh₃ catalyst shown below.

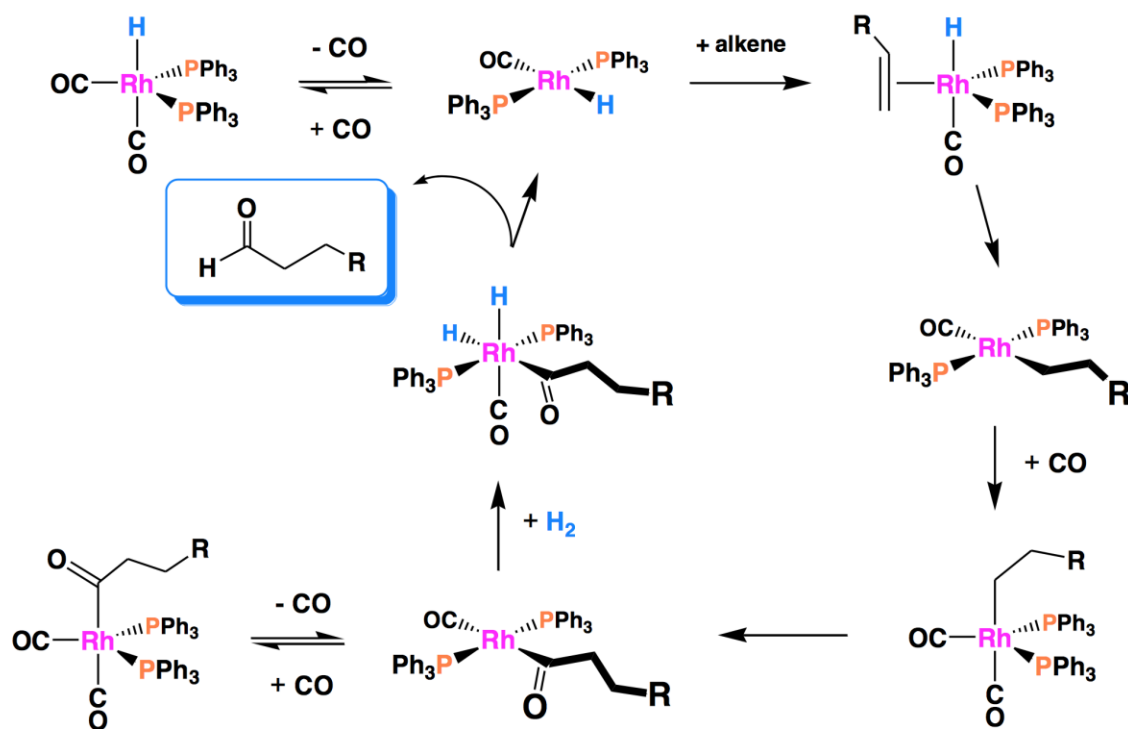


Figure 1.3. Rhodium-PPh₃ Hydroformylation Mechanism.

This Rh-PPh₃ catalyst was further improved by adding excess PPh₃ to the complex, which made it robust enough for commercial development. This discovery by Pruett (Union Carbide) and Booth (Union Oil), demonstrated a more selective and stable catalyst.¹⁴ PPh₃ does not coordinate very strongly to Rh and there is a very facile dissociation equilibrium in the presence of CO as shown in Figure 1.4.

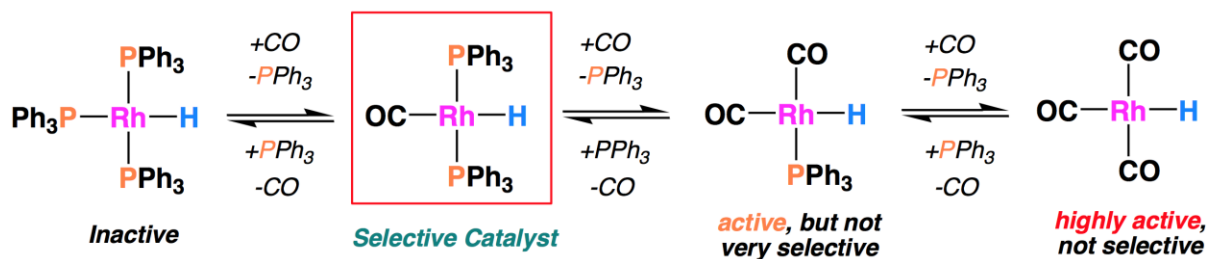


Figure 1.4. PPh₃ vs. CO and PPh₃ concentration Effects on Rhodium-PPh₃ system

The most selective and slowest hydroformylation catalyst is $\text{HRh}(\text{CO})(\text{PPh}_3)_2$ with two PPh_3 ligands coordinated. As the CO pressure is increased PPh_3 is replaced by CO and the activity of the complex increases, but the selectivity decreases. The use of high concentrations of PPh_3 favors the bisphosphine coordinated selective catalyst. This also minimizes the mono-phosphine catalyst that is active for Rh- PPh_3 orthometalation reactions and the oxidative addition of P-Ph bonds to the rhodium center. The oxidative addition of P-Ph bonds to the rhodium center is particularly serious as it leads to phosphide-bridged rhodium dimers and clusters that are inactive for hydroformylation and tend to precipitate out forming rhodium-phosphide sludge¹⁵. Rh- PPh_3 catalyst technology (or close variants) is used in about 75% of hydroformylation plants worldwide and operates at H_2 :CO pressures of 5-20 bar and temperatures of 40 to 120°C.

1.4 Chelating Ligands

A variety of ligands have been tested for hydroformylation including chelating ligands. Most metal-ligand bonds are weak compared to C-C or C-H bonds, and are prone to breaking and ligand dissociation from the metal center.¹⁶ Chelating ligands are much less likely to dissociate from a metal because of the chelate effect. The chelate effect involves two or more donor groups connected by an appropriate set of linking atoms to generate a geometric arrangement that allows both donor groups to coordinate to a single metal center. If one of the donor groups dissociates from the metal center, the other coordinated donor and connecting link keep the dissociated ligand to remain in proximity to the metal center, which kinetically favors re-coordination of the dissociated group back onto the metal center. Chelating ligands can provide great benefits to a catalyst by increasing stability and selectivity. Some common chelating ligands used for hydroformylation are shown Figure 1.5.

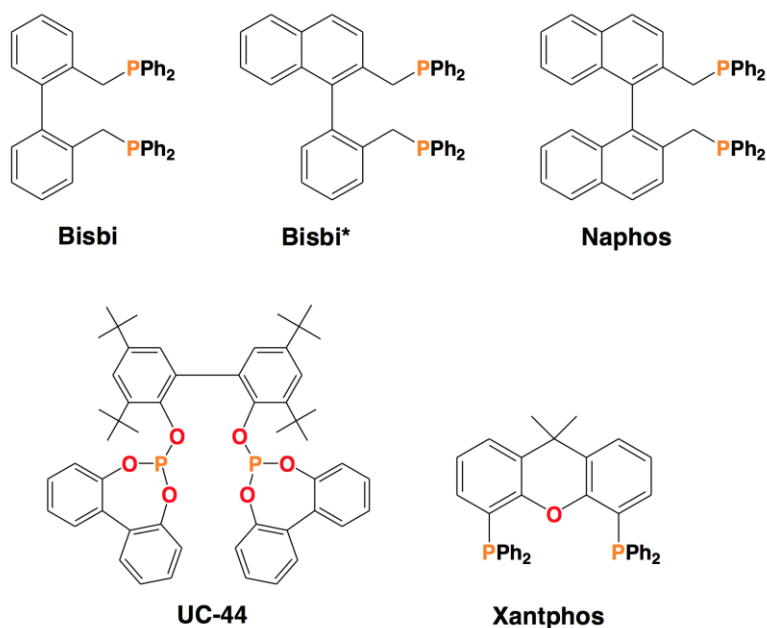


Figure 1.5. Chelating bisphosphine ligands that generate Rh hydroformylation catalysts with high aldehyde L:B selectivity.

These chelating ligands have shown to be excellent ligands for generating rhodium catalysts with high aldehyde L:B selectivity. Except for the bulky bisphosphite, UC-44, none of these ligands are used commercially due to Rh-induced phosphine fragmentation reactions that lead to catalyst deactivation. Rh/UC-44 may be used by Dow Chemical to hydroformylate 2-butene, considered a “trash” butane, to the linear aldehyde product. Rh/UC-44 is a good isomerization catalyst, unlike most of the Rh/phosphine catalysts, but also has enough steric directing ability to strongly favor the hydroformylation of 1-alkenes to linear aldehyde. UC-44, however, is very susceptible to reactions with water, aldehyde product, and Rh-induced fragmentations. Table 1 compares Rh/ PPh_3 to some of the Rh chelating ligand catalysts for the hydroformylation of 1-hexene.¹⁶

Table 1.1. Hydroformylation of 1-hexene using Rh-ligand catalysts

Catalyst	Initial TOF (min ⁻¹)	Aldehyde L:B	% isomerization
Rh/PPh ₃ ^a	13	9.1:1	< 0.5
Rh/Bisbi ^b	25	70:1	< 0.5
Rh/Naphos ^b	27	120:1	1.5
Rh/Xantphos ^b	13	80:1	5.0

Conditions: 90 °C and 6.2 bar 1:1 H₂/CO in Acetone. 1 mM Rh(CO)₂(acac) was combined with ^a 0.4 M PPh₃ (400 eq.) or ^b 5 eq. of ligand.

The table shows that the chelating ligands are able to give better rates and selectivity compared to the monodentate system. There are some disadvantages to the chelating ligands as they are more open to higher alkene isomerization side reactions and can be prone to Rh-induced ligand fragmentation reactions.

1.5 References

1. Trzeciak, A. M., Ziolkowski, J. J. *Coord. Chem. Rev.* 1999, 190-192, 883-900
2. Parshall, G. W. *Homogeneous Catalysis*, Wiley-Interscience, New York, 1980.
3. Whyman, R., *Applied Organometallic Chemistry and Catalysis*. Oxford University Press: 2001.
4. Borner, Armin & Franke, R. *Hydroformylation Fundamentals, Processes, and Applications in Organic Synthesis Volume II*, Wiley-VCH, Germany, 2016. Heck, R. F.; Breslow, D. S., The Reaction of Cobalt Hydrotetracarbonyl with Olefins. *J. Am. Chem. Soc.* 1961, 83, 4023-4027.
5. Heck, R. F.; Breslow, D. S., The Reaction of Cobalt Hydrotetracarbonyl with Olefins. *J. Am. Chem. Soc.* **1961**, 83, 4023-4027.
6. Whyman, R. *J. Organomet. Chem.* 1974, 81, 97-106.
7. Whyman, R. *J. Organomet. Chem.* 1974, 66, C23-C25
8. B. Cornils, *New Synthesis with Carbon Monoxide*, J. Falbe, Ed, 1980.
9. Slauch, L. H.; Mullineaux, R. D., *J. Organometal. Chem.* 1968, 13, 469-477.
10. Borner, A and Franke, R. *Hydroformylation*. Weinheim, Wiley-VCH, 2016.

11. "The Oxo Process." Encyclopedia of Chemical Technology, 3rd ed., 2000.
12. Unruh, J. D.; Christenson, J. R., A Study of the Mechanism of Rhodium/Phosphine Catalyzed Hydroformylation: Use of 1,1'-Bis(diarylphosphino)ferrocene Ligands. *J. Mol. Catal.* 1982, 14, 19-34.
13. Osborn, J. A.; Wilkinson, G.; Young, J. F., Mild Hydroformylation of Olefins using Rhodium Catalysts. *Chem. Commun.* 1965, 0, 17.
14. Pruett, R. L.; Smith, J. A. Hydroformylation of Unsaturated Organic Compounds US 3917661 A, November 4, 1975.
15. Bianchini, C.; Lee, H.; Meli, A.; Vizza, F., In Situ High-Pressure $^{31}\text{P}\{^1\text{H}\}$ NMR Studies of the Hydroformylation of 1-Hexene by $\text{RhH}(\text{CO})(\text{PPh}_3)_3$. *Organometallics*. 2000, 19, 848-853.
16. Aubry, D. A.; Bridges, N. N.; Ezell, K.; Stanley, G. G., Polar Phase Hydroformylation: The Dramatic Effect of Water on Mono- and Dirhodium Catalysts. *J. Am. Chem. Soc.* 2003, 125, 11180.

Chapter 2: Bimetallic Cooperativity: a Tetraphosphine Ligand Story

2.1 Bimetallic Catalyst

Although industry uses monometallic Co and Rh catalyst systems for hydroformylation, there is an interest in polymetallic homogeneous catalysts in hydroformylation research. These polymetallic catalyst systems can potentially provide new reactivity and selectivity for hydroformylation. Bimetallic cooperativity involves more than one metal working together to produce a product in catalysis. One of the first proposed bimetallic cooperative mechanisms was by Heck for cobalt catalyzed hydroformylation.¹ Heck's proposed bimetallic pathway, shown in figure 2.1, has two cobalt metal centers working together to produce an aldehyde product. This involved an intermolecular hydride transfer from $\text{HCo}(\text{CO})_4$ to $\text{Co}(\text{acyl})(\text{CO})_4$ to reductively eliminate the aldehyde product as opposed to the oxidative addition of H_2 to $\text{Co}(\text{acyl})(\text{CO})_4$ followed by reductive elimination of the aldehyde product (monometallic mechanism). The bimetallic pathway was not favored by Heck due to the low concentration of the bimetallic species.

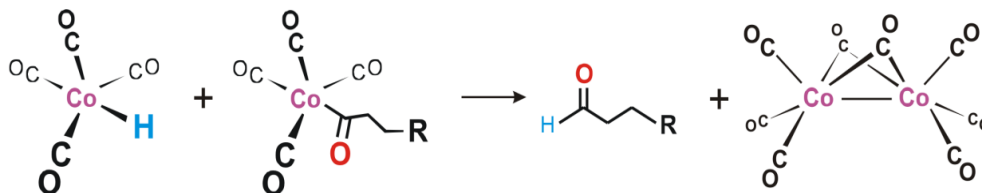


Figure 2.1. Heck's proposed bimetallic pathway

This mechanism led to other hydroformylation studies involving polymetallic catalysts. One example of a polymetallic catalyst was a cobalt cluster developed by Pitman, which

requiring high syn-gas pressures of 400-1000 psig and produced relatively low L:B ratios of 5:1 for 1-pentene.² $[\text{HRu}_3(\text{CO})_{11}]^-$ is a cluster catalyst discovered by Süss-Fink with a high L:B regioselectivity of 70:1 of propylene, but had an extremely low rate of 55 turnovers over the course of 66 hours.³ Kalk reported a highly active and regioselective catalyst when adding PPh_3 to a dirhodium thiolate-bridged catalyst.⁴ The catalyst was able to convert 1-hexene, and Kalk proposed that two intramolecular hydride transfers occurred during the hydroformylation process. This dirhodium catalyst unfortunately, suffered from fragmentation to make the Rh/PPh_3 monometallic catalyst, as studied by Southern and van Leeuwen.^{5, 6}

Research in Prof. Stanley's lab has shown highly effective bimetallic cooperativity for a dirhodium-tetraphosphine catalyst.⁷ The tetraphosphine ligand, $(\text{Et}_2\text{PCH}_2\text{CH}_2)(\text{Ph})\text{PCH}_2\text{P}(\text{Ph})(\text{CH}_2\text{CH}_2\text{PEt}_2)$, et,ph-P4, has the ability to chelate and bridge two rhodium metal centers keeping them in close proximity to promote bimetallic cooperativity (Figure 2.2). The ethylene link between the inner and outer phosphines allows for a chelate effect, while the bis(phosphino)methane unit acts as a bridging group to favor dirhodium complexes. The internal phosphines are chiral centers and produces two diastereomeric forms: *racemic* (*R,R* and *S,S*) and *meso* (*R,S*) as shown in Figure 2.2.

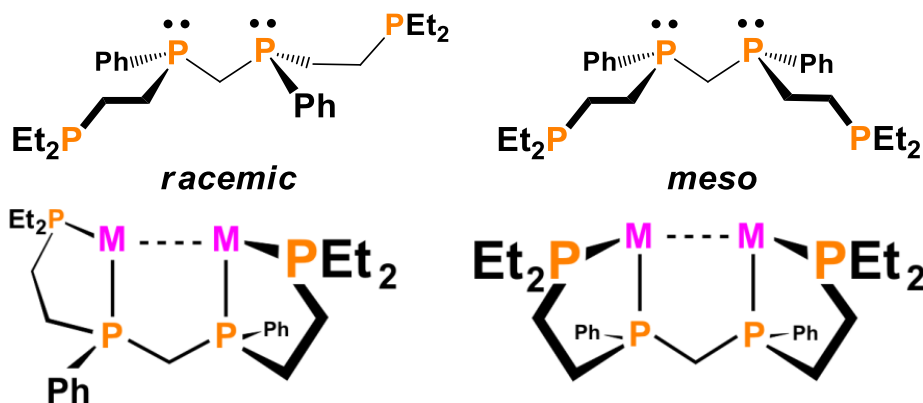


Figure 2.2. The *racemic* and *meso* diastereomers of the et,ph-P4 ligand

The tetraphosphine ligand reacts with two equivalents of $[\text{Rh}(\text{nbd})_2]\text{BF}_4$ to form the dirhodium catalyst precursor: $\text{Rh}_2(\text{nbd})_2(\text{et,ph-P4})](\text{BF}_4)_2$ (nbd = norbornadiene). The catalyst precursor is activated by H_2/CO to form a highly active and regioselective hydroformylation catalyst. The *racemic* diastereomer of the catalyst was shown to be far more active and selective than its *meso* counterpart. Table 2.1 compares the rates, selectivity, and isomerization of the two diastereomeric forms of the dirhodium-P4 catalyst and the Rh/PPh_3 monometallic catalyst.

Table 2.1. 1-Hexene Hydroformylation Comparisons

Catalyst (1 mM)	Initial TOF (min ⁻¹)	Aldehyde L:B ratio	Isomerization (%)	Alkane (%)
$[\text{Rh}_2(\text{nbd})_2(\text{rac-et,ph-P4})](\text{BF}_4)_2$	20	25:1	2.5	3.4
$[\text{Rh}_2(\text{nbd})_2(\text{meso-et,ph-P4})](\text{BF}_4)_2$	0.9	14:1	24	10
Rh/PPh_3 (1:820) ^a	9	17:1	1	<0.5

Conditions: 90°C, 90 psig, 1:1 H_2/CO , acetone, 1 mM catalyst, 1 M 1-hexene

^a $\text{Rh}(\text{CO})_2(\text{acac})$ was combined with ^a 0.82 M PPh_3 (820 eq.).

A critical reason for the dramatic difference between the *meso* and *racemic* dirhodium catalysts was the ability to transition to a close mode geometry. The *racemic* diastereomer is able to form a closed-mode structure with an edge-sharing bioctahedral structure that has all six coordination sites on the Rh available for ligand interactions (Figures 2.3 and 2.4).

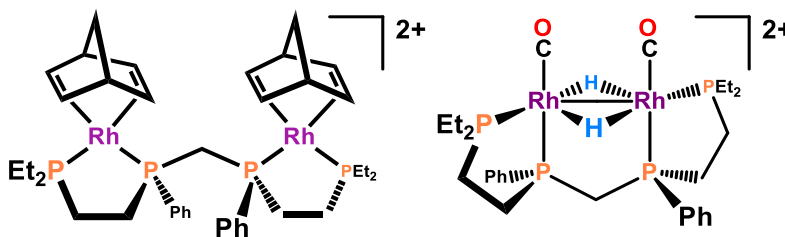


Figure 2.3. The *rac*- $\text{Rh}_2(\text{P4})$ catalyst precursor and the proposed active catalyst form, $[\text{rac-Rh}_2(\mu\text{-H})_2(\text{CO})_2(\text{et,ph-P4})]^{2+}$, (Et and Ph groups omitted for clarity).

The *meso* catalyst has a harder time transforming to the close mode geometry because of the position of the chelating phosphine arms which limits the coordination environment around the rhodium centers when performing the intramolecular step shown in Figure 2.4. The cisoidal arrangement of the chelate rings in the *meso*-diastereomer blocks out one or two of the rhodium coordination sites that point into the region between the chelate rings.

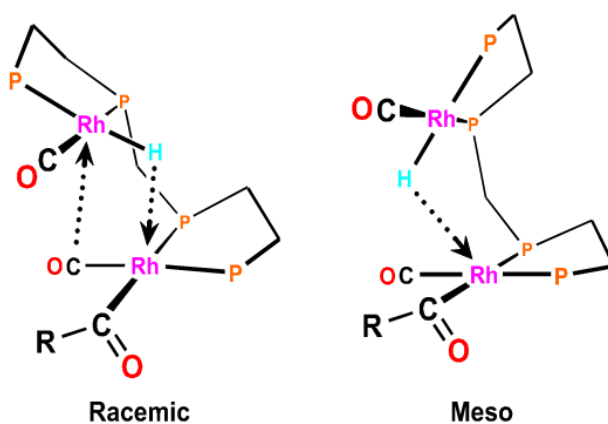


Figure 2.4. Intramolecular Hydride Transfer

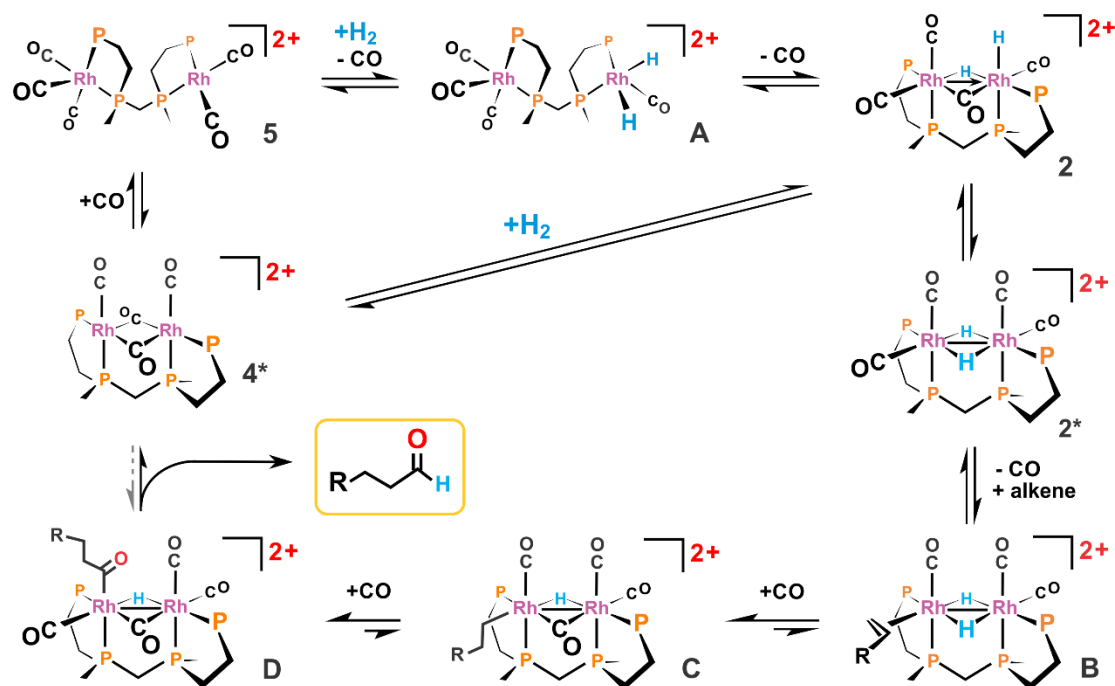


Figure 2.5. Proposed hydroformylation mechanism using *racemic* dirhodium catalyst.

The Stanley group has developed a proposed mechanism for dirhodium hydroformylation. The pentacarbonyl complex, **5**, undergoes oxidative addition of H_2 while a carbonyl is dissociated from the rhodium center to form **A**. Intramolecular hydride transfer occurs forming a bridging carbonyl and hydride (**2**). Based on DFT calculations by Dr. Ranelka Fernando, **2** rearranges to **2*** with two bridging hydride ligands. A metal-metal bond is formed between the two $\text{d}7$ $\text{Rh}(\text{II})$ centers once the complex has a symmetrical structure. $[\text{Rh}_2(\mu\text{-H})_2(\text{CO})_4(\text{rac-P4})]^{2+}$, **2***, is the key catalyst species that reacts with alkene to initiate hydroformylation. Dissociation of a CO ligand from **2*** allows coordination of the alkene to form **B**, followed by migratory insertion occurs between the alkene and hydride to form an alkyl group on the metal center (**C**). The empty coordination sites add CO ligands to do a second migratory insertion from the alkyl group and carbonyl ligand to form an acyl ligand (**D**). An intramolecular reductive elimination occurs between the acyl group and the bridging hydride to form the aldehyde product and the carbonyl-bridged species **4***. After the reductive elimination

both rhodium centers are in an oxidation state of +1 thus allowing two pathways for the hydroformylation cycle to finish. The first pathway involves CO-bridge breaking CO ligand addition to form the pentacarbonyl complex 5 to restart the cycle. The second pathway involves oxidative addition of hydrogen to 4* forming a bridging hydride-carbonyl complex 2.

To ensure bimetallic cooperativity was occurring monometallic chelating phosphine ligands were tested for hydroformylation. Monometallic chelating phosphine rhodium complexes were studied because of the possibility that the dirhodium complex could be acting as two independent monometallic complexes. Monometallic “half” analogs of the dirhodium P4 catalyst were prepared: $[\text{Rh}(\text{nbd})(\text{P}_2)] \text{BF}_4$ with $\text{P}_2 = \text{Et}_2\text{PCH}_2\text{CH}_2\text{PEt}_2$ (depe), $\text{Et}_2\text{PCH}_2\text{CH}_2\text{PMePh}$ (closest analog to half of the et,ph-P4 ligand), $\text{Et}_2\text{PCH}_2\text{CH}_2\text{PPh}_2$, or $\text{Ph}_2\text{PCH}_2\text{CH}_2\text{PPh}_2$ (dppe). All the $[\text{Rh}(\text{nbd})(\text{P}_2)] \text{BF}_4$ catalysts were shown to be terrible for hydroformylation with results of 1-2 turnovers per hour, 3:1 L:B aldehyde ratios, and 50-70% alkene isomerization and hydrogenation side reactions.⁸

Other model systems were tested to further demonstrate that bimetallic cooperativity was occurring for the dirhodium-P4 complex. By changing the methylene bridge of the et,ph-P4 ligand to a propylene or *p*-xylene bridge this spaced the rhodium centers apart to either have no interaction between the metal centers (*p*-xylene bridge) or very limited interactions (propylene bridge).

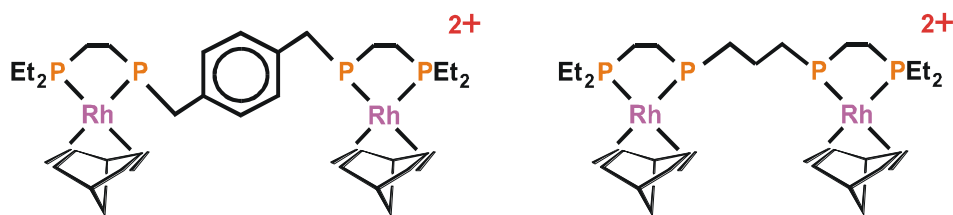


Figure 2.6. Different bridges for the dirhodium system

The modified P4 ligands resulted in very poor hydroformylation catalysts, similar to the monometallic models: 0.5-6 TO/h, 3:1 L:B product regioselectivity, 50-70% alkene isomerization and hydrogenation side reactions.

Stanley's bimetallic rhodium-P4 catalyst system showed great promise. Unfortunately, years of subsequent study revealed a serious flaw in the P4 ligand and dirhodium catalyst. The et,ph-P4 ligand was designed to coordinate strongly to the rhodium centers to maintain the bimetallic structure. NMR studies demonstrated that the ligand does not coordinate strongly enough and allows one of the rhodium centers to dissociate leading to deactivation of the $[\text{Rh}_2(\text{P4})]^{2+}$ catalyst system.^{9, 10}

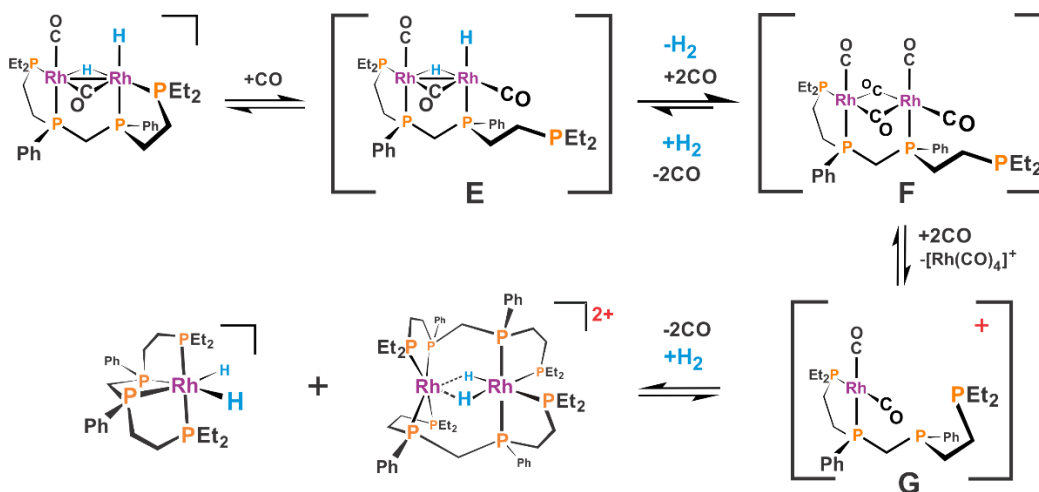


Figure 2.7. Proposed mechanism for the decomposition of the dirhodium catalyst system.

A mechanism was proposed for the dicationic dirhodium catalyst decomposition (Figure 2.7). The flexible ethylene bridge between the internal and external phosphine allows for phosphine dissociation to form complex **E** in Figure 2.7. This opens up the rhodium for CO coordination that reduces the electron density on the rhodium, which in turn promotes the reductive elimination of H_2 to form complex **F**. Additional CO coordination to this more

electron-rich rhodium center eventually peels off the one rhodium center to form complex **G**. Complex **G** can react with itself and H_2 to form the double-ligand dirhodium complex with two semi-bridging hydride ligands. The other complex is formed when the P4 ligand wraps around one metal center forming an inactive 18e- Rh(III) monometallic dihydride complex. In order to improve stability of the catalyst and to avoid the decomposition issue the ligand et,ph-P4 was modified for stronger chelation.

The Stanley group proposed a new tetraphosphine ligand, et,ph-P4-Ph, to avoid the decomposition issue. The new design modified the ethylene linkage between the internal and external phosphine by replacing the linkage with a phenylene linkage. This modified version of the ligand makes it a far stronger chelator because it will give the ligand more rigid arms to bind to the rhodium centers during the hydroformylation process. Similar to et,ph-P4, the new modified ligand forms two diastereomers: *racemic* and *meso*. Alexandre Monteil initially synthesized the et,ph-P4-Ph ligand and Katerina Kalachnikova and Marshall Moulis optimized the yields and separation of the diastereomers.¹¹

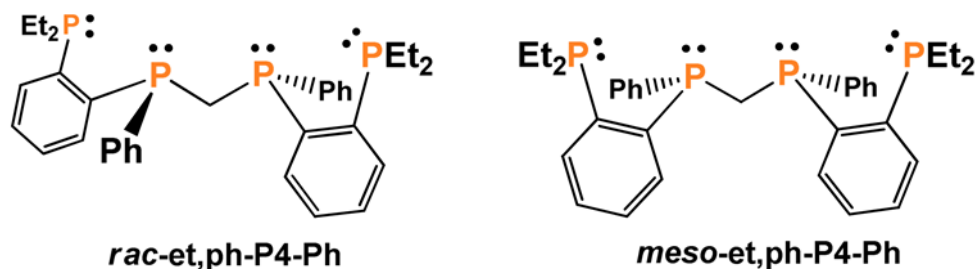


Figure 2.8. The *racemic* and *meso* diastereomers of et,ph-P4-Ph.

Marshall Moulis tested the new dirhodium catalyst based on the new P4-Ph ligand, $[Rh_2(nbd)_2(rac\text{-}et,ph\text{-}P4\text{-}Ph)](BF_4)_2$. Unfortunately, poor hydroformylation results with 1-

hexene were obtained with the new dirhodium-P4-Ph catalyst in acetone solvent: aldehyde L:B = 8.5, and 62% alkene isomerization with less than 50 turnovers. Different solvents were then tested by Moulis and the best results involved dimethylformamide, DMF, as a solvent. Running 1-hexene hydroformylation in DMF resulted in an improved aldehyde L:B ratio of 18.6, 3.3% alkene isomerization, and a low 1.1% hydrogenation with less than 100 aldehyde turnovers after 2 hours.

The next solvent tested was a 20% water/DMF mixture that resulted in a 16.1 L:B, 0.5% isomerization, 0.3% for hydrogenation with less than 100 turnovers after 2 hours. Those results were not better than the old ligand, which had a higher L:B, lower isomerization and hydrogenation as well as running faster than this new complex. The $[\text{Rh}_2(\text{nbd})_2(\text{rac-et, ph-P4-Ph})](\text{BF}_4)_2$ complex has not performed as well as the dirhodium catalyst based on the “old” et,ph-P4 ligand.

The new ligand was able to react with the rhodium starting material very easily to make the dirhodium catalyst precursor, but it has been very difficult to crystallize the precursor starting material, $[\text{Rh}_2(\text{nbd})_2(\text{rac-et,ph-P4-Ph})](\text{BF}_4)_2$. The best catalyst precursor to use in the past involved crystallized precursor, which is purer relative to crude precursor. Purity differences in catalyst precursors can cause dramatic differences hydroformylation runs.

Moulis changed the counterion from BF_4 to PF_6 , to aid in purification and better recrystallization. The new P4-Ph based catalyst precursor with PF_6 anions was able to crystallize better than the BF_4 system. The hydroformylation results, however, did not show better hydroformylation results relative to the old ligand-based catalyst because it showed lower L:B = 14:1 aldehyde ratios and initial TOF of 19 min^{-1} . NMR experiments later showed that the catalyst reacts with acetone solvent and PF_6^- to produce a PF_2O_2 anion and unidentified organic products.

Figure 2.9 shows the ^{31}P NMR reaction study with a septet at -145.5 ppm for the PF_6^- anion. The dirhodium P4-Ph complex has ^{31}P resonances between 54 to 76 ppm, while the PF_2O_2^- anion is the triplet-like pattern at -5.5 ppm.

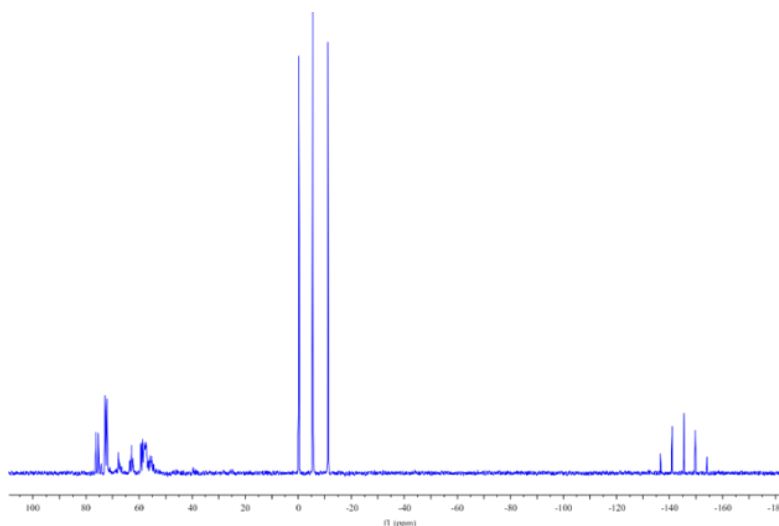


Figure 2.9. *In situ* $^{31}\text{P}\{^1\text{H}\}$ NMR $\text{Rh}_2(\text{nbd})_2(\text{rac-et,ph-P4-Ph})(\text{PF}_6)_2$ at 20 °C and 120psig of 1:1 H_2/CO in d_6 -acetone

The poor hydroformylation performance of $[\text{Rh}_2(\text{nbd})_2(\text{rac-et,ph-P4-Ph})](\text{PF}_6)_2$ was believed to be due to the unexpected reaction of the catalyst, PF_6^- , and acetone solvent to produce PO_2F_2^- and free fluoride anions. The NMR experiments did show signs that the dirhodium catalyst based on P4-Ph was considerably more stable than the old $[\text{Rh}_2\text{P4}]^{2+}$ catalyst. There was no significant difference between the ^{31}P NMR spectra of the catalyst under 120 psig of H_2/CO after one week as shown in Figure 2.10. The old $[\text{Rh}_2\text{P4}]^{2+}$ catalyst shows clear signs of extensive decomposition after 24 hours under H_2/CO pressure in acetone at room temperature.

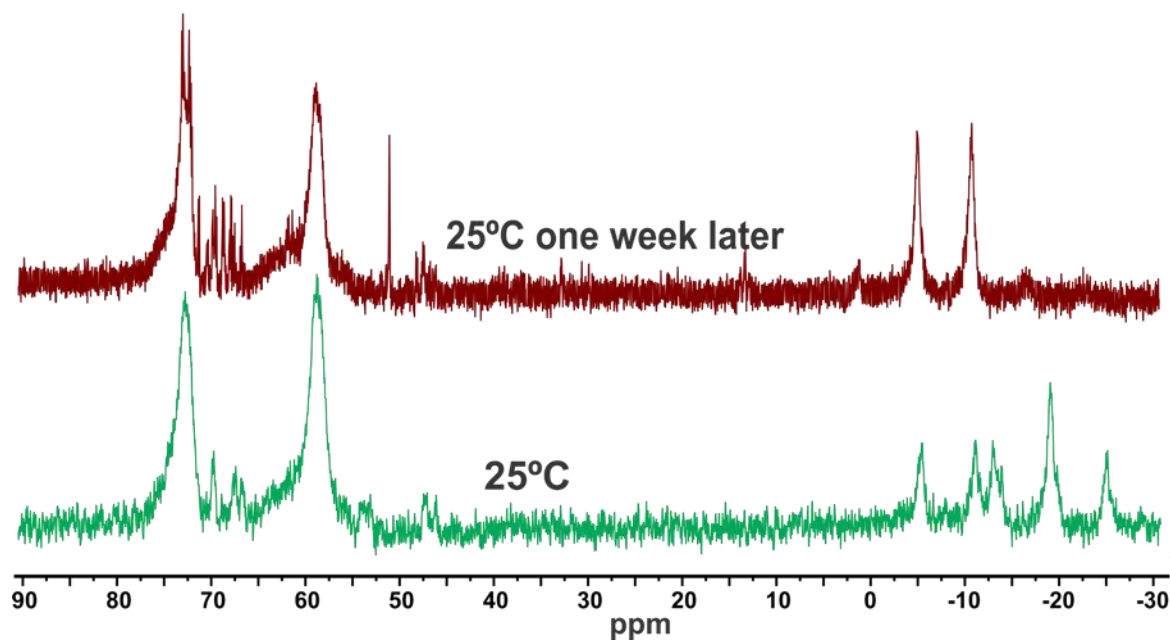


Figure 2.10. $^{31}\text{P}\{^1\text{H}\}$ NMR Pressurized with 120 psig H_2/CO in d_6 -acetone

2.2 $\text{Rh}_2(\mu\text{-CO})(\text{CO})_3(\text{rac-}i\text{-et,ph-P4-Ph})](\text{BF}_4)_2$

A new starting material was later discovered by Moulis to perform hydroformylation. The new catalyst was $[\text{Rh}_2(\mu\text{-CO})(\text{CO})_3(\text{rac-}i\text{-et,ph-P4-Ph})](\text{BF}_4)_2$. He prepared it by dissolving the precursor catalyst, $[\text{Rh}_2(\text{nbd})_2(\text{rac-}i\text{-et,ph-P4-Ph})](\text{BF}_4)_2$, in DCM, adding it to the autoclave, pressurized to 80 psig of H_2/CO , and heated to 70°C while stirring at 1000 rpm. After an hour the autoclave was cooled and depressurized. The dark red catalyst solution was removed by a syringe and placed in a Schlenk flask. H_2/CO was bubbled through the flask until a very concentrated solution was left and then placed in freezer for crystallization. Orange crystals formed and were isolated and spectroscopically characterized, along with a crystal structure shown in Figure 2.11. The complex is $[\text{Rh}_2(\mu\text{-CO})(\text{CO})_3(\text{rac-}i\text{-et,ph-P4-Ph})]^{2+}$ and was the first closed-mode dirhodium system we have characterized with either the old or new P4 ligands. The

Rh-Rh separation is 2.770 Å and the bridging CO is somewhat unsymmetrical with Rh1-C2 = 2.070 Å and Rh2-C2 = 2.075 Å.

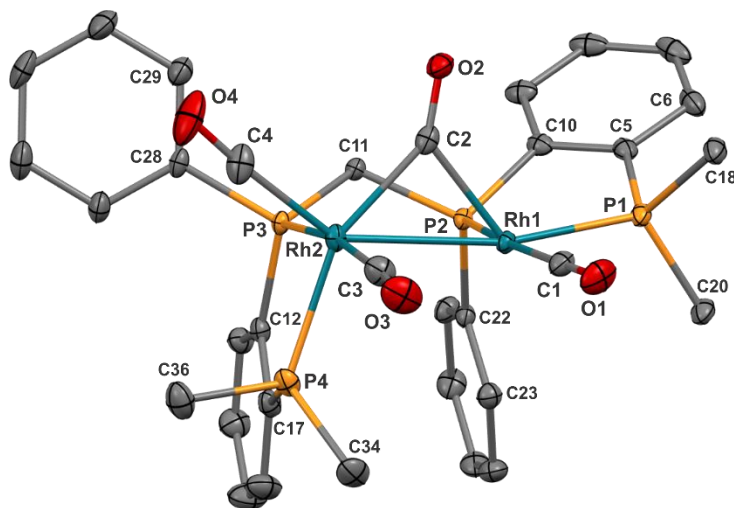


Figure 2.11. Crystal structure of $[\text{Rh}_2(\mu\text{-CO})(\text{CO})_3(\text{rac-et,ph-P4-Ph})](\text{BF}_4)_2$

$[\text{Rh}_2(\mu\text{-CO})(\text{CO})_3(\text{rac-et,ph-P4-Ph})]^{2+}$ turned out to be an excellent hydroformylation catalysts and ran 1-hexene well in acetone/water: initial TOF = 29.3 min^{-1} (ten minutes), aldehyde L:B = 17:1, alkene isomerization = 4.7%, and hydrogenation = 1.1%. Except for a somewhat lower L:B aldehyde ratio, these results compared extremely well with the old $\text{Rh}_2\text{P4}$ catalyst. DMF and DMF/water was also tested as a solvent system with very promising 1-hexene hydroformylation results for 25% water/DMF: initial TOF = 35.4 min^{-1} (ten minutes), L:B = 17.6:1, alkene isomerization = 1.9%, and alkene hydrogenation < 1%.

Although these results were extremely encouraging, the synthesis of $[\text{Rh}_2(\mu\text{-CO})(\text{CO})_3(\text{rac-et,ph-P4-Ph})]^{2+}$ was a serious problem. The autoclave synthesis was highly inconsistent when making the catalyst with generally low yields of expensive rhodium starting material. The fatal flaw to this synthesis method involves the amount of catalyst precursor that

has to be used to form the carbonyl species. At least 4 to 5 grams of $[\text{Rh}_2(\text{nbd})_2(\text{rac-et,ph-P4-Ph})](\text{BF}_4)_2$ has to be used to form less than half a gram of crystallized $[\text{Rh}_2(\mu\text{-CO})(\text{CO})_3(\text{rac-et,ph-P4-Ph})](\text{BF}_4)_2$, when it would crystallize. The effort, time, and cost that goes into separating the et,ph-P4-Ph ligand combined with the inconsistent and low yields of $[\text{Rh}_2(\mu\text{-CO})(\text{CO})_3(\text{rac-et,ph-P4-Ph})](\text{BF}_4)_2$ meant that we needed to find a much better catalyst precursor.

2.3 Probing the Catalyst Precursor, $[\text{Rh}_2(\text{nbd})_2(\text{et,ph-P4-Ph})](\text{BF}_4)_2$

I tested a wide variety of conditions with varying pressures, temperatures, and solvents in doing hydroformylation runs with $[\text{Rh}_2(\text{nbd})_2(\text{rac-et,ph-P4-Ph})](\text{BF}_4)_2$, some of which are shown in Table 1. Different solvents did not help, nor did higher pressures. Higher temperatures from 110°C-130°C led to black material precipitation and poor catalytic results, presumably due to catalyst decomposition. The initial soaking conditions for the catalyst precursor in the autoclave was varied from 20 total minutes of soaking at 90 psig 1:1 H_2/CO to 15 minutes H_2 at 80°C and 90 psig, then switching to pure CO for 30 minutes at 80°C and 110 psig, followed by 1:1 $\text{H}_2:\text{CO}$ when alkene is injected. These conditions also yielded very poor hydroformylation results with 1-hexene after 4 hours: aldehyde L:B = 12.5, alkene isomerization = 63.3%, with only 128 turnovers in an acetone/water solvent system. Altering the solvents, pressure, and temperature has not had a positive impact on the results of the reaction, so it was concluded that other factors surrounding the catalyst may be the issue.

Table 2.2. Catalytic Studies for the Hydroformylation of 1-Hexene using $[\text{Rh}_2(\text{nbd})_2(\text{rac-}i\text{-et,ph-P4-Ph})](\text{BF}_4)_2$

Time (hrs)	Solvent	Pressure (psig)	Temp. (°C)	Turnovers	Isomerization (%)	L:B
4	Pyridine	90	90	160	8.0	1.8
3	Acetophene	90	90	4	93.4	1.4
2	Acetone	225	70	223	65.2	2.6
6	t-glyme/30% H ₂ O	90	90	58	86.0	4.1

Conditions: 1 mM $[\text{Rh}_2(\text{nbd})_2(\text{rac-}i\text{-et,ph-P4-Ph})](\text{BF}_4)_2$, 1 M 1-hexene

The catalytic ability of the new dirhodium catalyst for hydroformylation was not comparable to that of our old ligand-based dirhodium catalyst. One issue that caused concern was the counterion. The new dirhodium catalyst promoted the reaction of the PF_6 counterion with acetone so perhaps the BF_4 anion could also be reacting with some solvents as well. Changing counterions could also help with crystallization and isolation of the catalyst precursor complex. We decided to test the tetrakis[3,5-bis(trifluoromethyl)phenyl]borate $[\text{BAr}^{\text{F}}_4]$ and tetrakis(pentafluorophenyl)borate $[\text{BF}_{20}]$ anions (Figure 2.12) to determine if they could make a better dirhodium catalyst precursor and catalyst for hydroformylation.

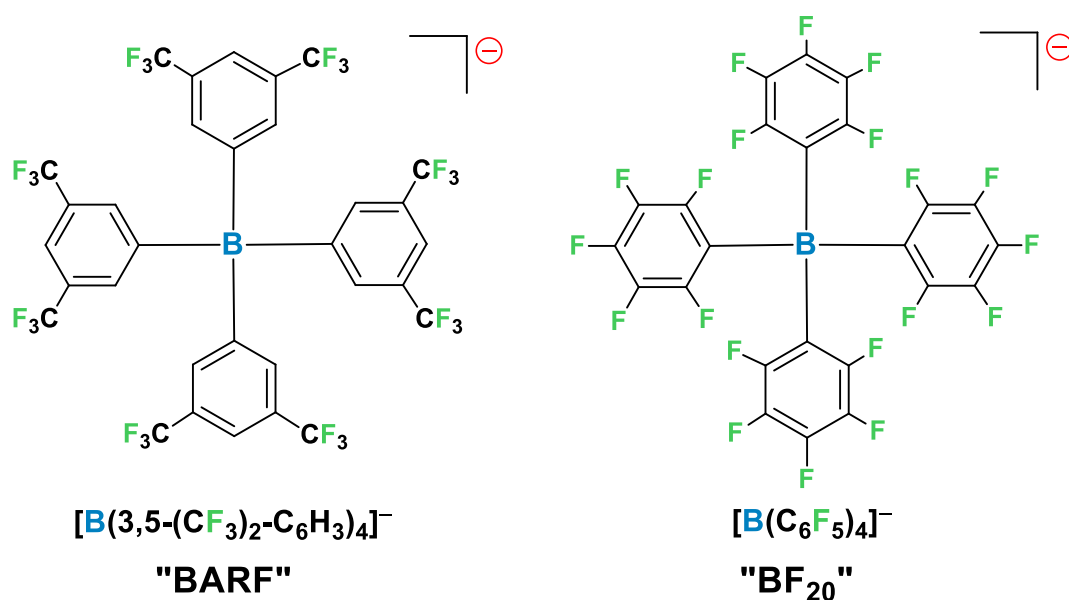


Figure 2.12. Drawings of the $[\text{BAr}^{\text{F}}_4]$ and $[\text{BF}_{20}]$ anions.

The BF₄ anions were for both *rac*- and *meso*-diastereomers of new dirhodium catalyst precursor were exchanged with [BAr^F₄] and [BF₂₀] counterions. I also exchanged the BF₄ anions for the old *rac*-catalyst precursor, [Rh₂(nbd)₂(*rac*-et,ph-P4)]²⁺ with [BF₂₀]⁻ and [BAr^F₄]⁻. The solubility of [Rh₂(nbd)₂(*rac*-et,ph-P4-Ph)](BAr^F₄)₂ and the [BF₂₀]- analog were quite similar to the original BF₄⁻ salts: soluble in polar solvents, insoluble in non-polar solvents.

Hydroformylation studies were done using different solvents and solvent combinations such as acetone, acetone/water, DMF, and acetonitrile. Testing the *meso* catalyst precursor for hydroformylation using 1-hexene, [Rh₂(nbd)₂(*meso*-et,ph-P4-Ph)]²⁺ with [BAr^F₄]⁻ and [BF₂₀]⁻ anions only showed alkene isomerization with all the solvents used with low turnovers from 20-40 in 3 hours.

The *racemic* catalyst precursors, [Rh₂(nbd)₂(*rac*-et,ph-P4-Ph)](BAr^F₄)₂ and [Rh₂(nbd)₂(*rac*-et,ph-P4-Ph)](BF₂₀)₂, also ran poorly showing mainly alkene isomerization between 40-60% and low hydroformylation turnovers less than 100 turnovers in two hours. The old catalyst precursor, [Rh₂(nbd)₂(*rac*-et,ph-P4)](BF₂₀)₂, did show similar results to the same precursor with the BF₄ anion with hydroformylation turnovers between 600-700 turnovers. I was unable to crystallize any of the new salts because only a small amount was made for each one. Changing the counterions did not reveal any different catalytic results from previous runs with the BF₄ counterion. The old ligand catalyst results demonstrated that the [BF₂₀] counterion had similar results as the BF₄ anion and didn't seem to have any significant effect on the catalysis. We did, however, observe that the [BAr^F₄]⁻ anion did decompose during the hydroformylation run based on the GC-MS analysis displaying fluorinated fragments.

Hydroformylation was also attempted using a modified version of the new P4-Ph ligand. Changing the R groups on the external phosphines of the tetraphosphine could increase reactivity

by not only changing electron density, but also impacting the steric effects. The modified ligand, $[\text{Rh}_2(\text{nbd})_2(\text{mixed-ph,ph-P4-Ph})](\text{BF}_4)_2$, has two phenyl groups on the outer phosphines instead of ethyl groups. Two 1-hexene hydroformylation experiments were run using this new P4-Ph substituted ligand. The first experiment was run at 90°C and 90 psig in 70% acetone/30% water; and the second was run at 90°C, with the pressure increased from 150 psig to 200 psig after two hours in 70% acetone/30% water. Both yielded similar terrible hydroformylation results with also isomerization increasing from 60% to 85% over time, a L:B ratio 2:1, no hydrogenation, and only 15 turnovers making aldehyde at 90 psig and 35 turnovers at 150 psig.

Previous hydroformylation studies in the group with the phenylated version of the old P4 ligand, ph,ph-P4, yielded very poor hydroformylation results. In that case Prof. Stanley proposed that the increased steric bulk prevented bimetallic cooperativity, which was important for hydroformylation catalysis. A methyl-substituted version of the P4-Ph ligand was also tested for hydroformylation using $[\text{Rh}_2(\text{nbd})_2(\text{mixed-me,ph-P4-Ph})](\text{BF}_4)_2$ as the catalyst precursor. This was also a very poor hydroformylation catalyst for 1-hexene with the following results after 2 hours: 33 turnovers to make aldehyde, aldehyde L:B = 3.6, and 63% alkene isomerization.

Table 2.3. Modified P4-Ph Ligand-Based 1-Hexene Hydroformylation

Ligand	Time (hrs)	Pressure (psig)	Aldehyde Turnovers	L:B	Isomerization (%)
<i>mixed-ph,ph-P4</i>	2	90	15	2	65
<i>mixed-ph,ph-P4</i>	2	150	35	2	70
<i>mixed-me,ph-P4</i>	2	150	33	3	63

Conditions: 1 mM $[\text{Rh}_2(\text{nbd})_2(\text{ligand})](\text{BF}_4)_2$ catalyst, 1 M 1-hexene, solvent = 30% water/acetone

After the initial hydroformylation studies with the new ligand, it was proposed that perhaps the norbornadiene (nbd) ligand on the new catalyst precursor, $[\text{Rh}_2(\text{nbd})_2(\text{rac-et,ph-P4-Ph})](\text{BF}_4)_2$, would be a better catalyst.

$\text{Ph})]^{2+}$, was not being displaced to generate the active catalyst, $[\text{Rh}_2(\mu\text{-H})_2(\text{CO})_x(\text{rac-}i\text{-et,ph-P4-Ph})]^{2+}$ ($x = 2\text{-}4$). FT-IR studies clearly demonstrated that the nbd ligand was very easily displaced by CO on the old ligand P4 dirhodium catalyst precursor. FT-IR studies on $[\text{Rh}_2(\text{nbd})_2(\text{rac-}i\text{-et,ph-P4-Ph})](\text{BF}_4)_2$ clearly showed H_2/CO reaction behavior that differed from the old ligand complex (Figure 2.13).

The FT-IR study in Figure 2.13 on the reaction of CO and H_2/CO with $[\text{Rh}_2(\text{nbd})_2(\text{rac-}i\text{-et,ph-P4-Ph})]^{2+}$ showed that nbd would compete with the carbonyls until around 40 psig, but when the pressure was decreased the nbd would rebind. The old ligand-based dirhodium catalyst did not have to constantly compete with the nbd ligand because the nbd would polymerize out in the autoclave, and the carbonyls could openly bind to the complex.¹²

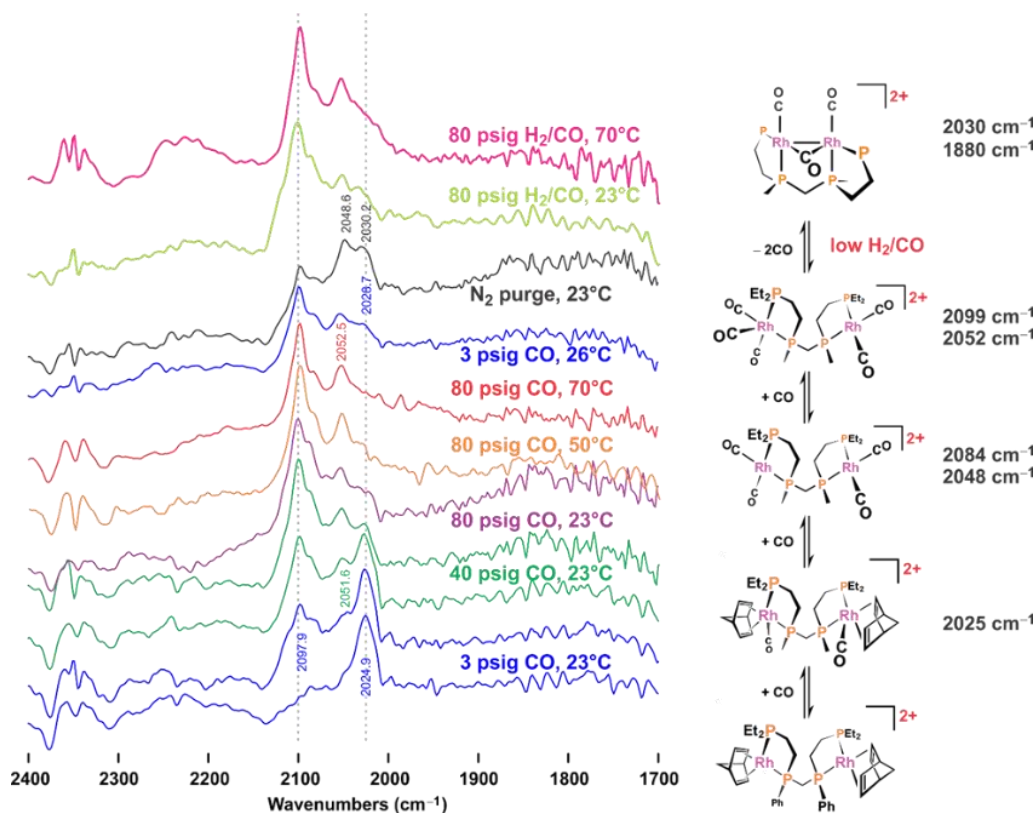


Figure 2.13. Stacked *in situ* FT-IR of $[\text{Rh}_2(\text{nbd})_2(\text{rac-}i\text{-et,ph-P4-Ph})](\text{BF}_4)_2$, the structures shown are drawn with the “old” *et,ph-P4* ligand for clarity as the 1,2-phenylene chelate rings complicate the structure drawings.

These results could be indicative as to why the new ligand complex has not been very active because if the nbd ligand rebinds during hydroformylation it will compete with 1-hexene coordination and slow hydroformylation.

2.4 The Degradation of the New Ligand

After looking at a variety of potential problems I decided to make a different precursor starting materials for the new tetraphosphine ligand. The norbornadienes on the dirhodium tetraphosphine complex were believed to be inhibiting the hydroformylation process by blocking coordination sites and acting as a competing coordinating ligand.

A number of different precursors were prepared and tested with the new tetraphosphine ligand. $[\text{Rh}_2(\text{N}\equiv\text{CCH}_3)_4(\text{rac-P4-Ph})](\text{BF}_4)_2$ was prepared replacing the norbornadiene ligands with acetonitriles. The $[\text{Rh}_2(\text{N}\equiv\text{CCH}_3)_4(\text{mix-et,ph-P4-Ph})](\text{BF}_4)_2$ precursor initially give good results for the hydroformylation of 1-hexene in 30% water/acetone solvent at 110 psig 1:1 H_2/CO and 90°C (2 hour results): 672 turnovers of aldehyde, 15.1 L:B aldehyde regioselectivity, 6.8% alkene isomerization, and low 0.8% alkene hydrogenation. Unfortunately, subsequent hydroformylation runs were inconsistent. A 1-hexene hydroformylation run using the *racemic* catalyst precursor, $[\text{Rh}_2(\text{N}\equiv\text{CCH}_3)_4(\text{rac-et,ph-P4-Ph})](\text{BF}_4)_2$, under the same conditions as the mixed precursor, $[\text{Rh}_2(\text{N}\equiv\text{CCH}_3)_4(\text{mixed-et,ph-P4-Ph})](\text{BF}_4)_2$, the results were very similar. The *racemic* complex after 2 hours had 660 turnovers of aldehyde, L:B = 12.3, 12.3% alkene isomerization, and low 0.9% alkene hydrogenation. These results indicated that there was not a significant difference between the *racemic* and *mixed* (*rac/meso*) mixture of catalyst precursor complexes. All our previous studies have clearly shown that the *racemic*-diastereomer is the active and selective dirhodium catalyst, while the *meso*-diastereomer is much slower and less

chemoselective. But in this case the *racemic* complex was worse than the mixed ligand complex with higher side reaction values and a lower total turnovers after 2 hours.

After these results it caused me to seriously question the purity of the *racemic* catalyst precursor that had used. A variety of experiments led me to believe the problem was with the new tetraphosphine ligand. I decided to make the catalyst precursor from a fresh batch of new ligand to produce the $[\text{Rh}_2(\text{nbd})_2(\text{mixed-et,ph-P4-Ph})](\text{BF}_4)_2$ complex.

Running this complex prepared with with fresh P4-Ph ligand under standard conditions (90 psig 1:1 H_2/CO , 90°C, 1 mM catalyst, 1 M 1-hexene) in 30% water/acetone gave good results after 2 hours: 548 aldehyde turnovers, 13.1 L:B, 13.5% alkene isomerization, and no alkene hydrogenation. This new batch mixed et,ph-P4-Ph ligand had only been through a DCM-alumina cleanup column and NOT our typical diastereomer separation column. The cleanup column removes most of the impurities in the mixed P4-Ph ligand, but does not separate the *rac* and *meso* diastereomers. The new batch of P4-Ph ligand compared to the batches that had gone through the separation column looked different via ^{31}P NMR (Figure 2.14 and 2.15).

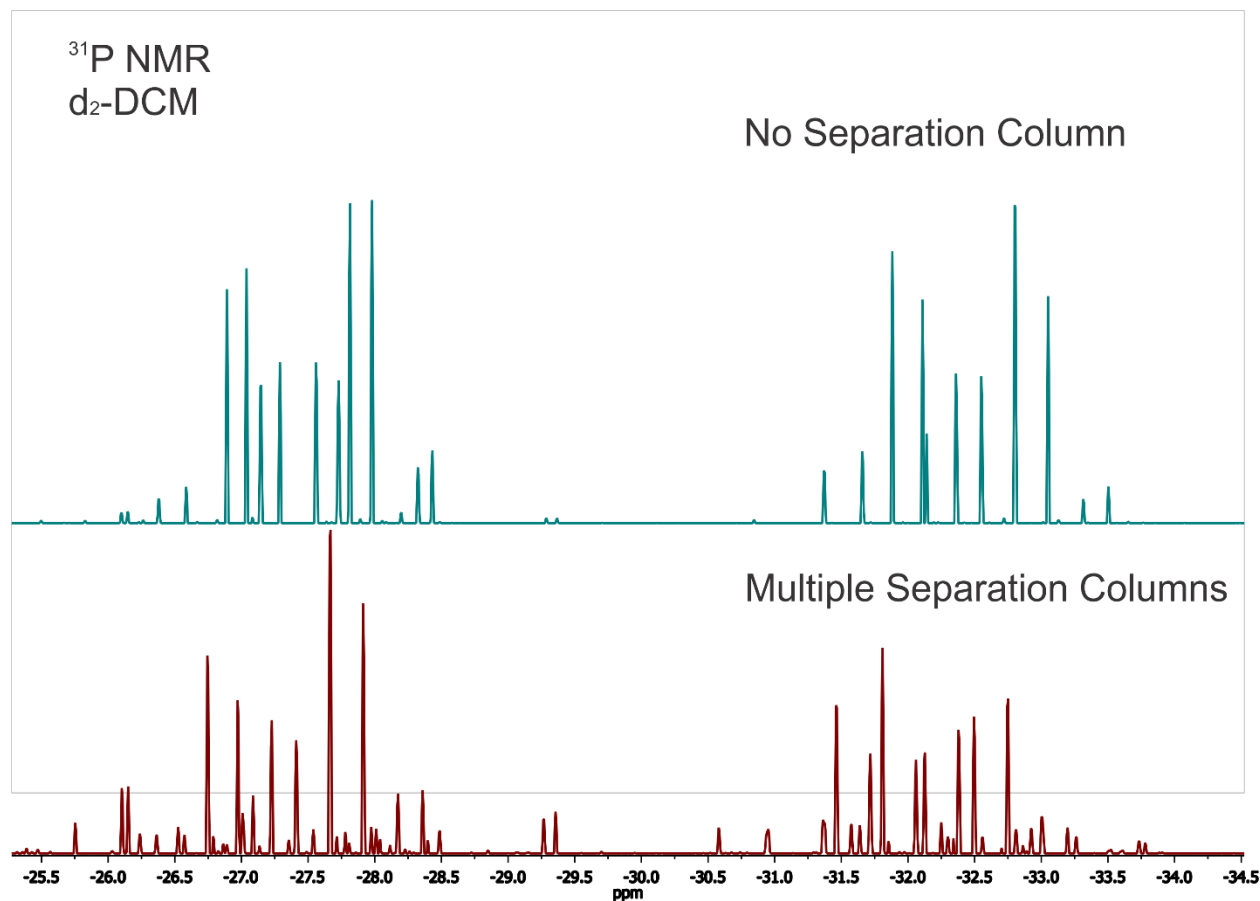


Figure 2.14. ^{31}P NMRs of mixed et,ph-P4-Ph ligand. Top green spectrum is P4-Ph ligand that has not gone through the separation column, only the clean-up column. Bottom red spectrum is the P4-Ph ligand that has passed through the separation column several times. A number of impurities are present in the red spectrum relative to the green spectrum.

When comparing the ^{31}P NMR spectra in Figure 2.14 and 2.15 the et,ph-P4-Ph ligand that has gone through several separation columns shows new impurities. The P4-Ph ligand goes through several separation columns because the amount of separated diastereomers quantities are not large enough to make a significant amount of dirhodium precursor catalyst. The P4-Ph ligand uses two columns: clean-up column and separation column. The clean-up column allows for the impurities initially on the P4-Ph ligand to stay on the column. The ligand is dissolved in DCM and passed through alumina column. The ligand is typically a yellowish color before the column and after the clean-up column turns to an opaque color. The separation column involves using a

1:4 DCM/Hexane mixture to elute the ligand from the column. Once off the column the ligand is collected by fractions and the solvent is boiled off.

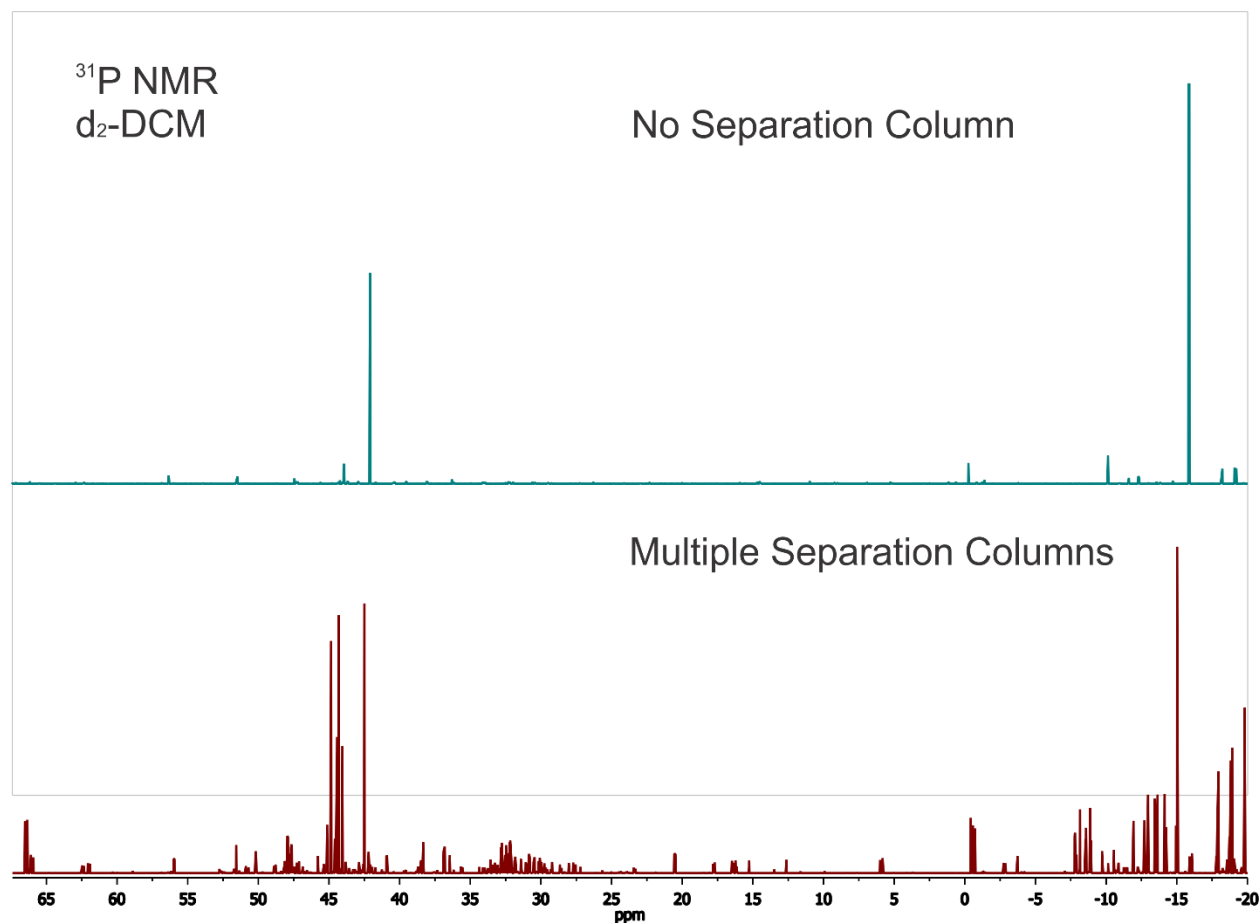


Figure 2.15. Stacked NMR of et,ph-P4-Ph ligand, green spectrum is new ligand that has not gone through column, red spectrum is new ligand under the column multiple times.

New resonances for the *rac*- and *meso*-diastereomers have appeared indicating that the P4-Ph ligand is being changed somehow when exposed to the separation column conditions too long. These impurities have come from the diastereomer separation column we use. The new ligand is very reactive to many solvents and DCM is one it is most reactive when exposed for too long a time. The separation column with run times ranging from 90 to 120 minutes and that is not including removing solvent from the fractions collected that can potentially add another hour or two of P4-Ph exposure to solvent. Consistently running a column to gather grams of ligand

can take considerable amounts of time and with the constant exposure to DCM and air the column deteriorates the new tetraphosphine ligand. The DCM reacts with the ligand somehow and causes these impurities to form. This would explain why the *racemic* and mixed ligand complexes displayed similar results because the *racemic* had been exposed to the DCM separation column longer resulting in a deteriorated *racemic* ligand complex.

The separation of the diastereomers has been investigated by former students and using the column to separate the ligand diastereomers has been the best method. The P4-Ph ligand reaction with DCM, however, is more serious than we previously believed and extra care in working with the P4-Ph ligand and its diastereomeric separation needs to be taken into account. I believe that the initial results from former graduate students in the lab when conducting hydroformylation runs with the P4-Ph used deteriorated ligand. The group usually stocks up the different diastereomers over months via multiple separations to gather grams of separated P4-Ph ligand. This ligand is then used for making the starting dirhodium precursor. Use of degraded P4-Ph ligand would explain the inconsistent results over time as well as why the nbd precursor was not active for hydroformylation. To avoid this problem I've made smaller batches of dirhodium complex using freshly separated ligand. Once the P4-Ph ligand coordinates to make the dirhodium precursor the ligand and complex appears to have good stability. With the ligand/catalyst problem solved I was able to further investigate and optimize the new dirhodium tetraphosphine ligand catalyst system.

2.5 References

1. R.F. Heck, D.S. Breslow, *J. Am. Chem. Soc.*, **1961**, 83, 4023.
2. Ryan, R. C.; Pittman, C. U., Jr. *J. Am. Chem. Soc.* **1977**, 99(6), 1986.
3. Süss-Fink, G.; Schmidt, G. F. *J. Mol. Catal.* **1987**, 42(3), 361.

4. Kalck, P. *Polyhedron* 1988, 7(22-23), 2441.
5. Davis, R.; Epton, J. W.; Southern, T. G. *J. Mol. Catal.* 1992, 77(2), 159.
6. Diéguez, M.; Claver, C.; Masdeu-Bultó, A. M.; Ruiz, A.; van Leeuwen, P. W. N. M.; Schoemaker, G. C. *Organometallics* 1999, 18(11), 2107.
7. Broussard, M. E.; Juma, B.; Train, S. G.; Peng, W. J.; Laneman, S. A.; Stanley, G. G., A Bimetallic Hydroformylation Catalyst: High Regioselectivity and Reactivity Through Homobimetallic Cooperativity. *Science*. 1993, 260, 1784.
8. Broussard, M. E.; Louisiana State University (Baton Rouge La.). Dept. of Chemistry. Thesis (Ph D), Louisiana State University, Baton Rouge, 1993.
9. Matthews, R. C.; Howell, D. K.; Peng, W.-J.; Train, S. G.; Treleaven, W. D.; Stanley, G. G., Bimetallic Hydroformylation Catalysis: In Situ Characterization of a Dinuclear Rhodium(II) Dihydrido Complex with the Largest Rh–HNMR Coupling Constant. *Angewandte Chemie International Edition in English* 1996, 35 (19), 2253-2256.
10. Matthews, R. C. *In Situ* Spectroscopic Studies of a Bimetallic Hydroformylation Catalyst. Louisiana State University, 1999; (b) Gueorguieva, P. G. Spectroscopic and Synthetic Studies Relating to a Dirhodium Hydroformylation Catalyst. Louisiana State University, 2004; (c) Polakova, D. Studies on a Dirhodium Tetrphosphine Hydroformylation Catalyst. Louisiana State University, Baton Rouge, 2012.
11. Monteil, A. R. Investigation into the Dirhodium-Catalyzed Hydroformylation of 1-Alkenes and Preparation of a Novel Tetrphosphine Ligand. Ph.D. Disseretation, Louisisana State University, 2006.
12. Moulis, M., unpublished material 2017.

Chapter 3: Optimization of the New Tetraphosphine Ligand (et,ph-P4-Ph)

3.1 Previous Results

The new P4-Ph tetraphosphine ligand took over 10 years to develop, however, our group does not have a significant amount of catalytic data due to problems discussed in the previous chapter. As previously mentioned, Marshall Moulis has been the only student to run the new ligand for hydroformylation with very mixed results. The high isomerization indicated that degraded *racemic* ligand was used to prepare the catalyst precursor, as discussed in Chapter 2. Testing catalyst precursors for hydroformylation that were prepared with good, fresh P4-Ph ligand (less impurities on the P4-Ph ligand) will be discussed in this chapter.

3.2 Standard Hydroformylation Procedure

To test the new dirhodium-tetraphosphine hydroformylation catalyst activity various methods and conditions were investigated using our standard catalytic protocols. All the hydroformylation runs require pressurized H₂/CO conditions and elevated temperatures. The reactions were conducted in a stainless steel Parr autoclave systems that were modified with quick-connects and solvent-resistant O-rings to allow faster assembly, disassembly, and cleaning. The current autoclave design uses 160 mL stainless steel Parr reactors equipped with three detachable stainless steel arms

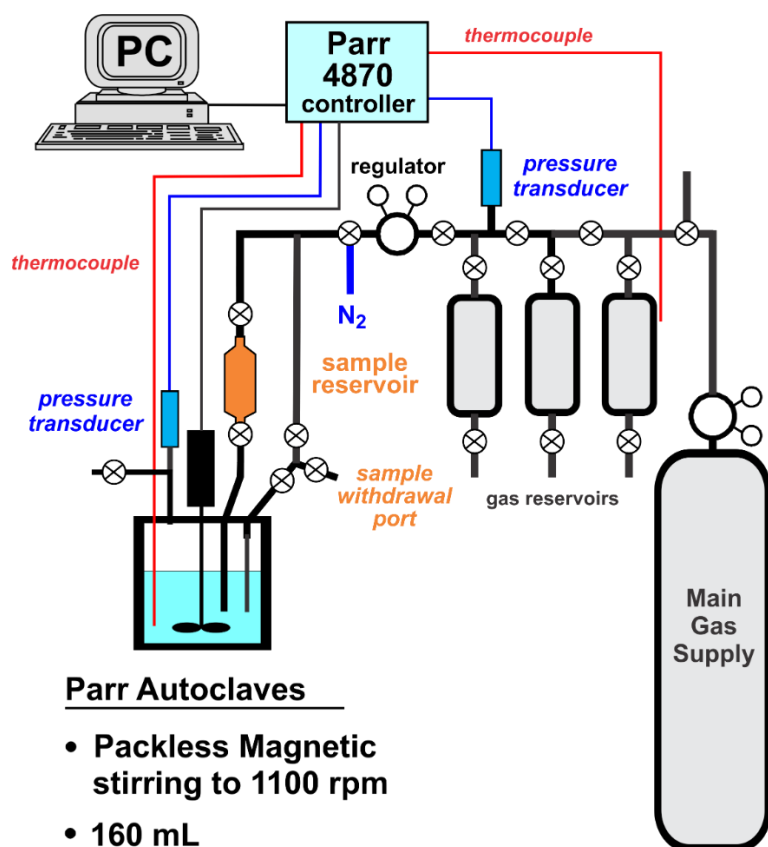


Figure 3.1. Schematic for the autoclaves used for hydroformylation in the Stanley lab.



Figure 3.2. Assembled Autoclave Reactor

The sampling arm allows for samples to be collected during the course of a hydroformylation run. The design allows for small samples to be withdrawn safely even under higher pressure conditions. The purge arm is used to add catalyst via cannula to the reactor vessel as well as used to vent gas at the end of a reaction. The pressure of the autoclave is monitored via an electronic pressure transducer attached to the purge arm. The olefin pressure injection arm allows for direct injection of the olefin to the activated catalyst under operating conditions. Gas is delivered through both the olefin pressure injection arm and sampling arm to allow for better mixing of gases into the catalyst mixture. A thermocouple is attached to the autoclave to allow monitoring and control of reaction temperature. There is a powerful magnetic stirrer system.



Figure 3.3. Autoclave Reactor Arms: Sampling Arm (left), Purge Arm with Pressure Transducer (middle), and Olefin Pressure Injection Arm (right)

The gas manifold system can accommodate up to four large gas cylinders. We typically use a premixed high purity 1:1 H_2/CO cylinder as the primary gas for hydroformylation runs. Individual CO and H_2 tanks allow mixing different ratios of these gases for specialized studies. The fourth gas cylinder is usually an inert gas (N_2 or Ar) or ethylene. Each gas cylinder has its own regulator and is connected to the common line that supplies gas to all four autoclave systems and the three smaller reservoir cylinders associated with each set of two autoclaves.

Each autoclave has a regulator that controls the gas pressure for the autoclave via stainless steel hoses as shown in the fully assembled autoclave (Figure 3.1). All our hydroformylation runs are done under constant pressure conditions.

The standard procedure used for hydroformylation reactions is as follows. The autoclave is assembled and vacuum line is connected to evacuate the air from the autoclave. In the glovebox, the catalyst solution and olefin are separately prepared in different flasks and sealed with a septum. The olefin is filtered through neutral alumina to remove any peroxide impurities. The catalyst solution and olefin are then transferred via cannula to the reactor vessel and olefin pressure injection arm, respectively. The autoclave is pressurized up with the desired operating pressure to purge the autoclave of any trapped air, and then heated up to the desired reaction temperature to allow for a soaking period with the H₂/CO gas as it stirs. After the soaking period the autoclave pressure is reduced by about 10 psig and the olefin is pressure injected into the catalyst solution. The reaction is held at a constant temperature and pressure with occasional samples being taken and analyzed via Gas Chromatography-Mass Spectrometry (GC-MS).

3.3 Cyclooctadiene precursor

As mentioned in Chapter 2 it was initially believed the problem that caused our hydroformylation problems was the catalyst precursor, [Rh₂(nbd)(*rac*-et,ph-P4-Ph)](BF₄)₂. The norbornadienes might be acting as competing ligands blocking the open rhodium coordination sites. The solution was to exchange the norbornadienes with other ligands that would dissociate more easily and not compete with the alkene substrate for hydroformylation. The original starting precursor material involved synthesizing bis(norbornadiene)rhodium(I) tetrafluoroborate, [Rh(nbd)₂](BF₄), using a synthesis the Stanley group had used prior to my arrival in the group.¹ The same method was used to make [Rh(cod)₂](BF₄), the only difference

involved instead of using norbornadiene the ligand was now 1,5-cyclooctadiene. The $[\text{Rh}(\text{cod})_2](\text{BF}_4)$ material was then used to make the dirhodium catalyst precursor. Using two equivalents of $[\text{Rh}(\text{cod})_2](\text{BF}_4)$ to react with mixed-et,ph-P4-Ph formed the new dirhodium precursor, $[\text{Rh}_2(\text{cod})_2(\text{mixed-et,ph-Ph-Ph})](\text{BF}_4)_2$. The mixed ligand was used initially for testing as the separation column did display signs of ligand degradation and I hadn't yet worked out the separation procedures to minimize the P4-Ph ligand degradation problem. The *mixed* ligand was used first to optimize conditions, and then the *rac*- and *meso*-diastereomers would be tested after optimization for hydroformylation. The initial properties of the $[\text{Rh}_2(\text{cod})_2(\text{mix-et,ph-Ph-Ph})](\text{BF}_4)_2$ were very similar to the dirhodium norbornadiene complex.² It was similar in color being a reddish-orange, and soluble in similar solvents: DCM, benzene, acetone, and other polar solvents. $[\text{Rh}_2(\text{cod})_2(\text{mix-et,ph-Ph-Ph})](\text{BF}_4)_2$ was not soluble in less-polar solvents like diethyl ether or hexanes.

The ^{31}P NMR shows similar resonances and chemical shifts as the norbornadiene precursor: a pair of doublet doublets around 52 and 49 ppm. The external phosphine is associated with the 52 ppm doublet of doublets and the 49 ppm resonance is associated with the internal phosphines on the dirhodium complex. There are additional peaks around 97 ppm and 4 ppm that are most likely an unidentified impurity.

The initial catalytic results for the cyclooctadiene dirhodium catalyst precursor material did not show great promise for hydroformylation. The catalytic runs were ran at 90°C and 110 psig based off the old catalyst conditions, however, the pressure was increased somewhat to make sure the cyclooctadienes would be replaced with hydrogen and carbonyls. Various solvents were attempted but all showed high isomerization and low turnovers overall. The runs that did have water present did perform better than without water. The best overall run was in 30%

water/acetone with the highest amount of turnovers overall and second highest L:B ratio. My initial thoughts led me to believe that this precursor was acting similar to the norbordiene species. I decided to go a different route with the precursor and find a ligand that could easily dissociate under these conditions.

Table 3.1. Hydroformylation of 1-Hexene with $[\text{Rh}_2(\text{cod})_2(\text{mixed-et,ph-P4-Ph})](\text{BF}_4)_2$

Solvents	Aldehyde Turnovers	Aldehyde L:B	Alkene Isomerization (%)	Alkane (%)
30% H ₂ O/acetone	481	13.4	24.0	0.6
DMF	93	6.0	41.8	0.3
30% H ₂ O/DMF	252	3.9	9.3	N/A
*Acetone (3hr)	30	1.9	91.8	N/A
H ₂ O	38	3.2	7.4	N/A
*30% H ₂ O/DMSO(1hr)	137	4.7	22.1	N/A
Acetonitrile	33	6.3	55.1	N/A
DMSO	100	4.8	25.3	N/A
30% H ₂ O/MeOH	284	11.8	20.4	0.85
30% H ₂ O/THF	59	31.8	35.8	N/A

Conditions: 1 mM catalyst, 1 M hexane, 90°C, 110 psig, samples were taken at 2 hours. * Samples taken at different times from other samples

3.4 Solvent-ligand Precursors

The norbordienes would polymerize and crystallize out in the old ligand dirhodium catalyst system, which eliminated it as a competing ligand during hydroformylation. I decided to look at solvent based ligands that could easily dissociate, and would not be a strong competing ligand during hydroformylation catalysis. The group had previously purchased a large amount of

[Rh(nbd)₂](BF₄). I wanted to use this rhodium starting material, but exchange the norbordienes for another ligand. I looked to use dioxane, pyridine, and acetonitrile. These solvent ligands were strong enough to bind to the rhodium and displace the norbordienes. New starting precursor materials were synthesized using the [Rh(nbd)₂](BF₄) material. The reaction involved using 70 mL of a solvent (acetonitrile, pyridine, dioxane) added to [Rh(nbd)₂](BF₄), followed by overnight reflux. The solvent the vacuum evaporated. [Rh(solvent)_x](BF₄) is dissolved in 10 mL of DCM, and the et,ph-P4-Ph ligand solution is added dropwise and allowed to stir for 10 minutes. The solution is vacuum evaporated and the solid is further dried by vacuum overnight. This was the method used to prepare all the solvent precursor materials.

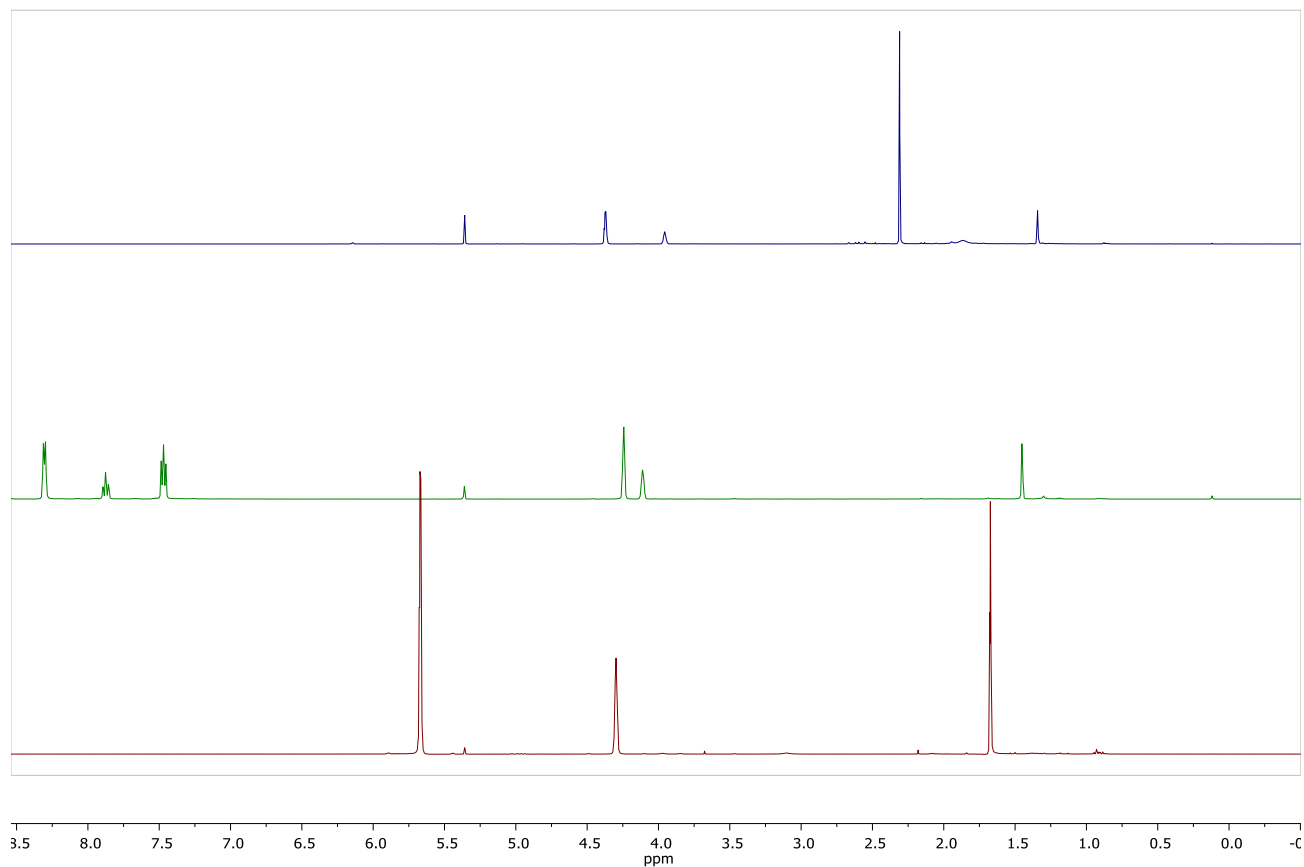


Figure 3.4. ¹H NMR of the solvent precursors in CD₂Cl₂. [Rh(nbd)₂](BF₄) (Top), [Rh(pyridine)₄](BF₄) (middle), [Rh(acetonitrile)₄](BF₄) (bottom)

The proton NMR (Figure 3.4) displays many similarities between the starting precursor complexes. There are certain differences in the spectra that indicates the norbornadiene ligand was replaced. The top spectra is the original material, $[\text{Rh}(\text{nbd})_2](\text{BF}_4)$ with a strong peak at 2.1 ppm. The exchange of the norbornadiene ligand is apparent when comparing the pyridine and acetonitrile spectra. The pyridine spectra shows the addition of pyridine by the new peaks in the 7-8 ppm range. The acetonitrile spectra shows the addition of acetonitrile with an intense peak at 1.6, 4.3, and 5.7 ppm.

The ^{31}P NMR of the catalyst precursors, $[\text{Rh}_2(\text{L})_x(\text{mixed-}i\text{et,ph-P4-Ph})](\text{BF}_4)_2$, $\text{L} = \text{nbd}$ ($x = 2$) or acetonitrile ($x = 4$), in Figure 3.4 shows overall similarities between the complexes with varying chemical shifts for each. There are two diastereomers (*racemic* and *meso*) present in the ^{31}P NMR. The *racemic* diastereomer has two pair of doublet doublets peaks (58 and 57 ppm and 52 and 51 ppm). The external phosphine arms have been assigned to 58 and 57 ppm, and the internal phosphines are assigned to 52 and 51 ppm peaks. The *meso* diastereomer also has two pair of doublet doublets with the external arms assigned to 56 and 55 ppm and the internal arms assigned to 44 and 42 ppm. The acetonitrile complex, however, does show a third set of resonances around 45 and 62 ppm that do not correspond to the nbd precursor. There are also a few other less intense peaks (e.g., 55 and 61 ppm) indicating that the acetonitrile system is

certainly more complex.

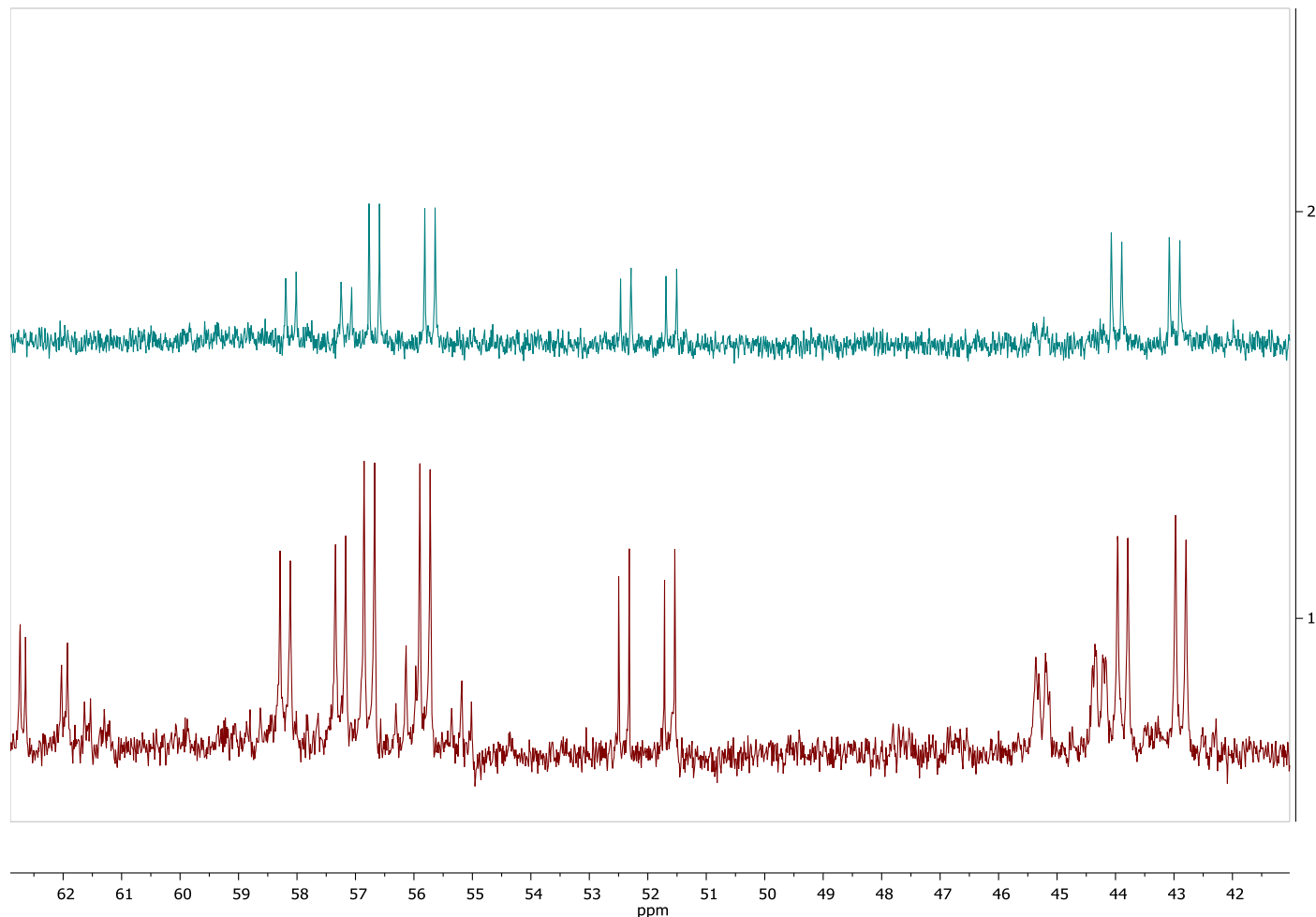


Figure 3.5. ^{31}P NMR of $\text{Rh}_2(\text{acetonitrile})_4(\text{mixed-et,ph-P4-Ph})](\text{BF}_4)_2$ (bottom) and $[\text{Rh}_2(\text{nbd})_2(\text{mixed-et,ph-Ph-Ph})](\text{BF}_4)_2$ (top) in CD_2Cl_2 .

Based off the previous results from the cod precursor complexes a 30% water/acetone solvent system was used for catalytic runs with the dioxane complexes. Running the catalytic run at 90°C and 110 psi the $[\text{Rh}_2(\text{dioxane})(\text{mix-et,ph-P4-Ph})](\text{BF}_4)_2$ catalyst precursor did 382 turnovers of aldehyde, 16.8 L:B aldehyde ratio, 4.9% alkene isomerization, and 0.5% alkene hydrogenation after 2 hours. Although the dioxane precursor showed some promise, I decided to focus on another solvent precursor due to the relatively low number of turnovers.

Staying with 30% water/acetone solvent the next catalyst precursor studied was $[\text{Rh}_2(\text{pyridine})_2(\text{mixed-et,ph-P4-Ph})](\text{BF}_4)_2$. Initially running the catalyst at the old ligand conditions, 90°C and 90 psig, revealed slower rates and higher side reactions. As the H_2/CO pressure was increased the side reactions decreased. 130 psig was found to be the optimal pressure as shown in Table 3.2, increasing the pressure further did not improve results. The pressure limit for the catalyst seems to be 150 psi as the turnovers decreased dramatically to 235 turnovers indicating that the catalyst either shifting to an open mode structure that is a very poor hydroformylation catalyst. Another possibility is that the catalyst is degrading under these more forcing conditions. The optimal pressure for this catalyst system seemed to be 130 psi. Even though these results shown great promise for the new ligand there was one more precursor to be observed.

Table 3.2. Hydroformylation of 1-Hexene using $[\text{Rh}_2(\text{pyridine})_4(\text{mixed-et,ph-P4-Ph})](\text{BF}_4)_2$ at 90°C under different H_2/CO pressures.

Pressure (psig)	Aldehyde Turnovers	Aldehyde L:B ratio	Alkene Isomerization (%)	Alkane (%)
90	562	12.2	16.5	0.7
110	371	16.4	3.3	0.5
130	635	15.8	2.3	0.6
150	235	18.1	9.6	0.3

Conditions: 1 mM catalyst, 1 M Hexene, 90°C, 30% water/acetone, results after 2 hours, except for the 90 and 110 psig runs that were sampled after 3 hrs.

The next catalyst precursor studied was $[\text{Rh}_2(\text{acetonitrile})_4(\text{mixed-et,ph-P4-Ph})](\text{BF}_4)_2$. Various solvents were tested with this precursor to study effects on hydroformylation. T-glyme and DMF were used for the hydroformylation of 1-hexene at 90°C and 110 psi with poor results: only 100 turnovers after 2 hours for both solvents with low L:B ranging from 3-5 and very high

alkene isomerization results ranging from 50-80%. Raising the H₂/CO pressure to 130 psig did not increase aldehyde turnovers with CH₂Cl₂ or 10% water/DMF solvents. Hydroformylation of 1-hexene using [Rh₂(acetonitrile)₄(*mixed*-et,ph-P4-Ph)](BF₄)₂ in DCM after 2 hours at 130 psig and 90°C only produced 114 turnovers of aldehyde, 6.4 L:B aldehyde ratio, and 83% alkene isomerization. Using 10% water/DMF was somewhat better, but still not good with 320 turnovers of aldehyde, 3.5 aldehyde L:B, and 7.7% alkene isomerization after 2 hours of reaction. The addition of water does improve the reaction by increasing the turnover number and lowering the side reactions.

The next step was to try the previous best solvent system, 30% water/acetone, with [Rh₂(acetonitrile)₄(*mixed*-et,ph-P4-Ph)](BF₄)₂. Table 3.3 shows the H₂/CO pressure effect for hydroformylation runs on 1-hexene at 90°C. The optimal pressure for the catalyst at 90°C is 110 psig giving the most turnovers (672) and the highest L:B ratio (15.1) after 2 hours of reaction. Higher pressures led to significantly poorer results.

Table 3.3. Hydroformylation of 1-Hexene using [Rh₂(acetonitrile)₄(*mixed*-et,ph-P4-Ph)](BF₄)₂ at 90°C and Various Pressures.

Pressure (psig)	Aldehyde Turnovers	Aldehyde L:B	Alkene Isomerization (%)	Alkane (%)
110	672	15.1	6.8	0.8-
130	529	11.8	9.6	N/A
150	366	11.2	10.3	N/A

Conditions: 1 mM catalyst, 1 M Hexene, 90°C, Acetone/ 30% H₂O, results after 2 hour

I decided to study which concentration of water in acetone solvent would work best with the [Rh₂(acetonitrile)₄(*mixed*-et,ph-P4-Ph)](BF₄)₂ catalyst precursor. Table 3.4 shows the pure acetone solvent hydroformylation results with those using increasing amounts of water by

volume. Comparing the concentration runs with each other it was apparent that the system with water is far superior than running it using only acetone.

Table 3.4. Hydroformylation of 1-Hexene using $[\text{Rh}_2(\text{acetonitrile})_4(\text{mixed-et,ph-P4-Ph})](\text{BF}_4)_2$ at 90°C and 130 psig 1:1 H_2/CO : Effect of Water in Acetone Solvent

Solvent	Aldehyde Turnovers	Aldehyde L:B ratio	Alkene Isomerization (%)	Alkane (%)
Acetone	202	7.7	76.4	N/A
5% $\text{H}_2\text{O}/\text{Acetone}$	539	7.1	20.0	0.7
10% $\text{H}_2\text{O}/\text{Acetone}$	622	13.3	10.1	0.8
15% $\text{H}_2\text{O}/\text{Acetone}$	830	11.1	3.4	0.8
20% $\text{H}_2\text{O}/\text{Acetone}$	745	11.9	4.8	0.8
25% $\text{H}_2\text{O}/\text{Acetone}$	774	12.4	5.2	N/A
30% $\text{H}_2\text{O}/\text{Acetone}$	529	11.8	9.6	N/A
40% $\text{H}_2\text{O}/\text{Acetone}$	732	12.9	2.3	N/A

Conditions: 1mM catalyst, 1M hexene, 90°C, 130 psig, 0.9% heptane as internal standard, all samples were taken after 2 hours of reaction.

The results from Table 3.4 demonstrate that water is important for the catalyst to hydroformylate effectively. The pure acetone results show high isomerization (76.4%) and very low aldehyde production of only 202 turnovers after 2 hours. The addition of water to the acetone solvent dramatically improved the hydroformylation of 1-hexene, especially between 15 and 25% water by volume. Some of the lower water concentration hydroformylation runs showed considerable inconsistencies. The 10% water/acetone study, for example, varied dramatically with one run giving 535 aldehyde turnovers after two hours, while another identical run produced 700 turnovers. The 15-25% water runs, however, were far more consistent and reproducible. Higher water concentration runs (30-40%) started to become inconsistent,

although the overall results still looked far better than the pure acetone runs. Above 40% water the 1-hexene solubility starts to drop off in this very polar mixed water-acetone solvent system, which negatively impacts hydroformylation.

3.5 Norbornadiene Precursor

The last catalyst precursor studied was the original new catalyst system, $[\text{Rh}_2(\text{nbd})_2(\text{mixed-et,ph-Ph-Ph})](\text{BF}_4)_2$. This catalyst precursor was prepared with fresh P4-Ph ligand and the hydroformylation of 1-hexene in 30% water/acetone at 90°C and 90 psig. After 2 hours aldehyde turnover = 548, with 13.1 L:B aldehyde ratio, and 13.5% alkene isomerization. These were considerably better results relative to that reported in Chapter 2, I decided to test the norbornadiene catalyst precursor with other conditions to get the best performance. The first reaction parameter studied was pressure. Running $[\text{Rh}_2(\text{nbd})_2(\text{mixed-et,ph-Ph-Ph})](\text{BF}_4)_2$ in 30% water/acetone at 90°C and 130 psig of 1:1 H_2/CO produced 663 turnovers of aldehyde, 8.4 L:B aldehyde ratio, and 10.7% alkene isomerization. The 130 psig H_2/CO pressure increased the number of turnovers but lowered the aldehyde L:B regioselectivity relative to the 90 psig study (8.4 vs. 13.1). Alkene isomerization decreased at the higher pressure (10.7% vs. 13.5%). Comparing this data with the 1-hexene hydroformylation studies done with the pyridine and acetonitrile dirhodium P4-Ph catalyst precursors showed similar results, which led me to believe that the exact catalyst precursor used is not particularly important for the hydroformylation of 1-hexene.

Different solvents were investigated with $[\text{Rh}_2(\text{nbd})_2(\text{mixed-et,ph-Ph-Ph})](\text{BF}_4)_2$ showing poor results as previously seen with the cod precursor (Table 3.1). The best solvent system for the nbd precursor catalyst was acetone/water. The main variable at this point was in discovering

the optimum pressure for each catalyst precursor. For example, the pyridine precursor runs better at 130 psig, but the acetonitrile complex ran much better at 110 psig in 30% water/acetone.

I decided to study the norbornadiene catalyst precursor and optimize it with regards to temperature and pressure. One reason to focus on the norbornadiene catalyst precursor is because it was better defined from a composition viewpoint. The various solvent based precursors could have different numbers of solvents associated with the catalyst precursor. Before starting the temperature and pressure study, I tested 15% and 25% water/acetone solvent mixtures for the hydroformylation of 1-hexene using $[\text{Rh}_2(\text{nbd})_2(\text{mixed-et,ph-Ph-Ph})](\text{BF}_4)_2$ at 90°C and 130 psig. The 25% water run was faster than 15% water/acetone, producing 774 turnovers of aldehyde after two hours, and having lower alkene isomerization of 8.9% compared to 15% for the 15% water/acetone study.

Table 3.5. Hydroformylation of 1-Hexene using $[\text{Rh}_2(\text{nbd})_2(\text{mixed-et,ph-P4-Ph})](\text{BF}_4)_2$ at 130 psig 1:1 H_2/CO : Effect of Temperature.

Temperature (°C)	Aldehyde Turnovers	Aldehyde L:B	Alkene Isomerization (%)	Alkane (%)
70	419	5.5	5.2	N/A
90	774	12.5	9.0	0.822
110	332	All Linear	23.8	N/A
130	0	N/A	28.7	N/A

Conditions: 1 mM catalyst, 1 M hexene, 130 psig, 0.9% heptane as internal standard, solvent: 25% water/acetone, samples were taken after 2 hours except for the 130°C run, which was sampled after 1 hour due to the poor results.

After choosing the 25% water/acetone solvent system, I experimented with different temperature conditions as shown in Table 3.5. The old ligand-catalyst optimal temperature conditions were always ran at 90°C. I had never tried different temperature conditions before, but I wanted to see what temperature worked best for the new ligand-catalyst. 90°C was found to be

the best temperature for the new dirhodium-P4-Ph catalyst. At 70°C, the results revealed that hydroformylation did occur, but at a slower rate and with lower L:B aldehyde regioselectivity. The 110°C run showed clear signs of catalyst degradation over the course of 2 hours with low turnovers and high alkene isomerization, and significant darkening of the red catalyst solution at the end of the run. At 130°C, the catalyst appeared to degrade immediately as no hydroformylation was observed, and after just one hour the color of the catalyst was a very dark red.

Table 3.6. Hydroformylation of 1-Hexene using $[\text{Rh}_2(\text{nbd})_2(\text{mixed-et,ph-P4-Ph})](\text{BF}_4)_2$ at 90°C: Effect of H_2/CO Pressure.

H_2/CO Pressure (psig)	Aldehyde Turnovers	Aldehyde L:B ratio	Alkene Isomerization (%)	Alkane (%)
70	611	14.1	12.7	0.9
90	686	16.0	7.5	0.9
110	408	14.1	17.5	0.9
130	774	12.5	9.0	0.8
150	881	10.4	5.5	0.8
200	713	8.0	11.7	N/A

Conditions: 1 mM catalyst, 1 M hexene, 90 °C, 0.9% heptane as internal standard, solvent: 25% water/acetone, all samples were taken after 2 hours of reaction.

Once the temperature experiments were concluded, and 90°C was observed to be the best temperature to run the new ligand catalyst, I studied different H_2/CO pressures with the $[\text{Rh}_2(\text{nbd})_2(\text{mixed-et,ph-Ph-Ph})](\text{BF}_4)_2$. In table 3.6, the turnovers increase as the pressure increased, however, 200 psi may be the catalyst highest limit before the pressure destroys the catalyst. It is noted at 110 psig the aldehyde turnovers were significantly lower than any other

pressures. At 150 psig the catalyst ran the fastest. . The L:B selectivity drops as the pressure increases above 90 psig.

The three best catalyst precursors were: $[\text{Rh}_2(\text{pyridine})_2(\text{mixed-}i\text{et,ph-P4-Ph})](\text{BF}_4)_2$, $[\text{Rh}_2(\text{acetonitrile})_4(\text{mixed-}i\text{et,ph-P4-Ph})](\text{BF}_4)_2$, and $[\text{Rh}_2(\text{nbd})_2(\text{mixed-}i\text{et,ph-Ph-Ph})](\text{BF}_4)_2$, but all were approximately comparable for the hydroformylation of 1-hexene under a similar set of conditions. The $[\text{Rh}_2(\text{pyridine})_2(\text{mix-}i\text{et,ph-P4-Ph})](\text{BF}_4)_2$ showed promise running at 90°C and 130 psig in a 30% water/acetone solvent system producing the lowest side reactions (2% alkene isomerization) and highest L:B ratio (15.8), however, it did have the lowest hydroformylation rate after 2 hours with 635 turnovers. The next two catalysts, the acetonitrile and nbd precursors, had similar results after optimizing their reaction conditions. The main difference between the two involved pressure with the nbd catalyst precursor having no clear-cut pressure dependence between 90 and 200 psig. The nbd precursors best run was at 90°C and 150 psig in a 25% water/acetone solvent system. It produced 881 turnovers of aldehyde, a L:B ratio of 10.4, 5.5% alkene isomerization, and 0.8% hydrogenation. This can be compared to the acetonitrile complex that produced 830 turnovers, 11.1 aldehyde L:B ratio, 3.4% isomerization, and 0.8 hydrogenation at 90°C and 130 psig in 15% water/acetone.

3.6 Racemic vs. Meso

The acetonitrile and nbd precursor catalyst were chosen to test the two different diastereomers because of the similarity in results conducted with the mixed ligand for the 1-hexene hydroformylation experiments. The *racemic* old ligand-based dirhodium catalyst was far superior to the *meso* diastereomer. I freshly separated both P4-Ph ligand diastereomers from each

other and made the dirhodium new ligand catalyst with both for testing.

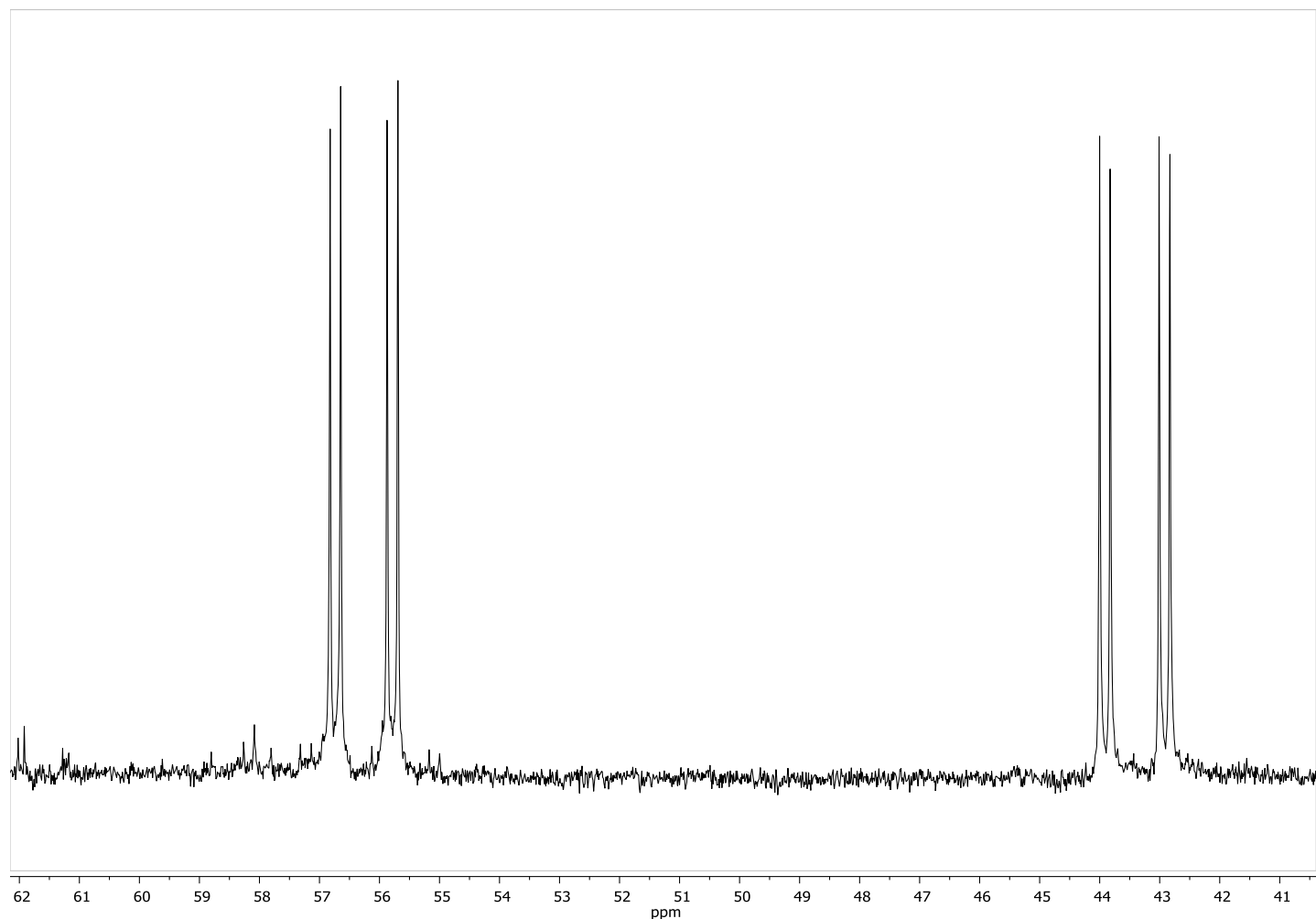


Figure 3.6. ^{31}P NMR of $[\text{Rh}_2(\text{nbd})_2(\text{meso-et,ph-Ph-Ph})](\text{BF}_4)_2$ in CD_2Cl_2 .

The $[\text{Rh}_2(\text{nbd})_2(\text{meso-et,ph-Ph-Ph})](\text{BF}_4)_2$ ^{31}P NMR displays a two pair of doublet doublets at 56 and 55 ppm and 44 and 43 ppm. The external phosphines are assigned to the 56 and 55 ppm peaks and internal phosphines are assigned to the 44 and 43 ppm peaks. The NMR for the *meso* complex appears to be quite pure, but the *racemic* catalyst, $[\text{Rh}_2(\text{acetonitrile})_4(\text{rac-et,ph-Ph-Ph})](\text{BF}_4)_2$, seems to have *meso* impurities on the complex. The separation column may not have separated the two diastereomers leading to an impure-*racemic* ligand collected. Observed in the ^{31}P NMR for the $[\text{Rh}_2(\text{acetonitrile})_4(\text{rac-et,ph-Ph-Ph})](\text{BF}_4)_2$ the external

phosphine has been associated to the 58 and 57 ppm peaks and the internal phosphines associated to the 52 and 51 ppm peaks. The *racemic* is the dominant diastereomer present, but there are *meso* impurities in the complex at 57, 56, 45, and 44 ppm. The *racemic* complexes that were made are not completely pure and will be referred to as the *impure-racemic*.

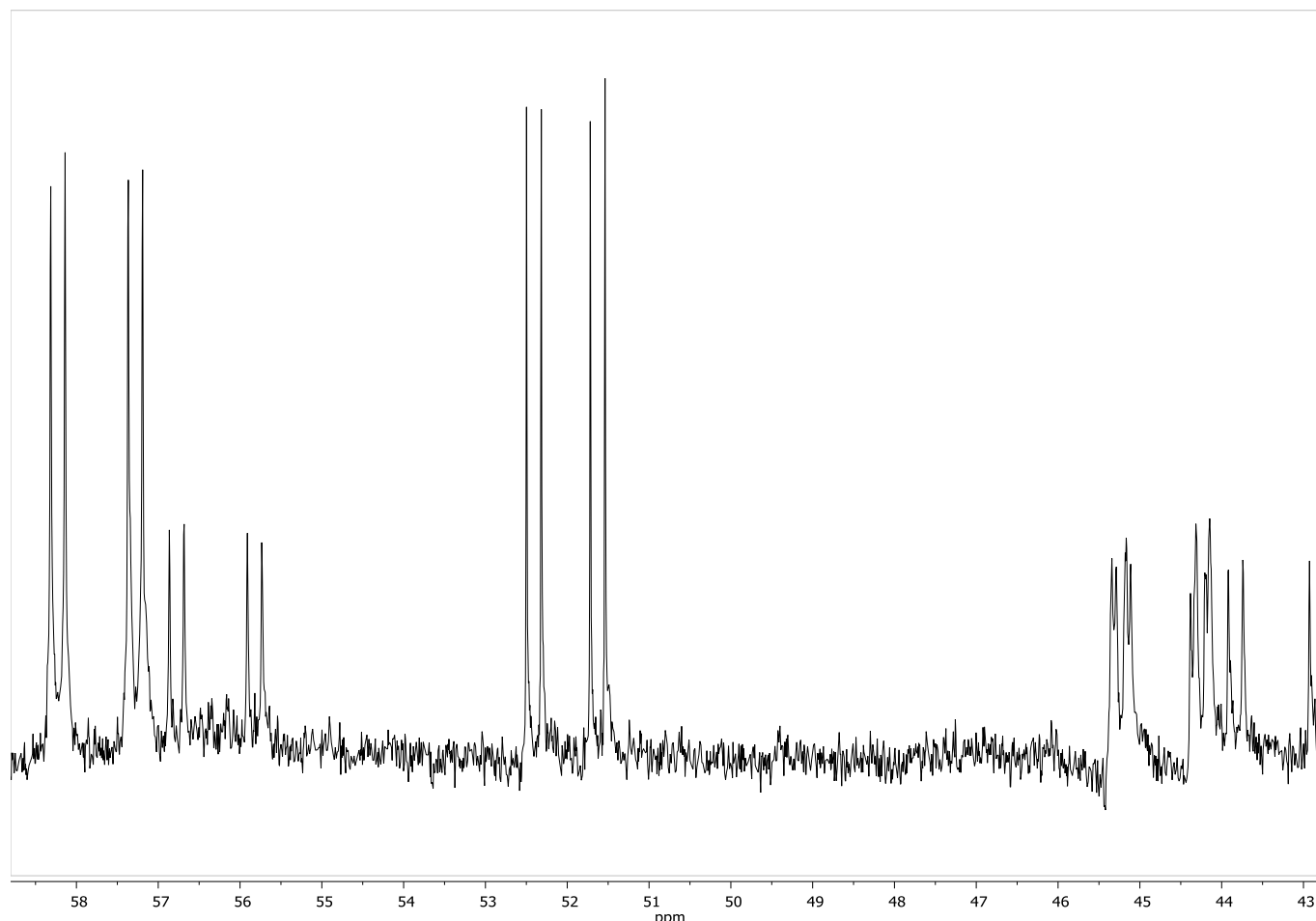


Figure 3.7. ^{31}P NMR of $[\text{Rh}_2(\text{acetonitrile})_4(\text{rac-et,ph-Ph-Ph})](\text{BF}_4)_2$ in CD_2Cl_2 .

The catalytic data displays a significant difference between the two diastereomers. The *meso* catalyst precursor generates a very poor hydroformylation catalyst. Running $[\text{Rh}_2(\text{nbd})_2(\text{meso-et,ph-Ph-Ph})](\text{BF}_4)_2$ in 25% water/acetone solvent mixture at 90°C and 90 psig with 1-hexene did not produce any aldehyde, but did 28.3% alkene isomerization. I decided to

run at a higher pressure to see if that would provide better hydroformylation results for the *meso* catalyst. Using the same solvent and temperature, the H₂/CO pressure was raised to 150 psig and after two hours the isomerization was 21% and 90 turnovers of aldehyde (all linear) were produced. Similar results were the obtained using [Rh₂(acetonitrile)₄(*meso*-et,ph-Ph-Ph)](BF₄)₂ with little turnovers produced (54 turnovers) and high isomerization percentage (39%). The *meso* diastereomer results indicate that it is a terrible hydroformylation catalyst and the main contribution to the *mixed* ligand-dirhodium results is increased alkene isomerization. The *racemic* diastereomer, therefore, must be the active diastereomer during the hydroformylation process based on the very poor results from the *meso* diastereomeric catalyst precursor.

Observing the catalytic data from running the [Rh₂(nbd)₂(*mixed*-et,ph-Ph-Ph)](BF₄)₂ and [Rh₂(nbd)₂(*meso*-et,ph-Ph-Ph)](BF₄)₂ indicated that the *racemic* catalyst was the active catalyst. I ran the catalyst in different solvents to see if reactivity would change with just the *racemic* catalyst. Running the [Rh₂(acetonitrile)₄(*racemic*-et,ph-P4-Ph)](BF₄)₂ catalyst in different solvent systems demonstrated similar results to the *mixed* ligand catalyst. At 90°C and 110 psig in pure acetone displayed alkene isomerization of 76%, hydrogenation of 0.6%, L:B of 8.7, and 201 aldehyde turnovers after two hours. There was also poor results when the catalyst was ran in 30% H₂O/acetonitrile, 30% H₂O/DMF, and 30% H₂O/t-glyme with high isomerization and low turnover number.

Running the impure-*racemic* ligand in different solvents displayed the same activity rates as the *mixed*, and the optimal temperature of 90°C was also the same as the *mixed* ligand. Acetophenone/water was one other solvent system that worked almost as well as acetone/water. After 2 hours in 30% H₂O/acetophenone at 90°C and 110 psi produced 697 aldehyde turnovers,

L:B of 14.0, isomerization of 14%, and hydrogenation of 1.27%. The pressure does have an impact on the catalyst turnover rate. As the pressure increases the turnovers increase.

Table 3.7. Hydroformylation of 1-Hexene using $[\text{Rh}_2(\text{acetonitrile})_4(\text{rac-}et,\text{ph-P4-Ph})](\text{BF}_4)_2$ at 90°C: Effect of H_2/CO Pressure.

H_2/CO Pressure (psig)	Aldehyde Turnovers	Aldehyde L:B ratio	Alkene Isomerization (%)	Alkane (%)
90	414	15.5	17.0	0.7
110	660	15.2	12.3	0.9
130	687	13.2	11.9	0.8

Conditions: 1mM catalyst, 1M hexene, 90 °C, solvent: 30% water/Acetone, all samples were taken at 2 hours

Overall the $[\text{Rh}_2(\text{acetonitrile})_4(\text{rac-}et,\text{ph-P4-Ph})](\text{BF}_4)_2$ did not show any signs of being a better catalyst than the *mixed* ligand because the *racemic* may not be pure enough. The *meso* diastereomer has shown to favor isomerization and display poor hydroformylation results. The interference with the *meso* diastereomer would be reason for the similar results to the mixed catalyst precursors. I believe the results of the *racemic* cannot improve with the current separation method. The separation column is most likely destroying the *racemic* ligand over time in DCM and it is not providing clean separation for the two diastereomers. The new ligand catalyst precursors do not want to crystalize, which could also be impacting the purity and catalytic results, especially for the *racemic* diastereomer.

3.7 Stability of the New ligand Catalyst

The lifetime experiment was to increase the amount of turnovers possible to test for the stability of the dirhodium catalyst system. Instead of using 1000 equivalents of 1-hexene the amount was increased to 10,000 equivalents. If the $\text{Rh}_2\text{-P4-Ph}$ catalyst has good stability it

should be able to convert more alkene to aldehyde over time. Initially I attempted the higher turnover runs at 90°C and 90 psi with soaking the catalyst at 45 psi using the old ligand soaking methods. I also decided to start with 5,000 equivalents of alkene.

After two hours the $[\text{Rh}_2(\text{nbd})_2(\text{mixed-et,ph-Ph-Ph})](\text{BF}_4)_2$ produced no aldehyde or isomers. I attempted to run it again using less alkene for a possible max of 3600 turnovers. I had been using the best solvent system in 25% water/acetone for all the runs. I was using lower amounts of catalyst precursor relative to the amount of alkene to increase the number of possible aldehyde turnovers. Lower catalyst concentrations are more susceptible to deactivation reactions and reactions with impurities. After 25 hours it produced 424 aldehyde turnovers, 79% alkene isomerization, and only produced linear aldehydes. The lifetime experiment was conducted again using 2100 equivalents of alkene in 25% water/acetone at 90 psig and 90°C. After 20 hours it produced 691 aldehyde turnovers, 10.7 L:B aldehyde ratio, 45% alkene isomerization, 0.8 hydrogenation. At the end of the run I noticed the material was a much darker red. These runs indicate that the $\text{Rh}_2\text{-P4-Ph}$ catalyst system is degrading under the conditions used for these higher turnover catalytic studies.

The new ligand, et,ph-P4-Ph, was designed to increase longevity and expand overall lifetime of the dirhodium catalyst via the much stronger chelate effect. The old ligand would degrade over time forming two inactive species: monometallic $[\text{RhH}_2(\kappa^4\text{-P4})]^+$, and a double-ligand species, $[\text{Rh}_2\text{H}_2(\text{P4})_2]^{2+}$ (see Figure 2.7). A simple catalyst stability test is to let it sit under H_2/CO at reaction conditions for some period of time without any alkene present, then testing it for hydroformylation activity. All monometallic rhodium-phosphine or phosphite-based catalysts with P-Ph, P-benzyl, or P-OR linkages will decompose within 24 hours under H_2/CO reaction conditions via rhodium-induced phosphine ligand fragmentation reactions. Unsaturated

rhodium centers are quite active at doing P-Ph, P-benzyl, or P-OR oxidative addition reactions to form phosphide-bridged rhodium dimers and clusters that are poor hydroformylation catalysts .

3,4

The problem with the old $[\text{Rh}_2(\text{P4})]^{2+}$ catalyst system was a too-weak chelate effect that led to loss of one of the rhodium centers and loss of bimetallic cooperativity. The old P4 tetraphosphine ligand had phosphine centers that were either fully alkylated (the terminal phosphines) or had two alkyl groups and only one phenyl group (the internal phosphines). Phosphines with three alkyl groups or two alkyl groups and one phenyl group are very resistant to rhodium-induced phosphine oxidative addition reactions. Indeed, despite thousands of hydroformylation runs with the old $[\text{Rh}_2(\text{P4})]^{2+}$ catalyst system under a wide variety of conditions no sign of rhodium-induced P4-fragmentation reactions have been observed unless the temperature was raised above 150°C.

The new P4-Ph tetraphosphine ligand, however, has internal phosphines with two P-aryl bonds and only one alkyl group (the central methylene bridge). These are considerably more reactive towards P-aryl group cleavage reactions. Prof. Stanley didn't think this would be a major problem for the new P4-Ph ligand, but the current studies clearly point to serious catalyst degradation reactions.

For example, $[\text{Rh}_2(\text{nbd})_2(\text{mixed-et,ph-Ph-Ph})](\text{BF}_4)_2$ was used to test the stability of the new ligand. The catalyst precursor was activated and soaked at 45 psig of 1:1 H_2/CO at 60°C for two hours in 25% water/acetone. 1000 equivalents of 1-hexene was pressure injected at this point to initiate hydroformation and after 2 hours the results revealed 256 turnovers of aldehyde, 20% alkene isomerization, and only linear aldehydes were produced. The hydroformylation activity has definitely decreased with an increase in side reactions. The L:B ratio was the highest

recorded with the new ligand catalyst. A second study was done by soaking $[\text{Rh}_2(\text{nbd})_2(\text{mixed-et,ph-Ph-Ph})](\text{BF}_4)_2$ for 80 minutes at 90°C and 90 psig. 1000 equivalents of 1-hexene was pressure injected and after two hours of reaction only 140 turnovers of aldehyde were produced as all linear aldehyde, and 15.7% alkene isomerization. We do not have an explanation for the production of all linear aldehyde, but the rate of hydroformylation and alkene isomerization side reactions point to serious degradation of the dirhodium catalyst.

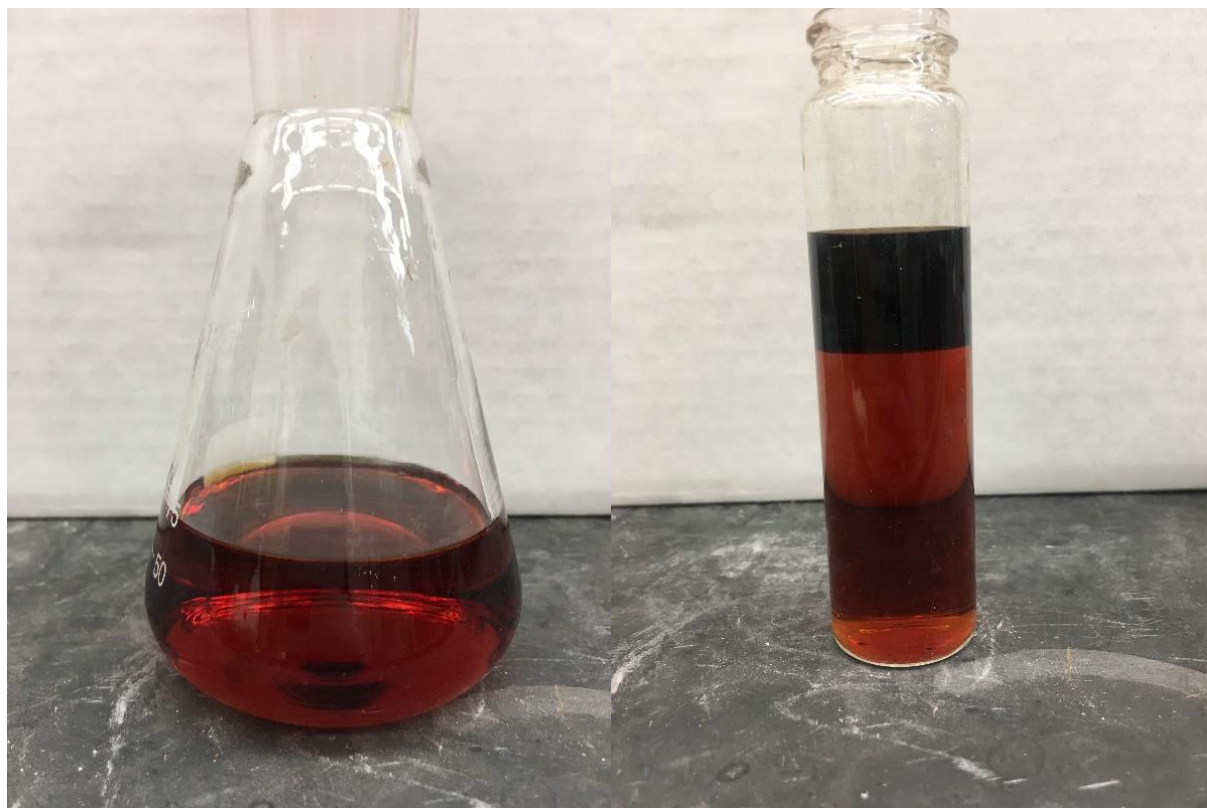


Figure 3.8. Catalyst degradation after soaking for 2 hours at 90°C and 90 psig before reaction (left) and after reaction (right) Aldehyde layer is on top with higher concentration of catalyst, and water/acetone layer on bottom.

These results indicate the catalyst is dying during the hydroformylation reaction. In figure 3.8 the catalyst is almost black compared to the reddish color it was before, and majority of the catalyst is in the top layer which is composed of aldehyde. The bottom layer was the solvent that

does have some catalyst in it as well. Both of the H₂/CO soaking runs lead to degradation of the new ligand, based on the lower amounts of hydroformylation and increased side reactions observed.

The new catalyst degrades in a different manner compared to the old catalyst. As mentioned previously the old catalyst degrades by losing a rhodium center and forming two inactive complexes. This fragmentation reaction occurs in acetone and in water/acetone at a slower rate. In water/acetone, the old catalyst displayed a better lifetime due to the cationic charges on the rhodium centers. The dicationic species was present in acetone, but in water/acetone the old catalyst transforms to a monocationic species. The old dicationic catalyst demonstrated high hydroformylation activity and regioselectivity in water/acetone.

The dicationic species has an Rh (2+) metal center that promotes metal-ligand bond weakening effects. The ligand weakening effects can be good for carbonyls which can speed the hydroformylation reaction, but this can also lead to weaker Rh-P bonding forming inactive species. In water/acetone the dicationic catalyst is deprotonated by water to form the monocationic species. The pH of the catalyst in water/acetone is 2.2 similar to a strong monoprotic acid species. This monocationic species was less prone to fragmentation reactions, but less active than the dicationic species. The rhodium centers for the monocationic species were less active because of the stronger Rh-CO π -backbonding causing alkene addition to occur at a slower rate. It is more resistant to fragmentation reactions which increases the concentration of the catalyst leading to an overall higher hydroformylation activity.

3.8 References

1. Broussard, M. E.; Juma, B.; Train, S. G.; Peng, W.-J.; Laneman, S. A.; Stanley, G. G., A Bimetallic Hydroformylation Catalyst: High Regioselectivity and Reactivity Through Homobimetallic Cooperativity. *Science* 1993, 260 (5115), 1784-1788.
2. Kalachnikova, K . Improved Synthesis, Separation, Transition Metal Coordination and Reaction Chemistry of a New Binucleating Tetrphosphine Ligand. Ph.D. Dissertation, Louisiana State University, Baton Rouge, LA, 2014.
3. A. G. Abatjoglou, D. R. Bryant, Mechanism of rhodium-promoted triphenylphosphine reactions in hydroformylation processes. *Organometallics* 3, 923-926 (1984)
4. A. G. Abatjoglou, D. R. Bryant, Aryl group interchange between triarylphosphines catalyzed by group 8 transition metals. *Organometallics* 3, 932-934 (1984)

Chapter 4: Characterization of the New Ligand Catalyst

4.1 NMR Studies of the Dirhodium Catalyst Based on et,ph-P4

Characterization of the dirhodium catalyst based on the old tetraphosphine ligand, et,ph-P4, took the Stanley group a considerable amount of time to understand the nature of the catalyst. The dirhodium catalyst was initially proposed in the 1993 *Science* paper to be a neutral complex. FT-IR studies helped demonstrate that the actual dirhodium catalyst was dicationic with Rh(II) oxidation state centers. The 1996 *Angew. Chemie* paper proposed a catalyst structure of $[\text{Rh}_2\text{H}_2(\mu\text{-CO})_2(\text{CO})_x(\text{rac-et,ph-P4})]^{2+}$, $x = 2\text{-}4$. The Stanley group started using high-pressure ^1H and ^{31}P NMR around this time to study the catalyst. The high pressure NMR experiments used a commercial Wilmad thick-walled NMR tube that can withstand pressures up to 300 psig.

Using high-pressure NMR led to the discovery of the inactive hydroformylation complexes that appear from the old P4 ligand dirhodium complex in acetone.

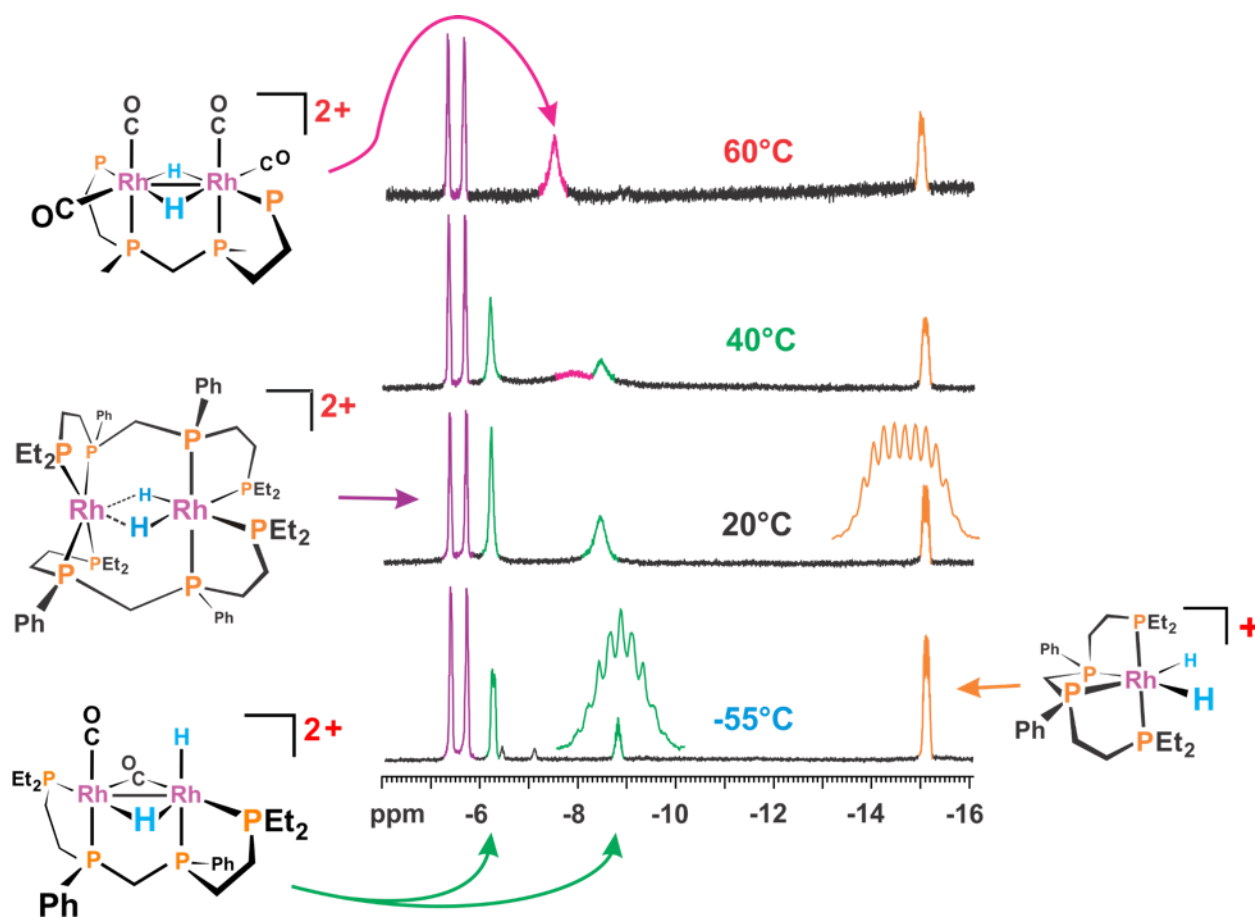


Figure 4.1. ^1H NMR of the hydride region of the mixture of complexes formed when $[\text{Rh}_2(\text{nbd})_2(\text{rac-}\text{et,ph-P4})]^{2+}$ is put under 200 psig of H_2/CO in d_6 -acetone.

At low temperatures hydride peaks were observed at -5.6 ppm, -6.3 ppm, -8.8 ppm, and -15.2 ppm; and combined with ^1H and ^{31}P COSY NMR experiments led to the identification of the various rhodium species. In figure 4.1, the -5.6 ppm and -15.2 ppm hydride peaks are assigned to the two inactive hydroformylation species: the double-ligand complex, $[\text{Rh}_2\text{H}_2(\text{rac-}\text{et,ph-P4})_2]^{2+}$, and monometallic dihydride complex, $[\text{RhH}_2(\text{rac-}\text{et,ph-P4})]^+$. These two inactive species are formed from the fragmentation of the old ligand dirhodium catalyst, $[\text{Rh}_2(\mu\text{-H})_2(\text{CO})_4(\text{rac-}\text{et,ph-P4})]^{2+}$, which leads to these two products that are inactive for hydroformylation. The double-ligand dirhodium complex is believed to be active for alkene isomerization and hydrogenation. The -6.3 ppm and -8.8 ppm peaks are associated with the

dirhodium catalyst with a bridging hydride and carbonyl, $[\text{Rh}_2\text{H}(\mu\text{-H})(\mu\text{-CO})(\text{rac-et,ph-P4})]^{2+}$. The bridging hydride is the -8.8 ppm peak which is coupled with two rhodium centers, three to four phosphines, and a hydride – all with approximately the same coupling constants producing a pseudo-nonet pattern. The terminal hydride is the unresolved peak at -6.3 ppm due to exchange reactions. As the temperature increased the two peaks associated with $[\text{Rh}_2(\mu\text{-H})(\mu\text{-CO})(\text{CO})_4(\text{rac-et,ph-P4})]^{2+}$ catalyst disappear and coalesce at 60°C into broad peak at -7.5 ppm, which is assigned to the active catalyst with two bridging hydrides, $[\text{Rh}_2(\mu\text{-H})_2(\text{CO})_x(\text{rac-P4})]^{2+}$, $x = 2\text{-}4$. Extensive DFT calculations by Dr. Ranelka Fernando pointed us to the complex with two bridging hydrides as the key catalyst species that reacts with alkene to start the hydroformylation cycle.

The stability of the old ligand catalyst was a significant problem. Bridges and Aubrey, unexpectedly helped solve the stability problem by using a very polar solvent system to phase separate the dicationic dirhodium P4 catalyst from the aldehyde product. Separating catalyst from product is a common problem for homogeneous catalysts. They added water to acetone to form a very polar solvent system, which should separate the less polar aldehyde product from the dicationic catalyst that should stay in the water-acetone solvent. Although the aldehyde did phase separate, the catalyst, unfortunately, was more soluble in the aldehyde instead of the water-acetone solvent. Unexpectedly a significant increase in turnover frequency (TOF), better L:B aldehyde regioselectivity, and a decrease in side products was observed.²

The Stanley group needed another 10 years of studies before the reason for the dramatic improvement of the dirhodium-P4 catalyst in water-acetone solvent was figured out. The addition of water leads to proton dissociation from the dicationic dihydride catalyst to generate a monocationic monohydride dirhodium system, $[\text{Rh}_2(\mu\text{-H})(\text{CO})_2(\text{rac-et,ph-P4})]^+$. This complex

was less active on a per-molecule basis relative to the dicationic $[\text{Rh}_2(\text{P4})]^{2+}$ catalyst, but deactivated far more slowly than the dicatonic catalyst. Thus, there was considerably more of the less active monocationic dirhodium catalyst, which yielded better overall TOFs for hydroformylation. The rhodium centers in the monocationic catalyst are more electron rich causing the carbonyl ligands to bind more strongly to the metal centers making it less active relative to the dicationic dirhodium catalyst. However, for the monocationic dirhodium catalyst also has stronger phosphine coordination and less chelate arm dissociation, which leads to loss of a rhodium center in the dicationic catalyst and deactivation. Overall the amount of active monocationic catalyst increased even though the monocationic monohydride species is not as active.

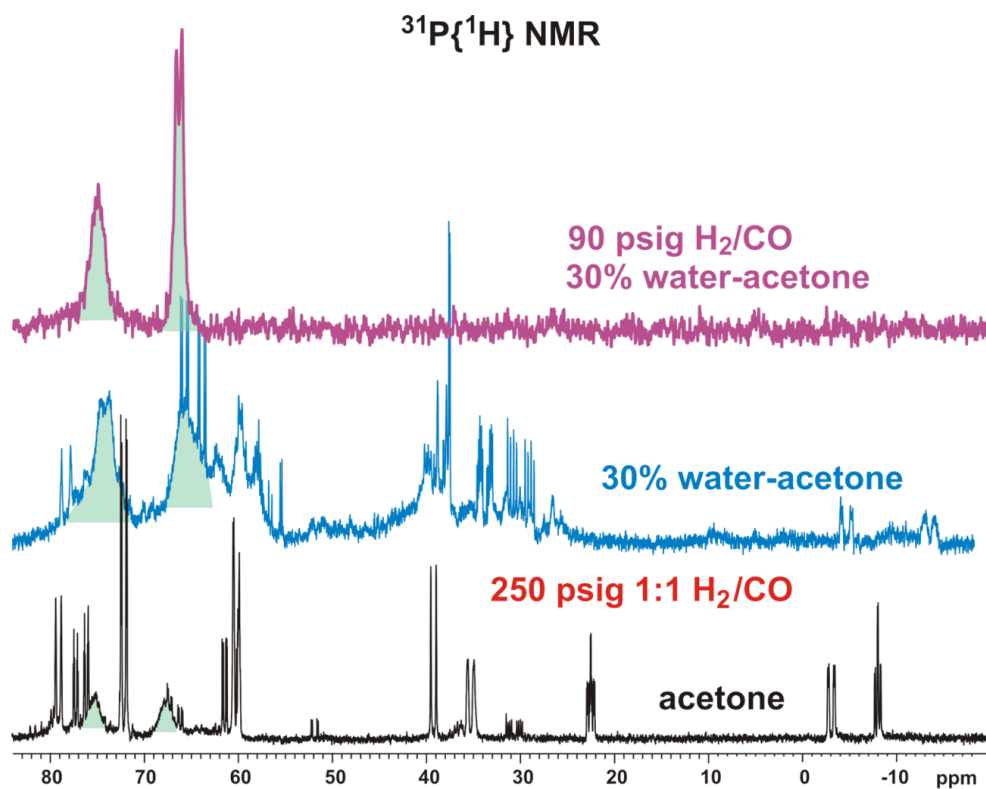


Figure 4.2. ^{31}P NMR spectrum of $[\text{Rh}_2(\text{nbd})_2(\text{rac-}\text{et,ph-P4})]^{2+}$ in acetone and acetone/water at room temperature under two sets of H_2/CO pressure.

In figure 4.2, the shaded green region is associated with the active hydroformylation catalyst. The acetone spectra has peaks at 77, 61, 23 ppm and -8 ppm assigned to the double ligand inactive species, but in the 30% water/acetone spectra these peaks are not present.³ The green shaded region representing active catalyst in water/acetone has a much large area corresponding to higher amounts of active catalyst. There are quite a few other very sharp ³¹P resonances present in the water/acetone spectrum at 250 psig that we have not assigned. This indicates that there is still some catalyst fragmentation/deactivation occurring, but much slower than for the dicationic catalyst in acetone. But lowering the pressure to 90 psig (temperature = 60°C) generates a very clean ³¹P NMR showing only active catalyst in water/acetone shown on top in Figure 4.2. The catalyst spectrum in acetone demonstrates the same fragmentation and complexity at 90 psig H₂/CO as it does at 250 psig.

Dr. Darina Polakova, ran the old ligand dirhodium catalyst in water/acetone showing signs of only one major hydride catalyst (Figure 4.3) instead of the more complex mixture of active and inactive hydride complexes in acetone (see Figure 4.1). The -9.5 ppm peak in the acetone spectra had been associated with the terminal hydride on the catalyst, however, it is missing in the acetone/water spectra.⁴ These studies lead to speculate the catalyst maybe monohydride species when in water/acetone. After studying the old ligand with various NMR experiments the new ligand was observed using NMR.

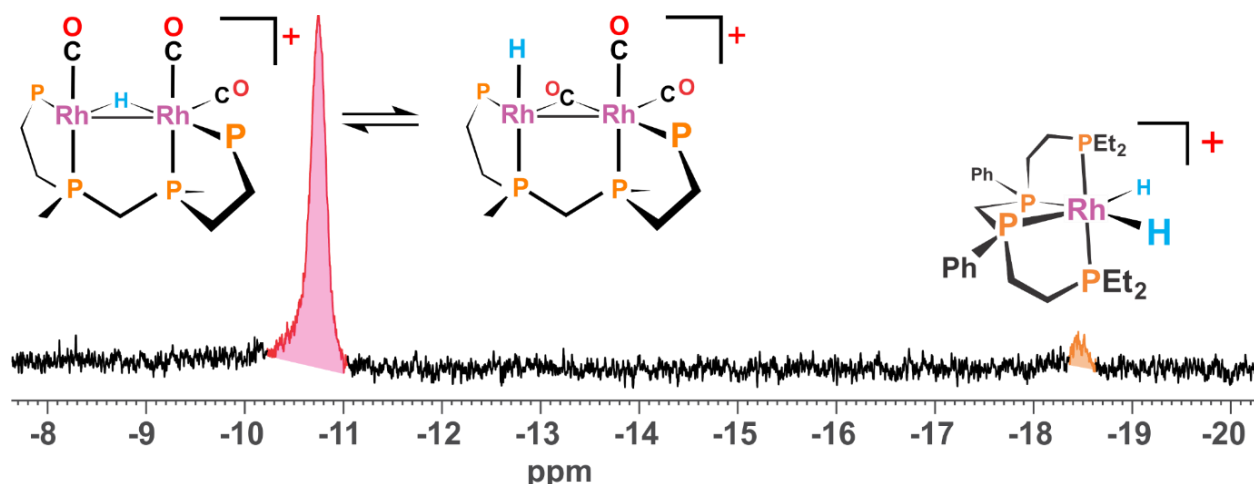


Figure 4.3. ^1H NMR of the hydride region of $[\text{Rh}_2(\text{nbd})_2(\text{rac-P4})](\text{BF}_4)_2$ in 30% water/acetone- d_6 solvent at 90 psig H_2/CO and 60°C . The major hydride resonance at -10.7 ppm represents a dynamic equilibrium between the terminal hydride and bridging hydride monocationic dirhodium catalyst species shown. A small amount of inactive monometallic $[\text{RhH}_2(\text{rac-P4})]^+$ is present at -18.5 ppm. No double-ligand dirhodium complex, $[\text{Rh}_2\text{H}_2(\text{rac-P4})_2]^{2+}$, is seen.

4.2 NMR Studies on New et,ph-P4-Ph Dirhodium Catalyst

Once the new P4-Ph ligand was developed Dr. Marshall Moulis ran many NMR experiments to study this system. The design and purpose for the new ligand was to increase stability and avoid fragmentation to inactive species. Figure 4.4 shows after one week in acetone and under 120 psig pressure the new catalyst appears to be relatively in the same condition. The peaks in the 0 ppm to -30 ppm range were caused by the reaction of PF_6^- anions with the catalyst and acetone- d_6 to produce PO_2F_2^- anions, free fluoride, and unidentified organic products from the acetone. There are other sharp ^{31}P resonances that appear in the 10-80 ppm region that do indicate catalyst fragmentation and ligand decomposition. For example, the sharp resonance in the top spectrum at 52 ppm doesn't show any rhodium or phosphorus coupling. This points to a monophosphine (or phosphine oxide) formed from the rhodium-induced fragmentation of the P4-Ph ligand.

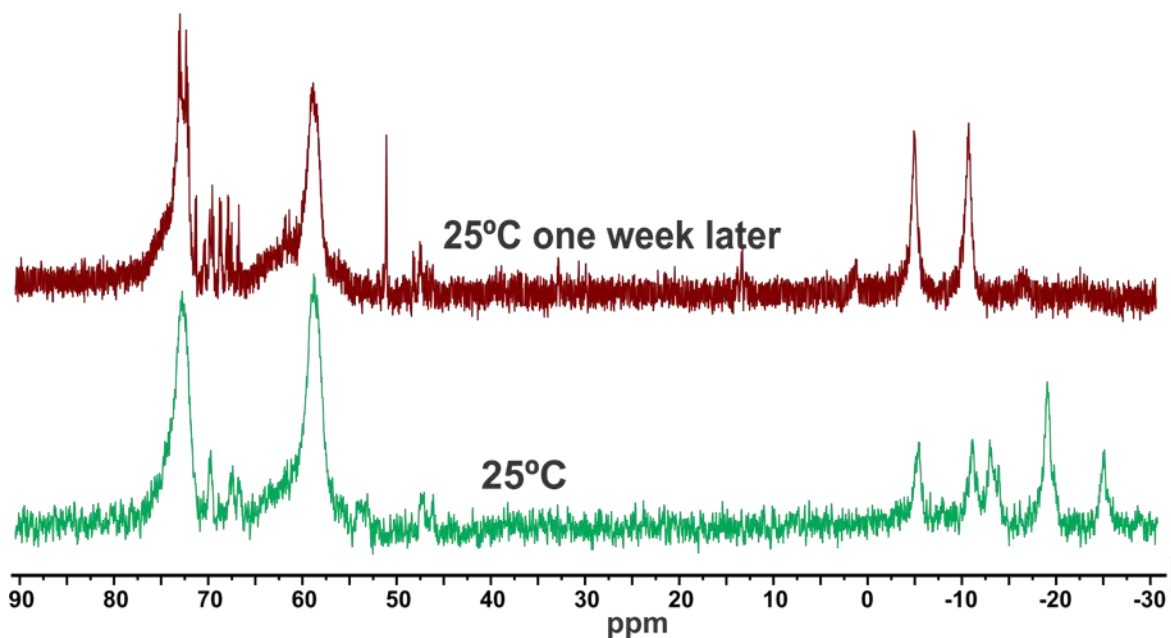


Figure 4.4. ^{31}P NMR of $[\text{Rh}_2(\text{nbd})_2(\text{rac-et,ph-P4-Ph})](\text{PF}_6)_2$ in d_6 -actone under 120 psi H_2/CO .

Further investigations into the new ligand dirhodium catalyst involved high pressure ^{31}P and ^1H NMR of the $[\text{Rh}_2(\text{nbd})_2(\text{rac-et,ph-P4-Ph})](\text{BF}_4)_2$ complex. Variable Temperature NMR experiments were carried out. The hydride region of ^1H NMR for bridging or terminal hydrides was studied as well as the ^{31}P NMR with the temperature increasing from -50°C to 90°C under

120 psig H₂/CO.

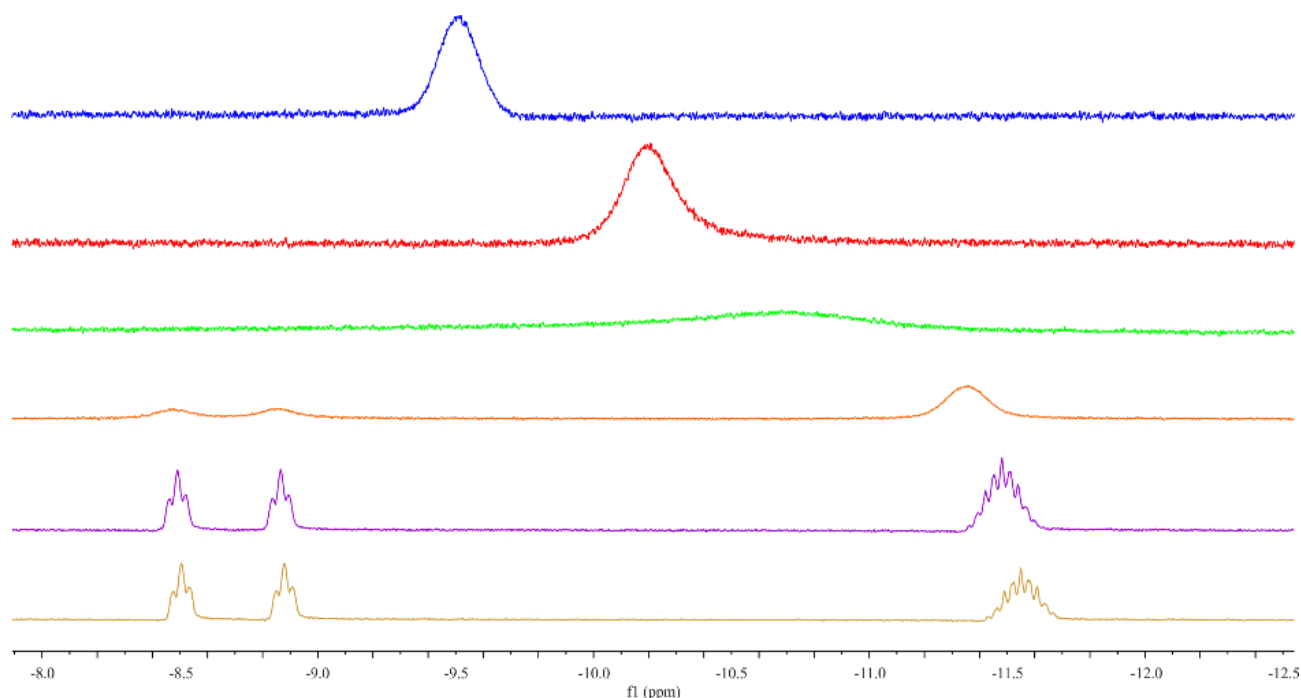


Figure 4.5. ¹H NMR of the hydride region for Rh₂(nbd)₂(*rac*-et,ph-P4-Ph)](BF₄)₂ at –50 °C, –30 °C, 0 °C, 30 °C, 60 °C, and 90 °C (from bottom to top) in DMF- d₇.

The ¹H NMR in Figure 4.5 displays the hydride region for the catalyst.⁵ The –50 °C spectrum shows a doublet of triplets at –8.7 ppm and a triplet of quartets (pseudo-nonet) at –11.6 ppm. The –8.7 ppm peak is assigned as a terminal hydride, and the –11.6 ppm peak as a bridging hydride. This corresponds to the catalyst [Rh(μ-H)(μ-CO)(H)(CO)_x(*rac*-P4-Ph)]²⁺, x = 2-4. As the temperature increases the separate hydride peaks exchange and coalesce to form a single broad hydride resonance at 60 °C located at –10.2 ppm, which shifts to –9.5 ppm at 90 °C. The broad peak at 90 °C is assigned to a bridging dihydride complex, [Rh₂(μ-H)₂(CO)_x(*rac*-P4-Ph)]²⁺, x = 2-4. These species and hydride behavior corresponds to the complexes assigned for the old P4-based dirhodium catalyst – only without the double-ligand and monometallic species formed from fragmentation of the catalyst.

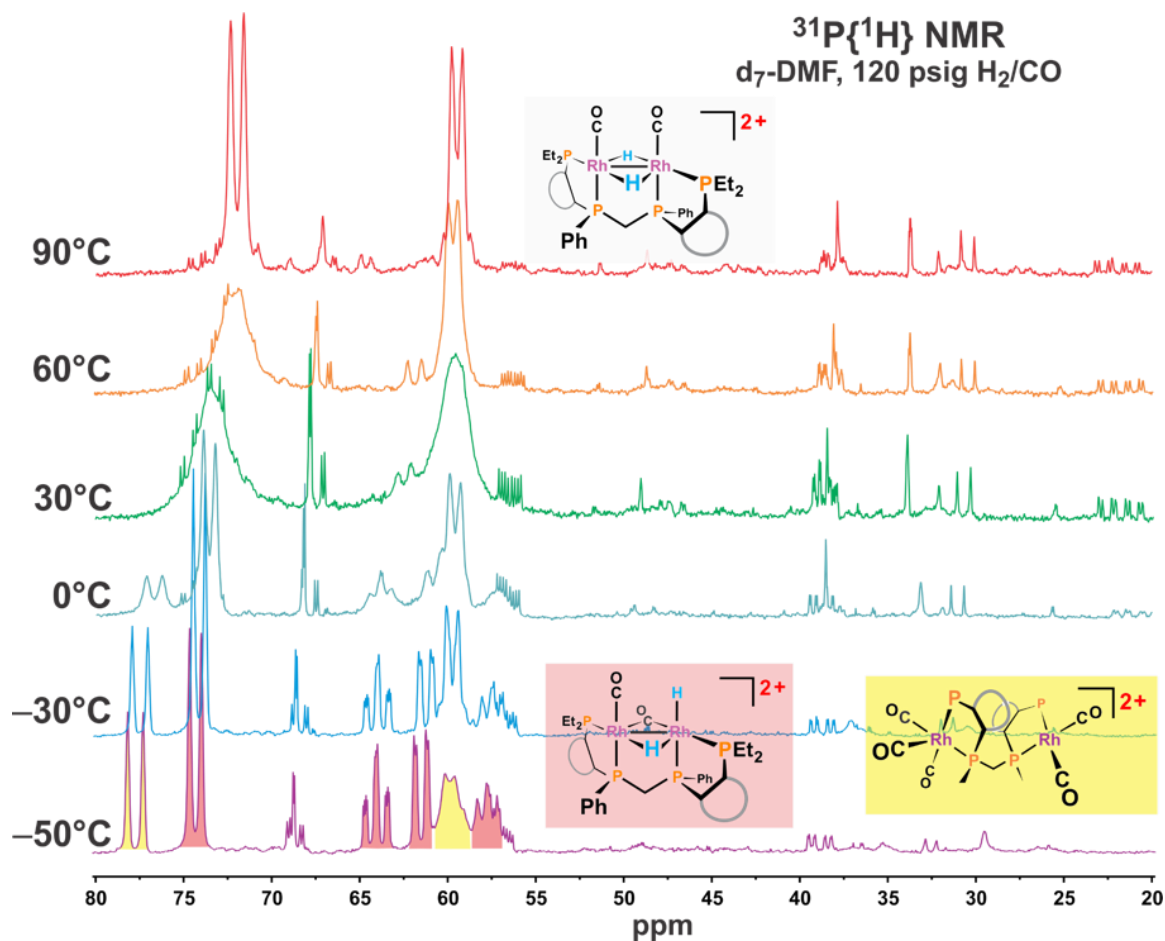


Figure 4.6. Variable temperature ^{31}P NMR of $\text{Rh}_2(\text{nbd})_2(\text{rac-et,ph-P4-Ph})](\text{BF}_4)_2$ in DMF-d_7 at 120 psig H_2/CO .

Figure 4.6 shows the variable temperature 120 psig H_2/CO ^{31}P NMR study that there are impurities or fragmentation products in the mixture in the range from 20 ppm to 40 ppm, the sharp peaks at 57 ppm, and resonances around 68 ppm. At the lower temperatures the pentacarbonyl species is believed to be formed with associated peaks at 77 ppm and 58 ppm and shaded in yellow. The peaks in the shaded pink region are associated to the $[\text{HRh}_2(\mu\text{-H})(\mu\text{-CO})(\text{CO})(\text{rac-et,ph-P4-Ph})]^{2+}$ complex having a bridging and terminal hydride as well as a bridging carbonyl. This species has four different phosphine resonances. As the temperature increases the peaks combine and broaden ultimately forming what is believed to be the symmetrical bridging dihydride complex.

I re-ran this experiment using the acetonitrile catalyst precursor, $[\text{Rh}_2(\text{acetonitrile})_4(\text{rac-P4-Ph})](\text{BF}_4)_2$ in DMF-d_7 to see if I would see any differences (Figure 4.7). Running under the same conditions (120 psig H_2/CO) the ^{31}P NMR was very similar to the experiment shown in Figure 4.6 with the nbd catalyst precursor. The 90°C ^{31}P NMR spectra in Figures 4.6 and 4.7 did not show significant differences. The similar impurities or fragmentation products still showed up as does the proposed $[\text{Rh}_2(\mu\text{-H})_2(\text{CO})_x(\text{rac-P4-Ph})]^{2+}$, $x = 2\text{-}4$, catalyst.

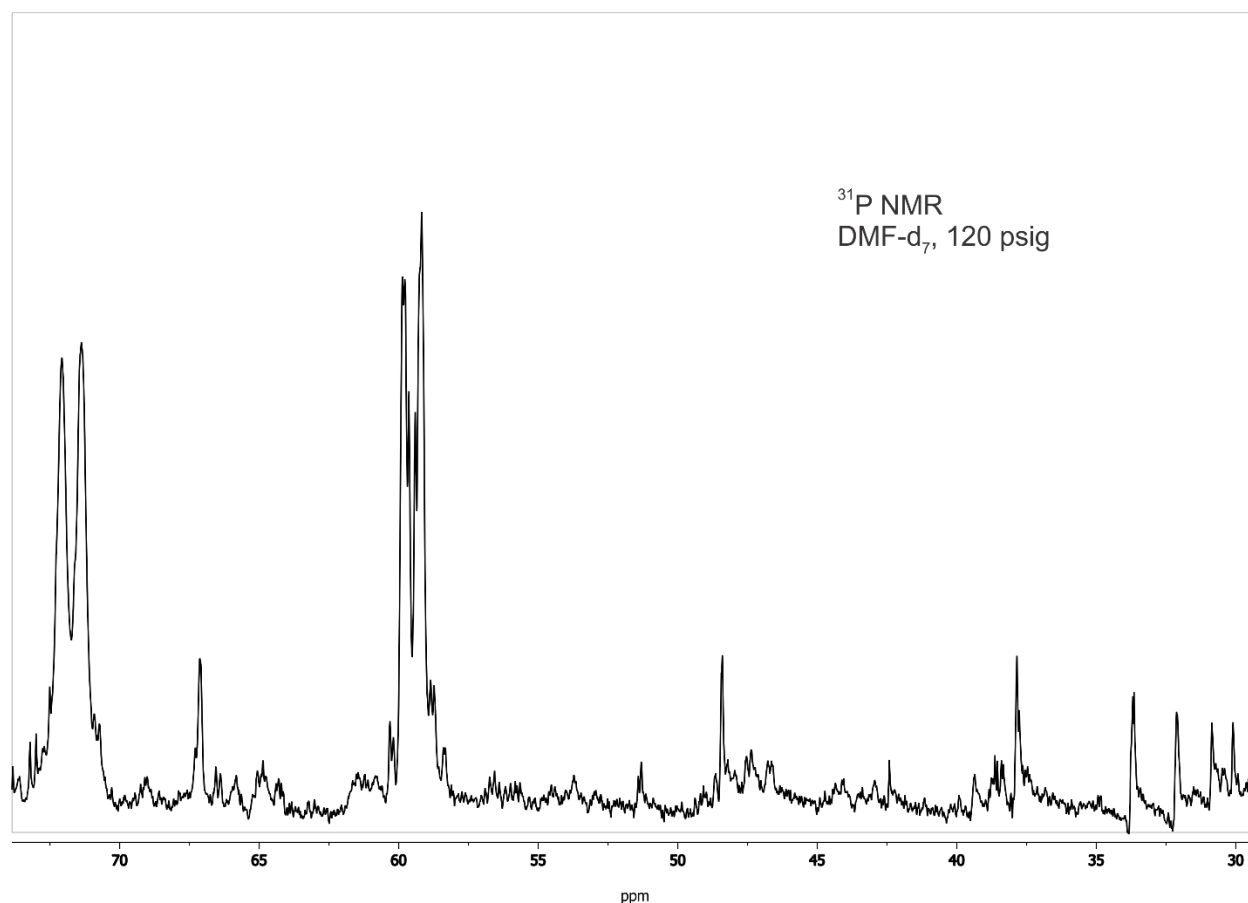


Figure 4.7. ^{31}P NMR of $\text{Rh}_2(\text{acetonitrile})_4(\text{rac-et,ph-P4-Ph})](\text{BF}_4)_2$ in DMF-d_7 at 120 psig H_2/CO and 90°C .

I also repeated the high-pressure ^{31}P NMR experiment using pure acetone- d_6 and the mixed-ligand $[\text{Rh}_2(\text{nbd})_2(\text{mixed-P4-Ph})](\text{BF}_4)_2$ precursor, as shown in Figure 4.8. These ^{31}P NMR spectra appear different due to the presence of both diastereomers. The ^{31}P NMR peaks that

broaden going from -30°C to 30°C are probably the *rac*-diastereomer, while the peaks that remain sharp are likely the *meso*-diastereomer. We believe the *meso*-diastereomer does not have the dynamic behavior of the *rac*-diastereomer. As the temperature increases the resonances for the dihydride-bridged *rac*-catalyst grow in at 59 and 71 ppm. The new ligand does have better stability under pressure over time in these NMR studies, however, when performing actual hydroformylation experiments in our autoclaves that is not the case.

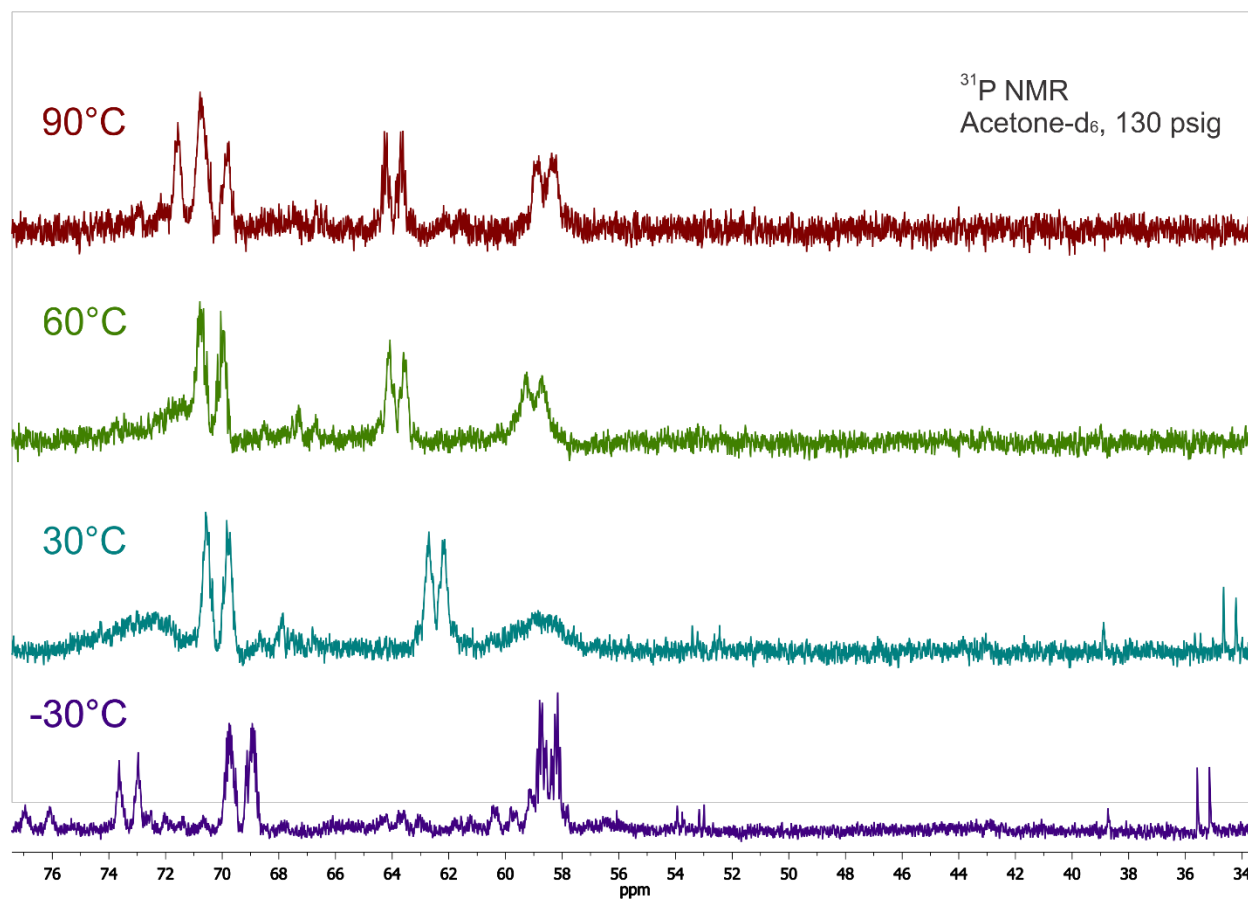


Figure 4.8. ³¹P NMR of Rh₂(nbd)₂(*mixed-et,ph-P4-Ph*)](BF₄)₂ in acetone-d₆ at 130 psig H₂/CO.

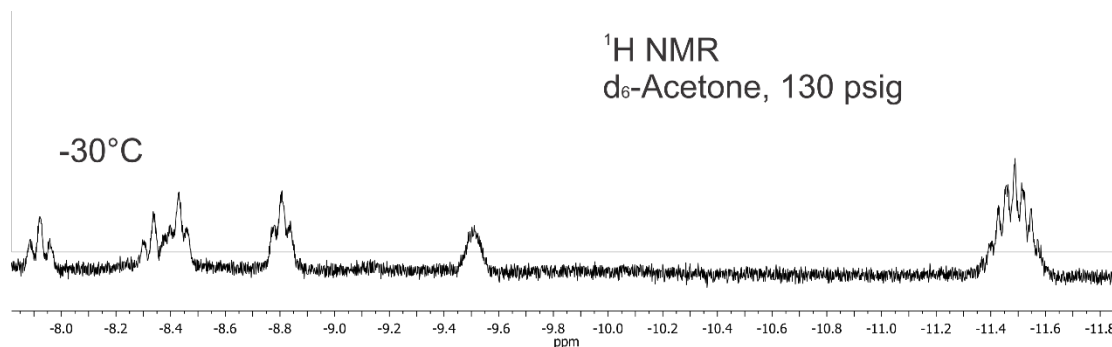


Figure 4.9. ^1H NMR of the hydride region for $\text{Rh}_2(\text{nbd})_2(\text{mixed-et,ph-P4-Ph})](\text{BF}_4)_2$ under 130 psig of 1:1 H_2/CO .

Figure 4.9 shows the ^1H NMR for the hydride-containing complexes generated from the mixed-ligand precursor, $\text{Rh}_2(\text{nbd})_2(\text{mixed-et,ph-P4-Ph})](\text{BF}_4)_2$ under 130 psig of 1:1 H_2/CO at -30°C . Hydride resonances are clearly seen at low temperature. The doublet of triplets centered at -8.6 ppm (terminal hydride) and the pseudo-nonet at -11.5 ppm (bridging hydride) are assigned to the *racemic*-diastereomer with terminal and bridging hydrides, $[\text{Rh}_2(\mu\text{-H})(\mu\text{-CO})(\text{H})(\text{CO})_x(\text{rac-P4-Ph})]^{2+}$, $x = 1\text{-}3$, as discussed earlier. There is a second set of hydride peaks that are assigned to the *meso*-diastereomer, also with a terminal and bridging hydride, but probably no bridging carbonyl: $[\text{Rh}_2(\mu\text{-H})(\text{H})(\text{CO})_x(\text{meso-P4-Ph})]^{2+}$, $x = 2\text{-}3$. The terminal hydride is the doublet of triplets centered at -8.1 ppm, while the bridging hydride is the broad unresolved peak at -9.5 ppm.

Raising the temperature caused all the hydride resonances to disappear. We believe this is due to H/D exchange reactions with the acetone- d_6 solvent. The Stanley group has observed this very slow acetone- d_6 /hydride exchange reaction with the old-P4 dirhodium catalyst over the course of several days. The new P4-Ph based dirhodium catalyst, however, appears to be far more reactive with acetone- d_6 as indicated by the $\text{PF}_6^-/\text{acetone}$ reaction chemistry observed by Dr. Marshall Moulis (discussed earlier), who also observed rapid exchange between Rh-H species and acetone- d_6 .

Performing the pressurized H₂/CO NMR study of the mixed-ligand precursor, Rh₂(nbd)₂(*mixed-ct,ph-P4-Ph*)](BF₄)₂, in 25% H₂O/acetone-d₆ did show a broad hydride peak at 60°C under 130 psig at –10.1 ppm, as shown in Figure 4.10. We tentatively assign this to the bridging hydride on the *meso*-catalyst diastereomer, which should be the least reactive to acetone-d₆. The *rac*-catalyst is apparently more reactive to acetone-d₆ exchange reactions that prevents observation of the hydride resonances. The other possibility is that H/D exchange with H₂O is fast, which broadens out the hydride resonances for the *rac*-catalyst.

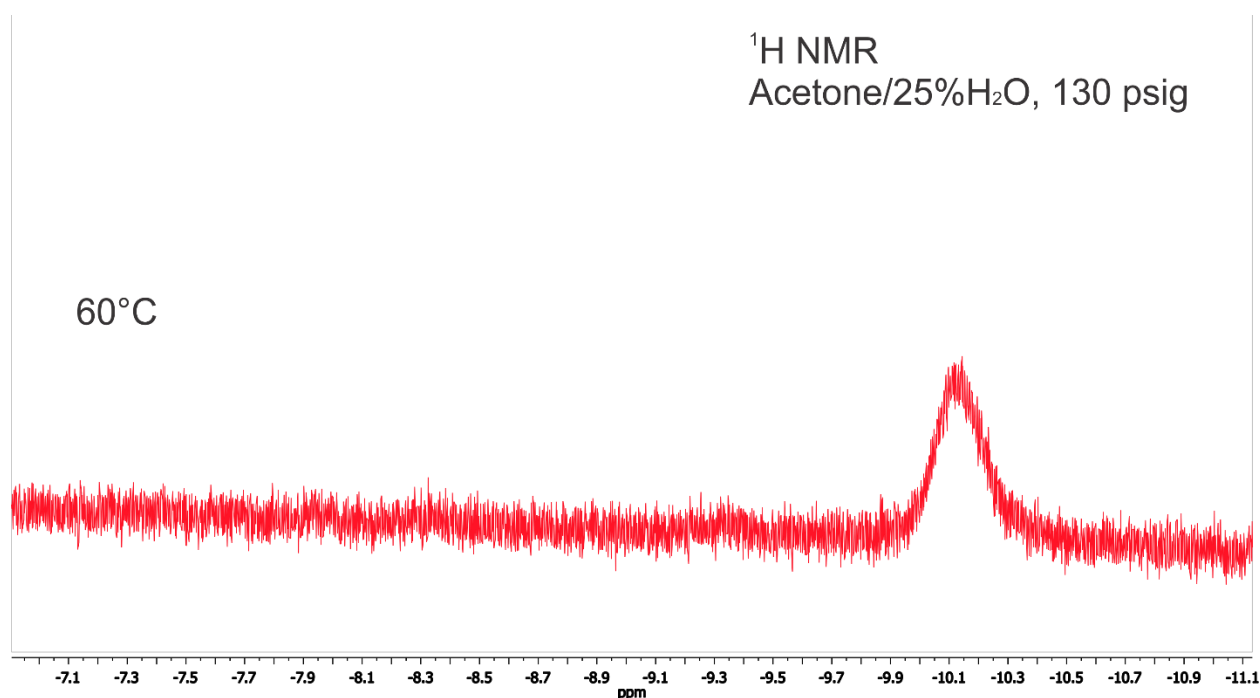


Figure 4.10. ¹H NMR of the hydride region for Rh₂(nbd)₂(*mixed-ct,ph-P4-Ph*)](BF₄)₂ under 130 psig of 1:1 H₂/CO using 25% H₂O/acetone-d₆ solvent.

4.3 FT-IR Studies on the Old P4-Based Dirhodium Catalyst

Fourier transform infrared spectroscopy (FT-IR) has been very useful studying hydroformylation mechanisms and structures that occur during the reaction. High-pressure FT-IR cells have shown a great value in obtaining data for catalyst over time. Developed in the late

sixties, these cells allowed for IR studies under actual hydroformylation conditions when investigating a modified cobalt catalyst.^{6, 7} Metal-carbonyls are observed during FT-IR studies which can display strong, easily observed bands between 1700 cm⁻¹ and 2100 cm⁻¹. Important information on catalyst structure can be obtained from carbonyl band positions that usually clearly identify the presence of terminal and/or bridging carbonyls. The position of the terminal carbonyl bands also provides important information about the electron density on the metal center: electron-rich or electron-deficient. A number of studies have used high-pressure IR cells to investigate unmodified rhodium carbonyls,⁸ rhodium-phosphine,⁹ rhodium-diphosphine,¹⁰ and rhodium-phosphite.¹¹ A thiolate-bridged dirhodium complex, initially proposed to be doing hydroformylation catalysis via bimetallic cooperativity, was investigated using high pressure FT-IR and shown to be fragmenting into active monometallic catalyst species.¹² High pressure IR studies can provide much insight to catalysts, especially those using CO, by providing information on active forms, degradation products, and additional complexes that may form during the catalytic cycle.

Various FT-IR experiments have been performed over the years to analyze the old ligand dirhodium catalyst. Dr. Catherine Alexander performed a study on [Rh₂(nbd)₂(*rac*-et,ph-P4)]²⁺ increasing CO pressure and temperature over time to study the carbonyl complexes formed. [Rh₂(nbd)₂(*rac*-et,ph-P4)]²⁺ was very reactive to CO even at low pressures. The 2015 cm⁻¹ band is associated with the norbornadiene precursor adding one CO to each rhodium center to form [Rh₂(nbd)₂(CO)₂(*rac*-P4)]²⁺. Additional CO ligands add and displace the norbornadiene ligands to generate the pentacarbonyl open-mode dirhodium complex, [Rh₂(CO)₅(*rac*-P4)]²⁺, which has CO bands at 2095 and 2043 cm⁻¹.

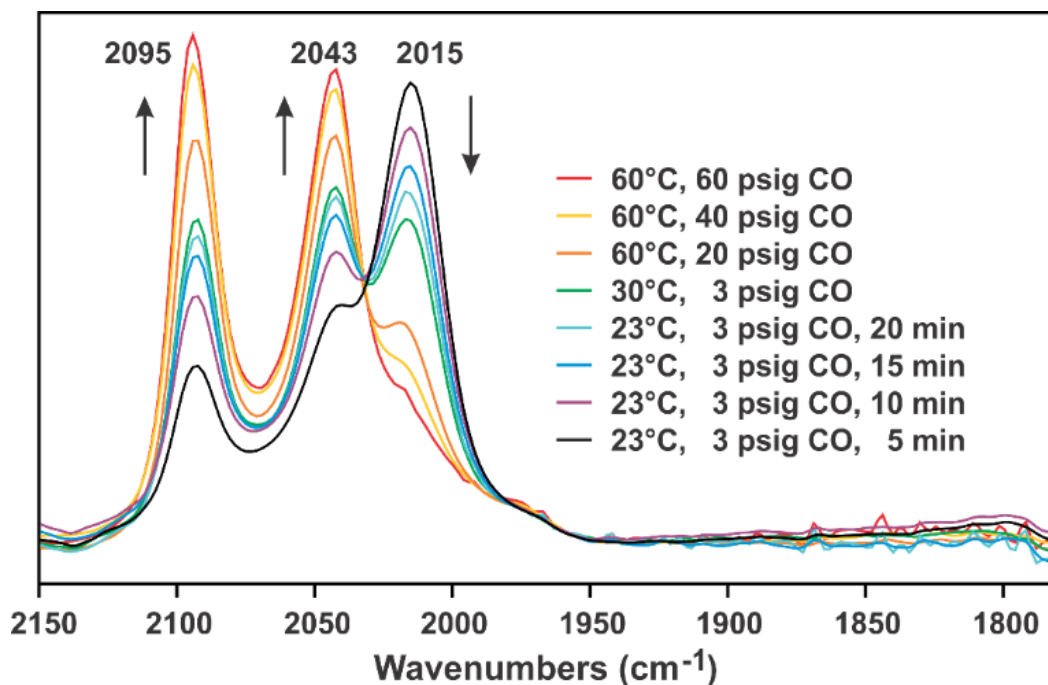


Figure 4.11. FT-IR spectra of $\text{Rh}_2(\text{nbd})_2(\text{rac-}et,\text{ph-P4})](\text{BF}_4)_2$ under CO pressure at different temperatures.

Dr. Catherine Alexander did the first high-pressure IR study on the old-P4-based dirhodium catalyst in water/acetone solvent to try and explain the much better hydroformylation results seen for the old-dirhodium catalyst when water was added to the acetone solvent. Figure 4.9 shows the FT-IR spectra for the old-P4-based dirhodium catalyst in acetone and 30% water/acetone, along with two dirhodium carbonyl complexes. Although the catalyst spectra in acetone and 30% water/acetone look similar, there are some key differences. The most important is that the terminal carbonyl bands in water/acetone are shifted to lower wavenumbers. For example, the 2094 cm^{-1} band is barely present in water/acetone and the 2075 cm^{-1} band has lower intensity. The entire terminal carbonyl band average position has shifted to lower wavenumbers and has higher intensity compared to the bridging carbonyls.

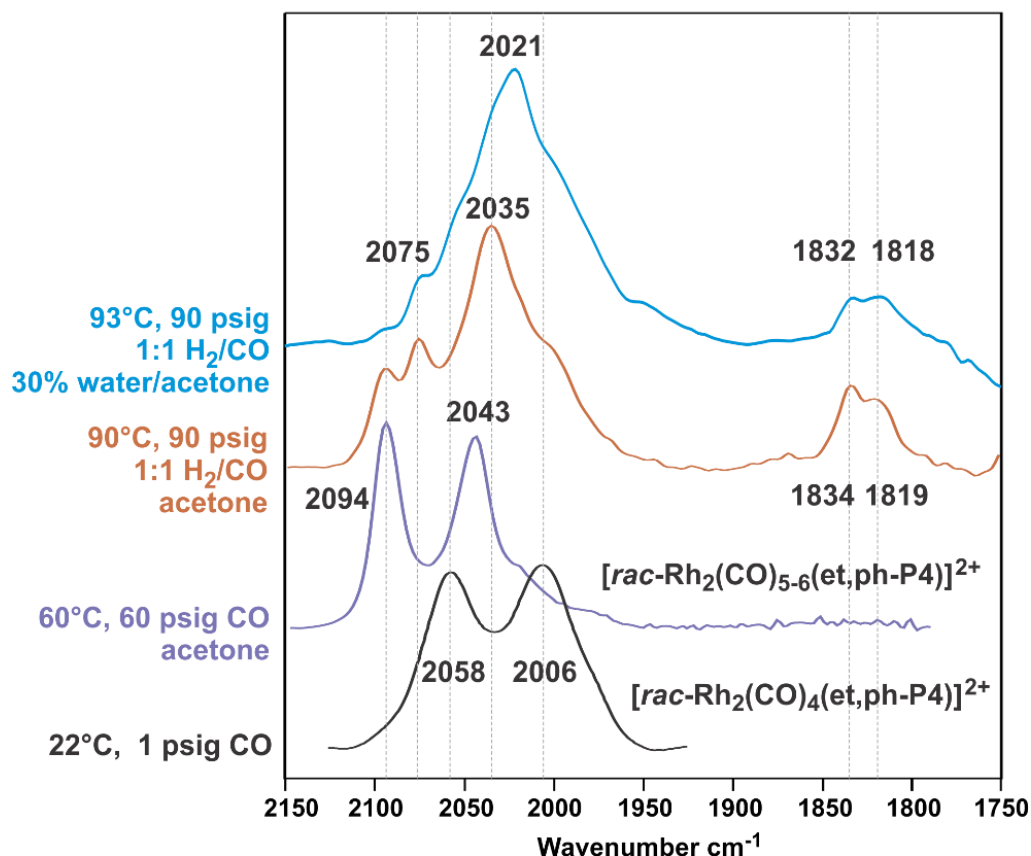


Figure 4.12. Old Ligand Dirhodium catalyst in acetone and water/acetone under CO or H₂/CO.

This means that the dirhodium catalyst in water-acetone is more electron-rich, which results in more π -backbonding to the terminal carbonyl ligands. Water is not a good donating ligand, so water coordination to the dirhodium catalyst is not the main factor causing the terminal carbonyl shift to lower wavenumbers. What the Stanley group eventually figured out was that the dicationic dihydride catalyst, $[\text{Rh}_2(\mu\text{-H})_2(\text{CO})_x(\text{rac-P4})]^{2+}$, $x = 2\text{-}4$, was dissociating a proton into the water/acetone solvent to generate a monocationic, monohydride dirhodium catalyst: $[\text{Rh}_2(\mu\text{-H})(\text{CO})_x(\text{rac-P4})]^+$, $x = 2\text{-}4$. Water is an excellent solvent for stabilizing proton dissociation via hydrogen-bonding.

The monocationic, monohydride dirhodium catalyst, $[\text{Rh}_2(\mu\text{-H})(\text{CO})_x(\text{rac-P4})]^+$, $x = 2\text{-}4$, is more electron-rich, which shifts the terminal carbonyls to lower wavenumbers consistent with

more π -backbonding. Although this makes it less reactive for hydroformylation relative to the dicationic catalyst, it is far less susceptible to loss of a rhodium center and catalyst deactivation. Thus there is considerably more of the monocationic dirhodium catalyst present, which compensates for its lower activity compared to the dicationic catalyst system.

4.4 High pressure FT-IR Reactor Design

Previous FT-IR studies have mainly used a SpectraTech High Pressure *In-Situ* Circle Reaction FT-IR Cell equipped with a ZnSe or silicon crystal rod. Most of my current studies use the Mettler-Toledo ReactIR 45m FT-IR system connected to a high-pressure IR cell designed by Mettler-Toledo and Parr Instruments (Figure 4.10).¹⁴

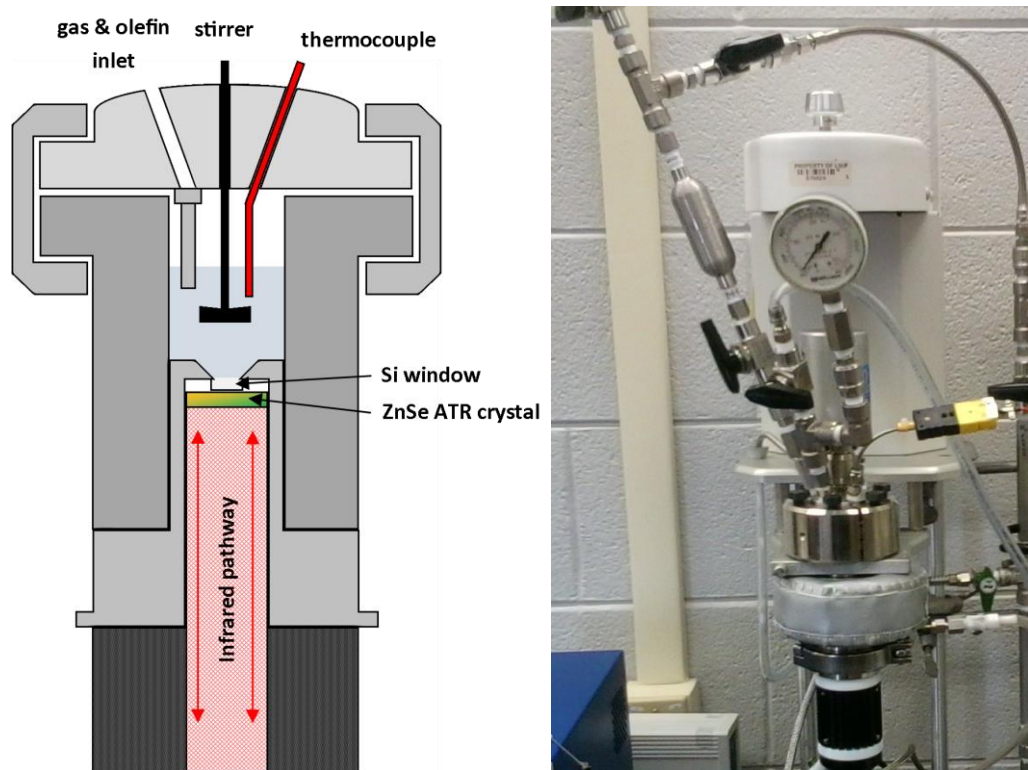


Figure 4.13. High Pressure *In-Situ* ReactIR Autoclave Design

This high-pressure IR cell uses a ZnSe focusing crystal attached to the Si ATR crystal window. The IR beam is directed to the cell via a fiber optic conduit, then directed to one edge of the silicon crystal where it is reflected through the crystal via attenuated total reflectance (ATR) and collects the IR spectrum of anything in contact with the silicon window. The top part of the IR cell is essentially a Parr autoclave with the IR probe inserted from the bottom and screwed in with a Teflon o-ring seal.

The top part of the cell has been modified with quick-connects equipped with solvent-resistant o-rings, similar to what we use on the in the Stanley lab. The design includes a stirrer, thermocouple, olefin addition arm, and vent arm equipped with an electronic pressure transducer. The olefin arm is used as the gas inlet and for pressure injecting alkene or other reactants. The vent arm is used to inject the catalyst solution and to vent pressure. A needle valve can be added to either the olefin or vent arms to allow very slow and controlled venting of the cell.

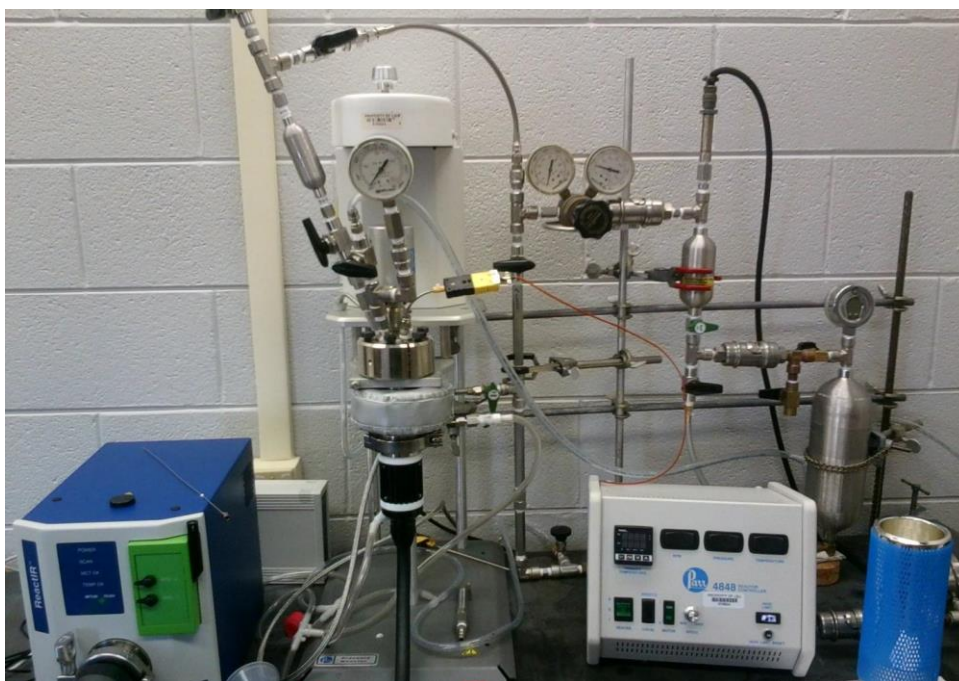


Figure 4.14. ReactIR spectrometer (left), high-pressure FT-IR reactor cell (center), gas manifold system (back/right), and temperature/stirring controller (front/right).

Figure 4.11 shows the entire setup of the FT-IR involving using a gas manifold system equipped with a regulator for pressurizing the cell. A 1 liter portable stainless steel gas cylinder is used as the gas source which is beneficial for transporting different gases such as pure CO or H₂/CO mixtures that can hold pressures up to 2000 psig. The standard FT-IR runs performed used the same procedure after the IR cell was assembled. Nitrogen is flowed through the olefin arm from the gas inlet, and purged through the vent arm allowing the autoclave to be purged of air. The ReactIR spectrometer MCT detector dewar is filled with liquid nitrogen to operating conditions, and an empty cell energy check is done and blank background collected. Background scans of the solvent being used were collected at various temperatures prior to the experiment and stored. The refractive index of the silicon ATR crystal (& ZnSe focusing crystal) changes with temperature and this affects the data being collected. Subtracting solvent spectra collected at the temperature being studied gives much better experimental spectra.

Once the system is purged with nitrogen gas the catalyst solution is added via syringe through the vent arm. Once inserted the catalyst is pressurized with the reaction gas with stirring and heating to various temperatures studied. The software allows for FT-IR spectra to be collected at certain time intervals over the course of the study. We typically collect 256 scans per spectrum at 8 cm⁻¹ resolution, which takes just over a minute. Spectra collected at different pressures and temperatures show changes to the catalyst due to these conditions.

4.5 FT-IR Studies on the New P4-Ph Dirhodium Catalyst.

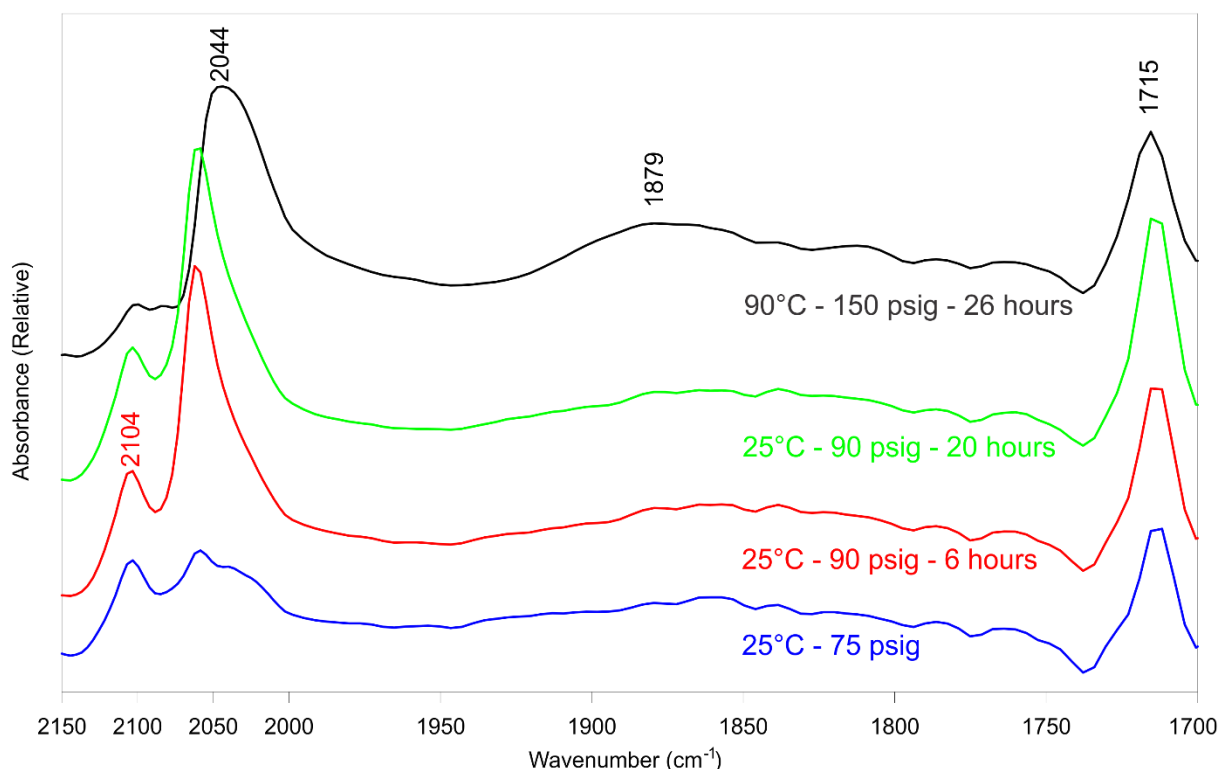


Figure 4.15. FT-IR spectra of $[\text{Rh}_2(\text{acetonitrile})_4(\text{mixed-et,ph-P4-Ph})](\text{BF}_4)_2$ under 1:1 H_2/CO pressure and temperatures indicated in CH_2Cl_2 (DCM) solvent.

The ReactIR was used to study the new P4-Ph ligand dirhodium catalyst. The mixed ligand dirhodium catalyst precursor complexes were studied first. 10 mmol of $[\text{Rh}_2(\text{acetonitrile})_4(\text{mixed-et,ph-P4-Ph})](\text{BF}_4)_2$ was dissolved in 15 mL of DCM and added to the IR cell for the first ReactIR study. DCM is used to observe the catalyst because it does not interfere with the metal-carbonyl region. The H_2/CO pressure was raised to 75 psig while the temperature remained at room temperature (Figure 4.12).

There is peak at 1715 cm^{-1} and as the pressure and temperature increases the peak stays about the same over time. This peak is most likely associated with the acetonitrile precursor since it is not present with the norbornadiene precursor, although we do not have a specific

assignment. We are more interested in the metal-carbonyl region that shows terminal CO bands between 2000 and 2150 cm^{-1} at 75 psig and 25°C.

As the H_2/CO pressure is increased the Rh-carbonyl peaks grow more prominent on the FT-IR spectra, especially the 2050 cm^{-1} band. There is a smaller Rh-carbonyl peak at 2104 cm^{-1} . These two peaks are similar to the pentacarbonyl dirhodium complex, $[\text{Rh}_2(\text{CO})_5(\text{rac-P4})]^{2+}$, seen with the old ligand (see Figure 4.9). The carbonyl bands for the new complex are shifted to somewhat higher energies, consistent with the P4-Ph ligand that is a somewhat poorer electron-donating ligand due to the 1,2-phenylene bridges. Studies on the old catalyst indicate that it doesn't react with H_2 at lower temperatures and the new dirhodium P4-Ph complex should have similar behavior. So the proposal of a pentacarbonyl open-mode dirhodium complex forming at lower temperatures is quite reasonable. There is essentially no change in the Rh-CO bands over 16 hours at room temperature as indicated in Figure 4.12.

The terminal Rh-CO bands change shape, position, and broaden significantly on heating to 90°C. The addition of H_2 should cause a change in the terminal carbonyl pattern and a shift to somewhat lower wavenumbers, which is observed for the main band that moves from 2050 to 2044 cm^{-1} . There might be a broad, low intensity band at 1879 cm^{-1} indicating a bridging carbonyl. However, the broadening and lack of band structure compared to the old catalyst IR studies, could indicate catalyst degradation.

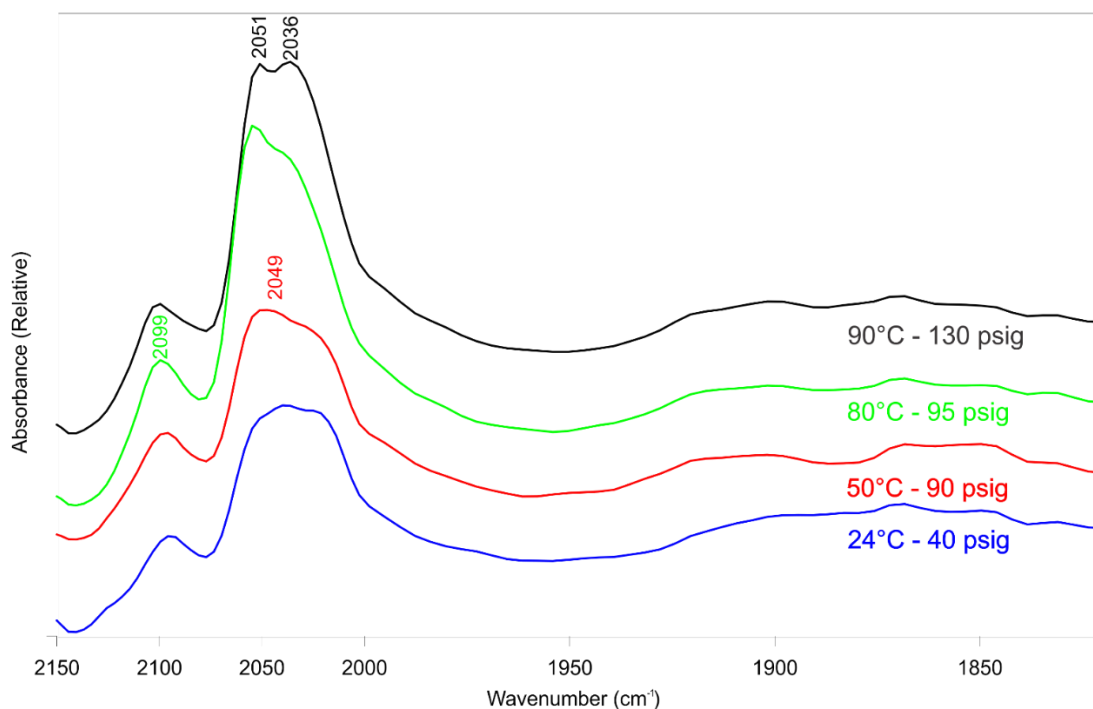


Figure 4.16. FT-IR spectra of $[\text{Rh}_2(\text{nbd})_2(\text{meso-et,ph-P4-Ph})](\text{BF}_4)_2$ under 1:1 H_2/CO pressure in DCM

The next ReactIR study involved the *meso* catalyst precursor (Figure 4.13). Unlike the *racemic*-diastereomer, the *meso*-P4-Ph ligand can be obtained in high purity. Hydroformylation studies on the *meso* precursor, $[\text{Rh}_2(\text{nbd})_2(\text{meso-et,ph-P4-Ph})](\text{BF}_4)_2$, clearly showed it was an extremely poor hydroformylation catalyst. The terminal Rh-carbonyls for the *meso*-complex in Figure 4.13 are somewhat similar to that seen for the mixed acetonitrile catalyst precursor in Figure 4.12, but the main band between 2000 and 2070 cm^{-1} appears broader with some structure indicating a broader spread of terminal Rh-CO frequencies. This can also be assigned to a pentacarbonyl complex: $[\text{Rh}_2(\text{CO})_5(\text{meso-P4-Ph})]^{2+}$, that could exist in several different rotational conformations giving rise to the greater spread of terminal Rh-CO frequencies. If the *racemic* pentacarbonyl complex is more symmetrical with a narrower and more intense Rh-CO band around 2050 cm^{-1} , the combination of the two could yield that seen in Figure 4.12.

As the temperature and pressure increases two Rh-CO peaks become resolved at 2051 cm^{-1} and 2036 cm^{-1} (90°C and 130 psig). We believe this is a mixture of the pentacarbonyl complex and a dihydride bridged species, $[\text{Rh}(\mu\text{-H})_2(\text{CO})_2(\text{meso-P4-Ph})]^{2+}$. Due to the different stereochemistry of the *meso* diastereomer and fewer coordinated CO ligands, this dihydride complex is not active for hydroformylation. The lower energy 2036 cm^{-1} band can be assigned to this dihydride complex, while the higher energy bands are due to the pentacarbonyl complex.

Remember that the ^1H NMR of the hydride region in Figure 4.9 showed that both *rac*- and *meso*-precursors react with H_2/CO to form hydride complexes. At low temperature, both appear to have one bridging hydride and one terminal hydride. But as the temperature is raised, these complexes convert to dihydride-bridged complexes with only terminal carbonyls.

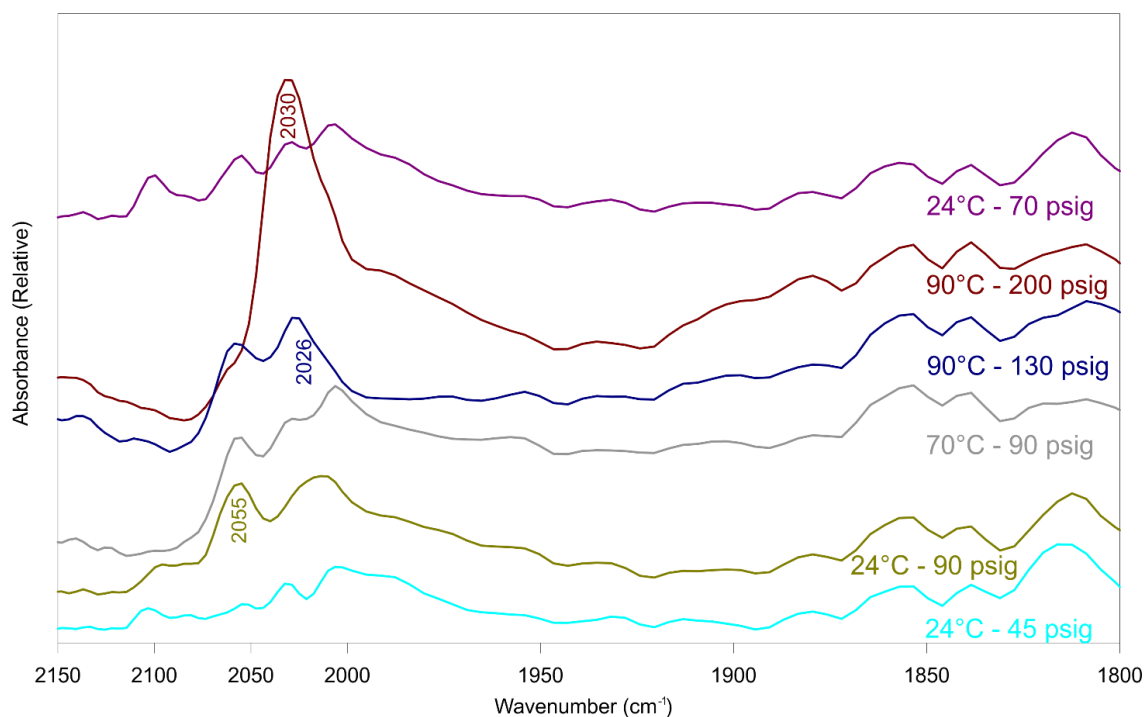


Figure 4.17. FT-IR spectra of $[\text{Rh}_2(\text{nbd})_2(\text{mixed-et,ph-P4-Ph})](\text{BF}_4)_2$ under 1:1 H_2/CO pressure in 25% water/Acetone solvent.

The catalyst does not perform hydroformylation well in DCM, and I decided to run the FT-IR of the new ligand dirhodium catalyst in water/acetone to see if there would be a difference. Water/acetone appears to be the best solvent for hydroformylation using the new ligand dirhodium catalyst system. Running 10 mmol $[\text{Rh}_2(\text{nbd})_2(\text{mixed-et,ph-P4-Ph})](\text{BF}_4)_2$ in 15 mL of 25% water/acetone solvent displayed different FT-IR results from the DCM spectra. Figure 4.14 shows terminal carbonyl peaks at 2120, 2055, 2026, and 2030 cm^{-1} as the temperature and pressure increase. A prominent peak at 2030 cm^{-1} when the pressure was increased to 200 psig at 90°C. One might be tempted to assign some weak bridging carbonyl peaks in the range between 1875 cm^{-1} to 1825 cm^{-1} , except that this region is very susceptible to solvent subtraction artifacts from the water and acetone. Carefully comparing the FT-IR spectra in Figure 4.14 with those in Figures 4.12 and 4.13 reveals a general shift to lower wavenumbers for the terminal CO bands and a more defined separation of the higher energy peaks from the lower set. We interpret this as indicating the presence of the open-mode pentacarbonyl complex at lower temperatures and mostly a monocationic monohydride complex, $[\text{Rh}_2(\mu\text{-H})(\text{CO})_x(\text{mixed-P4-Ph})]^+$, $x = 2\text{-}4$, formed via proton dissociation from the dicationic dihydride complex. This is directly analogous to the old dirhodium catalyst system. The *racemic* monohydride dirhodium species should be active for hydroformylation, but will eventually suffer from Rh-induced P4-Ph degradation reactions that leads to catalyst deactivation. The dicationic dirhodium catalyst based on the P4-Ph ligand is considerably more susceptible to rhodium-induced P4-Ph degradation reactions, which is why acetone-water works better than acetone as a hydroformylation solvent.

4.6 Hydroformylation Catalytic Cycle

NMR, FT-IR, catalytic results, and Density Functional Theory (DFT) calculations have been used to propose the mechanistic steps during hydroformylation using the old ligand dirhodium catalyst system – both for the dicationic and monocationic versions.¹⁵

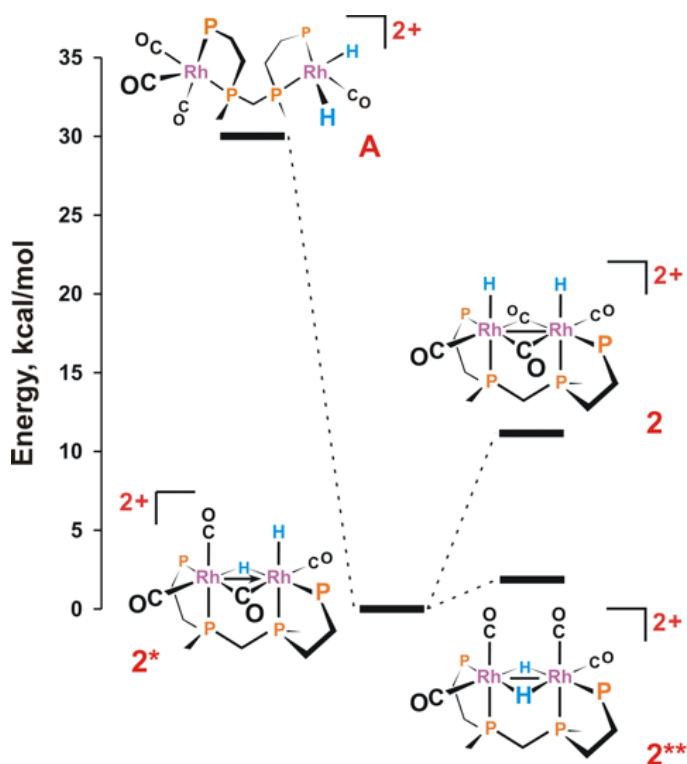


Figure 4.18. DFT relative energies for four different dirhodium dihydride isomers

Four dirhodium dihydride structures were initially studied via the DFT calculations. The lowest energy isomer involved a bridging and terminal hydride on the catalyst, which is supported by the low-temperature ^1H NMR results that show terminal and bridging hydride ligands. The next likely complex was a bridging dihydride species, which Prof. Stanley did not believe was important because terminal hydrides are considered far more reactive for migratory

insertion reactions with alkenes. The ^1H NMR shows a broad symmetrical hydride species that forms at higher temperatures, this is consistent with either the terminal dihydride or bridging dihydride complexes. The FT-IR, however, showed two bridging carbonyl bands, which initially led Prof. Stanley to favor the terminal dihydride dirhodium complex as the key catalytic species that reacted with alkene. DFT, however, indicated that the terminal dihydride structure was 12.5 kcal higher and was unlikely to form during the reaction. Ranelka Fernando would later redo the DFT calculations and include transition state calculations studying all the proposed mechanistic steps in our hydroformylation cycle.^{16, 17}

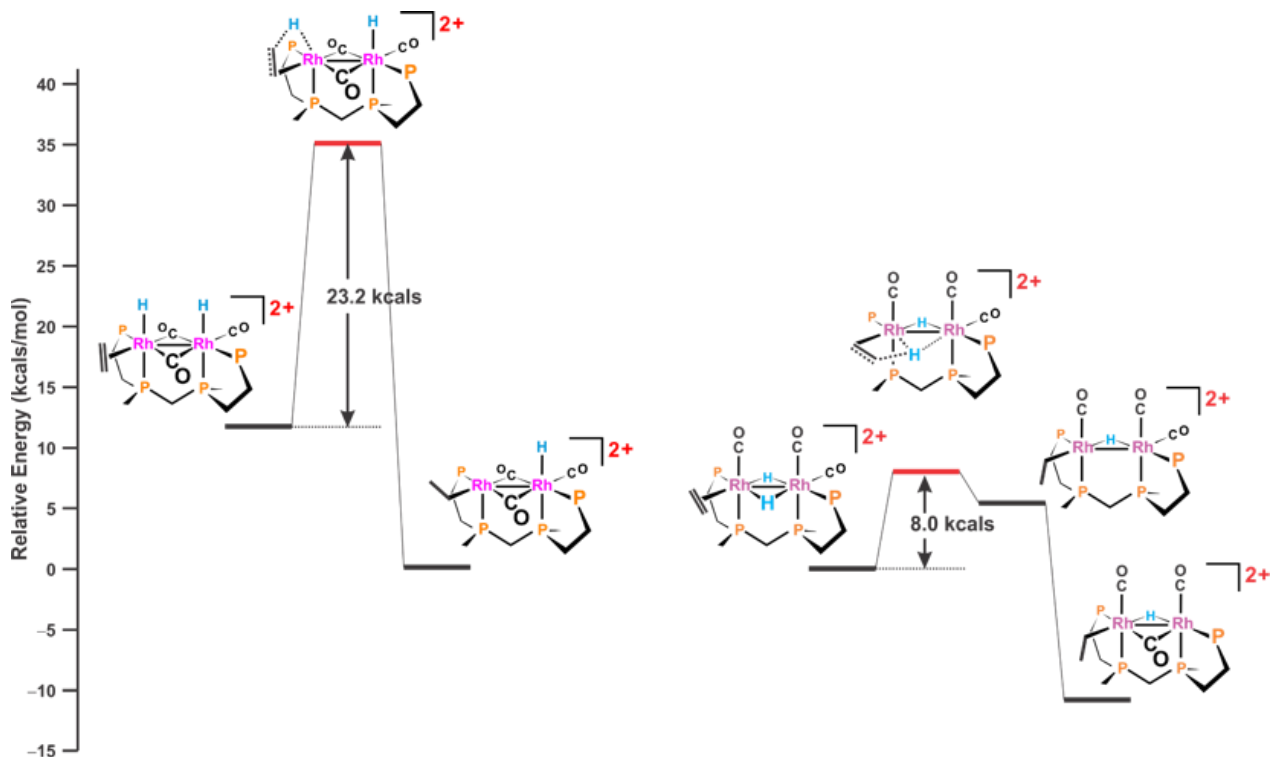


Figure 4.19. DFT transition state energies for the migratory insertion of an alkene with terminal and bridging hydrides on the dicationic dirhodium catalyst based on the P4 ligand.

The energy barrier for the insertion of an alkene with the terminal hydride species was 23.2 kcal compared to the bridging hydride complex of only 8 kcal. DFT clearly predicts that the bridging hydride complex was not only far lower in energy than the terminal species but was

also far more reactive for the key alkene-hydride migratory insertion step. This lead to the current proposed mechanism for the dicatonic old ligand dirhodium catalyst. The bridging dihydrides complex is now proposed as the key catalyst species for reacting with the alkene.

The rest of the mechanism is essentially identical to monometallic hydroformylation. Carbonyl dissociation opens a coordination site allowing alkene to bind to the rhodium center. Migratory insertion from one of the bridging hydrides takes place with the alkene to form an alkyl group. Carbonyl migratory insertion with the alkyl group forms the acyl group, followed by carbonyl coordination to fill empty binding sites. The last bridging hydride and the acyl are cisoidal to one another and can readily reductively eliminate to produce the aldehyde product. After the aldehyde is produced the catalyst can revert to an open-mode pentacarbonyl species, followed by oxidative addition of H_2 on one rhodium center converting it back to the close-mode bridging and terminal hydride species. This readily converts to the dihydride bridged species at higher temperatures.

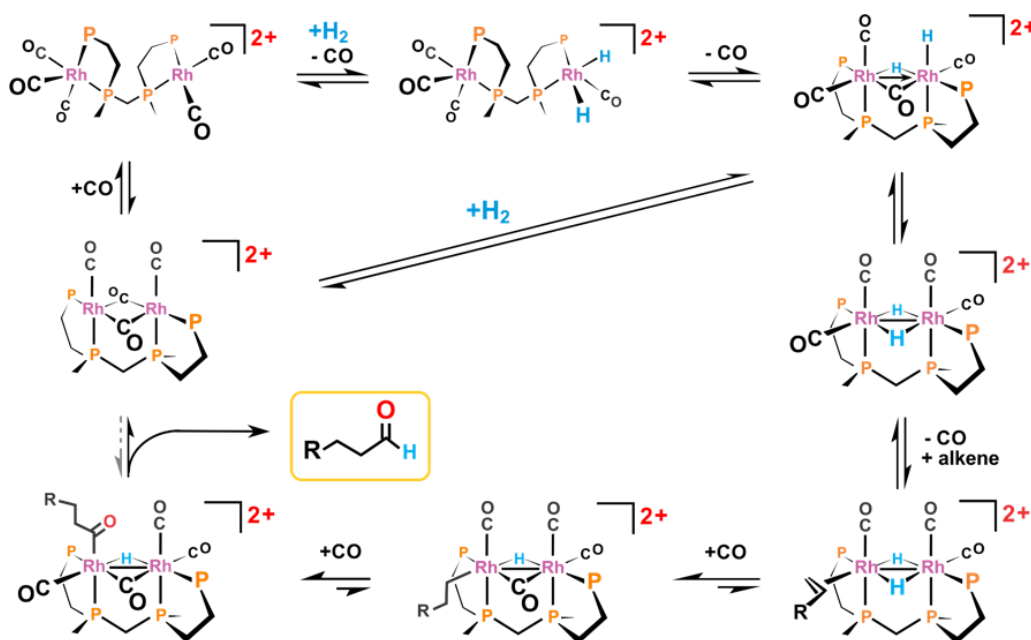


Figure 4.20. Proposed hydroformylation mechanism for the dicatonic catalyst, $[Rh_2(\mu-H)_2(CO)_4(rac-et,ph-P_4)]^{2+}$.

The addition of water to the acetone solvent was an attempt to get the product aldehyde to phase separate similar to the Shell higher olefin process.¹⁸ The water allowed the dicationic dihydride catalyst to do a proton dissociation generating a monocationic monohydride dirhodium catalyst, $[\text{Rh}_2(\mu\text{-H})(\text{CO})_x(\text{rac-P4})]^+$, $x = 2\text{-}4$. The monocationic dirhodium catalyst was far more stable with respect to catalyst deactivation than the dicationic system.

NMR and FT-IR spectroscopy were used with DFT calculations to propose catalyst complexes and a hydroformylation mechanism for the monocationic system. NMR indicated the active monocationic catalyst had one broad peak in the hydride region at -10.5 ppm. DFT calculations found that the most stable complexes for the monocationic catalyst, which are mainly in the Rh(I) oxidation state, prefer an A-frame-like geometry with only one bridging ligand. Dirhodium complexes with a bridging carbonyl and hydride were found to be very close in energy, with the bridging hydride complex only 1.82 kcal higher in energy. Once again transition state DFT calculations clearly indicated that the bridging hydride complex had a much lower activation barrier for alkene migratory insertion relative to the terminal hydride species: 16.8 kcal vs. 34.1 kcal. The proposed mechanism is shown in Figure 4.18.

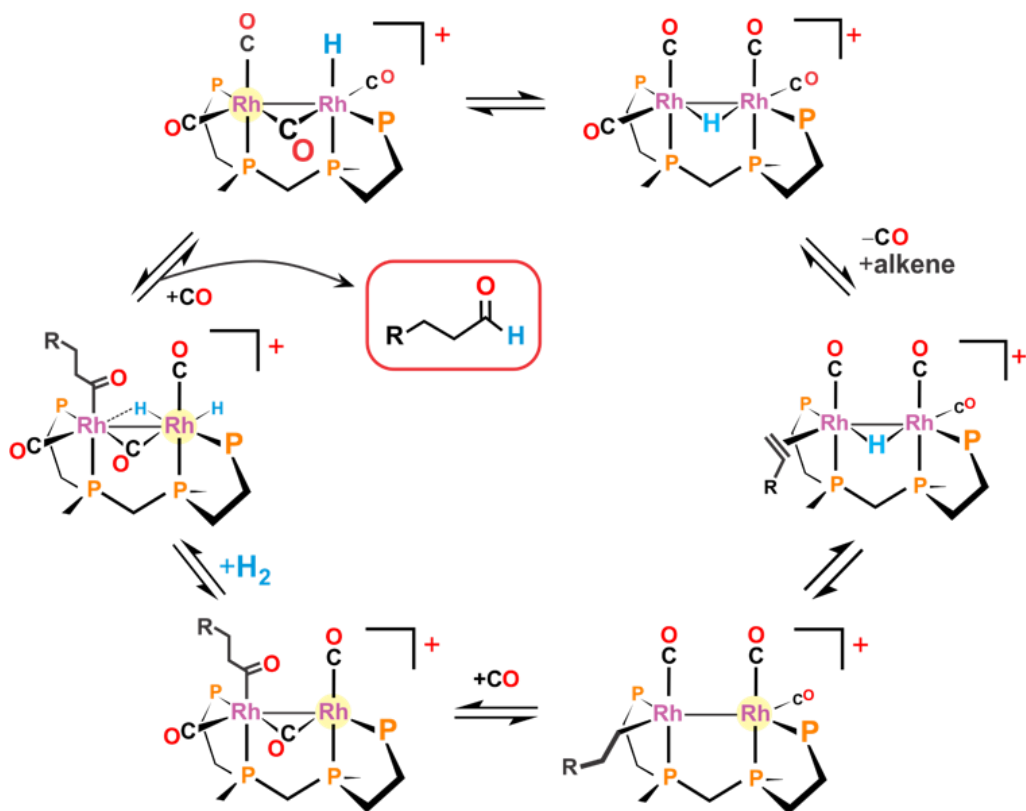


Figure 4.21. Proposed hydroformylation mechanism for $[\text{Rh}_2(\mu\text{-H})(\text{CO})_4(\text{rac-}i\text{-et,ph-P4})]^+$, rhodium centers highlighted in yellow are formally cationic and will have more labile carbonyl ligands.

The monohydride bridged dirhodium species is proposed to be the active hydroformylation catalyst. Carbonyl dissociation opens up a coordination site for alkene binding. Due to the lower cationic charge on this dirhodium complex, the rhodium centers are more electron-rich and CO dissociation will be slower than the dicationic catalyst. Migratory insertion of the bridging hydride and alkene take place to form an alkyl group. The alkyl group undergoes migratory insertion with a carbonyl ligand to form an acyl group, followed by CO coordination to fill empty coordination sites and reformation of a CO-bridged complex. Oxidative addition of H_2 occurs on the cationic rhodium metal center that will have more labile carbonyl ligands, forming a terminal and bridging hydride complex. The bridging hydride and the acyl group reductive eliminates to form the aldehyde product. A carbonyl is added to the

open coordination site and the complex rearranges back to the starting hydride-bridged dirhodium catalyst to repeat the process.

4.7 Conclusion

The new ligand, *et*,*ph*-P4-Ph, based-dirhodium hydroformylation catalyst most likely acts in the same way as the old ligand dirhodium catalyst with dicationic and monocationic versions. Catalytic data shows that the dirhodium catalysts based on the new ligand degrade via P-Ph bond oxidative additions to the rhodium center leading to fragmentation of the P4-Ph ligand and catalyst.

The additional P-arene bonds in the new P4-Ph ligand make it far more susceptible to rhodium-induced phosphine fragmentation reactions, similar to what happens with monometallic rhodium-PPh₃ and bisphosphite catalysts. This problem, unfortunately, negates the much stronger chelate effect of the P4-Ph ligand.

The new P4-Ph ligand is also more problematic and harder to work with compared to the old ligand due to increased reactivity with solvents, especially CH₂Cl₂, which is used to separate the racemic and meso ligand diastereomers. I found it incredibly difficult to obtain pure *racemic-et*,*ph*-P4-Ph ligand and make clean dirhodium catalyst precursors. The issues with the separation of ligand diastereomers, catalyst crystallization and purification, and rhodium-induced ligand degradation reactions, unfortunately all worked together to demonstrate that this was not a better hydroformylation catalyst system relative to the old P4-based dirhodium catalyst.

4.8 References

1. Horvath, I. T.; Millar, J. M. *Chem. Rev.* 1991, 91 (7), 1339-1351.

2. Aubry, D. A.; Bridges, N. N.; Ezell, K.; Stanley, G. G., Polar Phase Hydroformylation: The Dramatic Effect of Water on Mono- and Dirhodium Catalysts. *J. Am. Chem. Soc.* 2003, 125, 11180.
3. Gueorguieva, P. Spectroscopic and Synthetic Studies Relating to a Dirhodium Hydroformylation Catalyst. Ph.D. Dissertation, Louisiana State University, Baton Rouge, LA, 2004.
4. Polakova, D. Studies on a Dirhodium Tetrphosphine Hydroformylation Catalyst. Ph.D. Dissertation, Louisiana State University, Baton Rouge, LA, 2012.
5. Moulis, M. Hydroformylation and Aldehyde-Water Shift Catalysis by Dirhodium Tetrphoshine Complexes . Ph.D. Dissertation, Louisiana State University, Baton Rouge, LA, 2017.
6. Heck, R. F.; Breslow, D. S. *J. Am. Chem. Soc.* 1961, 83, 4023-4027.
7. Whyman, R. *J. Organomet. Chem.* 1974, 81, 97-106.
8. Fyhr, C.; Garland, M. *Organometallics* 1993, 12 (5), 1753-1764.
9. Moser, W. R.; Papile, C. J.; Weininger, S. J. *J. Mol. Catal.* 1987, 41 (3), 293-302.
10. Bronger, R. P. J.; Kamer, P. C. J.; van Leeuwen, P. *Organometallics* 2003, 22 (25), 5358-5369; (b) Silva, S. M.; Bronger, R. P. J.; Freixa, Z.; Dupont, J.; van Leeuwen, P. *New J. Chem.* 2003, 27 (9), 1294-1296.
11. Kamer, P. C. J.; van Rooy, A.; Schoemaker, G. C.; van Leeuwen, P. *Coord. Chem. Rev.* 2004, 248 (21-24), 2409-2424.
12. Bayon, J. C.; Esteban, P.; Real, J.; Claver, C.; Polo, A.; Ruiz, A.; Castillon, S. *J. Organom. Chem.* 1991, 403 (3), 393-399; (b) Dieguez, M.; Claver, C.; Masdeu-Bulto, A. M.; Ruiz, A.; van Leeuwen, P.; Schoemaker, G. C. *Organometallics* 1999, 18 (11), 2107-2115.
13. Alexander, C. Ph.D. Dissertation, Louisiana State University, Baton Rouge, LA, 2009.
14. Barnum, A. Studies of A Dirhodium Tetrphosphine Catalyst For Hydroformylation and Aldehyde-Water Shift Catalysis. Ph.D. Dissertation, Louisiana State University, Baton Rouge, LA, 2017.
15. Wilson, Z. S. Electronic Structural Investigations of Bi- and Polymetallic Complexes Using Quantum Mechanical Methods. Ph.D. Dissertation, Louisiana State University, Baton Rouge, LA, 2004.
16. Fernando, S. R. G. Computational Studies on Bimetallic Catalysis and X-Ray Absorption

Spectroscopy. Ph.D. Dissertation, Louisiana State University, Baton Rouge, LA, 2015.

17. Fernando, R. G.; Gasery, C. D.; Moulis, M. D.; Stanley, G. G., Bimetallic Homogeneous Hydroformylation. *In Homo and Heterobimetallic Complexes in Catalysis*, 1; Kalck, P.; Springer: Switzerland, 2016.
18. Lutz, E., Shell higher olefins process. *Journal of Chemical Education* 1986, 63 (3), 202.

Chapter 5: Cationic Cobalt(II) Hydroformylation

5.1 Introduction

Cobalt was the first metal to be used for hydroformylation. The first, and perhaps the best cobalt hydroformylation catalyst, $\text{HCo}(\text{CO})_4$, was accidentally discovered by Otto Roelen in 1938. Richard Heck proposed the first widely-accepted mechanism for hydroformylation with $\text{HCo}(\text{CO})_4$ in 1961.¹ The Heck mechanism is considered the best description today for almost any metal catalyst system that is active for hydroformylation catalysis. $\text{HCo}(\text{CO})_4$ is often referred to as the high-pressure unmodified cobalt catalyst system. This is because $\text{HCo}(\text{CO})_4$ readily decomposes to cobalt metal as the temperature is raised. High partial pressures of carbon monoxide are needed to stabilize $\text{HCo}(\text{CO})_4$ from decomposing to cobalt metal. In fact, the CO pressure needs to be increased logarithmically as the temperature is increased.²

The $\text{HCo}(\text{CO})_4$ high-pressure catalyst system is used by BASF, ExxonMobil, Sasol, and others for the hydroformylation of internal, branched alkenes that are very difficult to hydroformylate. Typical industrial conditions for $\text{HCo}(\text{CO})_4$ hydroformylation are 160-200°C, 250-350 bar, 1:1 H_2/CO . Once you are past a certain minimum CO pressure, all hydroformylation catalysts run more slowly as the CO pressure is increased. This is because CO is the best ligand in hydroformylation and needs to dissociate from the catalyst in order to open up empty coordination sites for alkene and H_2 to coordinate.

Slaugh and Mullineaux at Shell Chemical Co. developed the phosphine-modified cobalt hydroformylation process in the mid-1960s.³ By adding a strongly-donating, sterically bulky alkylated phosphine ligand to the cobalt, they stabilized the $\text{HCo}(\text{CO})_3(\text{PR}_3)$ catalyst with respect to decomposition to cobalt metal. The donating ability of the alkylated phosphine made the cobalt more electron-rich, which, in turn, increased the π -backbonding to the carbonyl ligands

and the overall Co-CO bond strength. This allowed them to design an industrial hydroformylation process that ran at medium CO pressures. The stronger cobalt-carbonyl bonds, however, made the catalyst considerably less active for hydroformylation. This requires higher temperatures and very high catalyst loadings to compensate for the lower catalyst activity.⁴ The phosphine ligand had two other major effects on the cobalt catalyst:

- 1) The steric bulk of the phosphine ligand increased the aldehyde L:B ratio up to 8:1, which was highly desired for the products that Shell makes and sells.
- 2) The donating ability of the phosphine makes the Co-H more hydridic and active for the hydrogenation of aldehyde to alcohol. Shell wants to make alcohols from the aldehydes, so this is a highly desired reaction. Unfortunately, the increased hydrogenation activity also converts alkene into alkane, an unwanted side reaction.

Shell runs a large hydroformylation plant in Geismar, LA (just south of Baton Rouge). Typical reaction conditions for the Shell phosphine-modified catalyst are 60-80 bar 2:1 H₂/CO, 180-220°C, 2400 ppm cobalt, and a small excess of a proprietary bulky alkylated phosphine ligand. Note that Shell uses a 2:1 H₂/CO gas mixture due to the hydrogenation of aldehyde to alcohol. Aldehyde that isn't hydrogenated during hydroformylation is hydrogenated in a subsequent reactor using a heterogeneous hydrogenation catalyst.³

The Stanley Group has been working on dirhodium tetraphosphine hydroformylation for thirty years to study bimetallic cooperativity. One reason rhodium was used was that it is 1000 times more active than cobalt for hydroformylation and its stronger Rh-Rh bonding would favor bimetallic cooperativity.⁵ When the new P4-Ph tetraphosphine ligand with a much stronger chelate effect was developed, Prof. Stanley wanted to study dicobalt P4-Ph systems for hydroformylation.

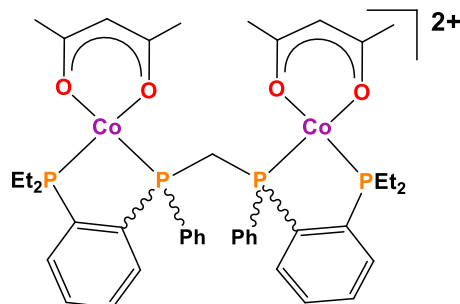


Figure 5.1. Structural drawing of the dicobalt P4-Ph catalyst precursors.

Drew Hood synthesized a dicatonic dicobalt catalyst precursor, $[\text{Co}_2(\text{acac})_2(\text{et,ph-P4-Ph})](\text{BF}_4)_2$, using the new tetraphosphine ligand (Figure 5.1).⁶ Hood tested this catalyst precursor for the hydroformylation of 1-hexene and observed high reactivity under mild conditions (31 bar H_2/CO) for cobalt. The *mixed* diastereomeric dicobalt precursors were initially tested, then the separate *racemic* and *meso*- $[\text{Co}_2(\text{acac})_2(\text{P4-Ph})](\text{BF}_4)_2$ precursors were studied. The *racemic* and *meso* precursors displayed very similar results (Table 5.1) with good activity for 1-hexene, low L:B ratios, and a good bit of alkene isomerization. Both $\text{HCo}(\text{CO})_4$ and $\text{HCo}(\text{CO})_3(\text{PR}_3)$ catalyst systems are also very active for alkene isomerization, so this aspect was not unexpected.

Table 5.1. 1 1-Hexene Hydroformylation by Dicobalt Tetraphosphine Diastereomers

Catalyst	Time	L:B	Aldehyde (%)	Alcohol (%)	Isomer (%)	Alkane (%)
$[\text{Co}_2(\text{acac})_2(\text{meso-P4-Ph})]^{2+}$	10 min.		38.3	N/A	52.3	0.9
	2 hrs.	0.9	78.5	10.5	8.6	2.0
$[\text{Co}_2(\text{acac})_2(\text{rac-P4-Ph})]^{2+}$	10 min.		31.6	N/A	57.7	0.8
	2 hrs.	0.9	65.3	8.6	23.5	1.8

Conditions: reactions were run in dimethoxytetraglyme (t-glyme) with 1 M 1-hexene at 160°C under 31 bar (450 psig) of 1:1 H_2/CO gas with 0.1 mol % catalyst (1 mM, 120 ppm)

What was very odd was that the the *meso* dicobalt catalyst actually ran faster than the *racemic* diastereomer. 30 years of bimetallic rhodium hydroformylation in the Stanley group with *rac*- and *meso*-P4 or P4-Ph ligands has clearly demonstrated that the *racemic*-dirhodium catalyst is highly active and selective, while the *meso*-diastereomer is a very poor hydroformylation catalyst. This is the case when the catalyst is using bimetallic cooperativity with the two metal centers working together to do hydroformylation.⁷ The results in Table 5.1 clearly indicated that the dicobalt catalysts were operating as open-mode monometallic hydroformylation catalysts. Therefore, monometallic analogs were prepared and studied.

5.2 Monometallic Cationic Cobalt(II) Hydroformylation Catalysts

The similar results between the two different dicobalt diastereomers indicated that the bimetallic catalyst was actually acting as two separate monometallic catalysts for hydroformylation. Monometallic cobalt(II) catalyst precursors with two different classes of chelating bisphosphine ligands were tested. One bisphosphine was based on the 1,2-phenylene chelate, which is one of the strongest chelates known, while the other used the weaker, but far more common, ethylene chelate (Figure 5.2). Phenyl and alkyl R groups were tested to probe electronic effects on the hydroformylation catalysis.

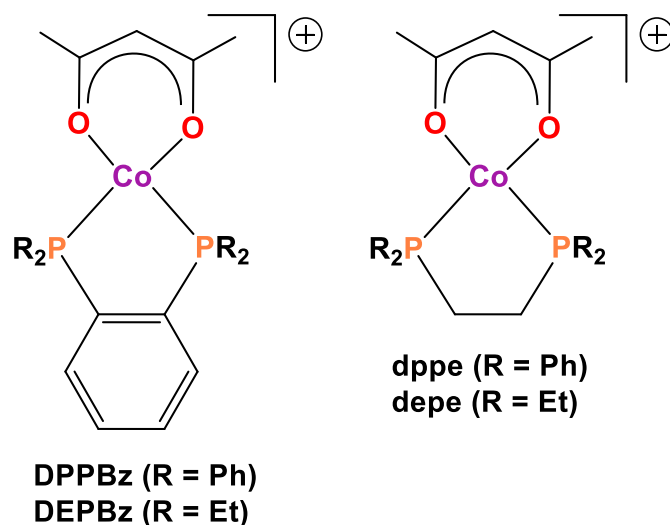


Figure 5.2. Structural drawings of the monometallic cobalt catalyst precursors studied. $[\text{Co}(\text{acac})\{(\text{R}_2\text{P}-1,2-\text{C}_6\text{H}_4)\}^+]$ and $[\text{Co}(\text{acac})(\text{R}_2\text{PCH}_2\text{CH}_2\text{PR}_2)]^+$ (R = Et, Ph). BF_4^- counteranions are present for each complex. Biphosphine ligand abbreviations shown.

The monometallic catalysts performed considerably better than the dicobalt catalysts, especially if you take into account that only one cobalt center is present, the catalyst is much simpler, and far easier to make. I joined the project at this point to help study this remarkable hydroformylation catalyst that represented a major breakthrough as an extremely active cobalt catalyst that operated at medium pressures. I worked with Drew and Dr. Alex Carpenter at ExxonMobil to study temperature and pressure effects on hydroformylation, different alkene substrates, and different phosphine ligands.

Table 5.2 shows the results from an extensive 1-hexene hydroformylation study using $[\text{Co}(\text{acac})(\text{DPPBz})](\text{BF}_4)$ as the catalyst.

Table 5.2. Temperature and Pressure Studies for the Hydroformylation of 1-Hexene with [Co(acac)(DPPBz)](BF₄).

TEMP (°C)	PRESSURE (BAR)	INITIAL TOF (MIN ⁻¹)	ALDEHYDE (%)	L:B	HYDRO. (%)	ISO. (%)
120*	50	26.5	59.4	1.7	0	7.6
140*	50	43.6	71.3	1.3	0.3	17.9
160	50	66.0	76.8	1.1	1.4	18.9
PRESSURE (BAR)	Temp (°C)	Initial TOF (min ⁻¹)	Aldehyde (%)	L:B	Hydro. (%)	Iso. (%)
30	160	52.5	49.0	0.94	1.4	45.7
50	160	66.0	76.8	1.1	1.4	18.9
70	160	94.8	84.0	1.3	1.2	12.1
90	160	103.2	87.3	1.4	1.0	9.1

Conditions: DPPBz = (Ph₂P)₂-1,2-C₆H₄. Catalysis conditions: 1 mM catalyst (61 ppm Co), 1 M 1-hexene, 0.1 M heptane standard, solvent = dimethoxytetraglyme (t-glyme), 1:1 H₂:CO, 1000 rpm stirring under constant pressure. TOF = initial turnover frequency based on a sample taken at 2 min. Other results based on sampling after 1 hour. *The reaction mixture was heated to 160°C for 5 mins to activate the catalyst then cooled to operating temperature before the alkene was injected. TOF = initial turnover frequency based on a 5 min sample.

Table 5.2 shows the results of the temperature and pressure study using the DPPBz ligand. The [Co(acac)(DPPBz)](BF₄) catalyst precursor needs to be activated under H₂/CO at 140°-160° to generate active catalyst, which is what we did for the lower temperature runs. It will activate slowly at lower temperatures under H₂/CO pressure. The temperature study in Table 5.2 shows a steady increase in rate with temperature. Decomposition starts increasing above 160°, so we usually limit our maximum temperature to that. As the temperature increases the L:B aldehyde selectivity drops and the alkene isomerization activity increases. This is standard behavior for most hydroformylation catalysts.⁸

For the pressure study we used the optimal temperature 160°C and noticed as the pressure increased the conversion of aldehyde increased and isomerization decreased. The 30 bar study showed signs of decomposition when some cobalt metal was found in the autoclave. Due the limits

of our autoclave system 90 bar was the highest pressure we were able to use. The fact that as the H₂/CO pressure increased the rate steadily increased as well is remarkable and unique for hydroformylation. All known hydroformylation catalysts, after an initial positive rate dependence on CO pressure, are inhibited by increasing CO pressures.

So we are not sure what the maximum pressure is for the DPPBz-based cobalt catalyst. We do believe that the catalyst will slow down once the CO pressure is increased enough. This catalyst shows remarkable activity compared to industry catalysts which require higher temperatures, pressures, and much higher catalyst concentrations.

Table 5.3. 1-Hexene Hydroformylation by [Co(acac)(DEPBz)](BF₄).

TEMP (°C)	PRESSURE (BAR)	INITIAL TOF (MIN ⁻¹)	ALDEHYDE (%)	L:B	HYDRO. (%)	ISO. (%)
120*	50	25.4(5.0)	74.6(5.4)	1.6	0	7.9(1.1)
140	50	61.5(6.1)	84.7(1.2)	1.3	0	10.0(1.2)
160**	50	76.8(2.0)	78.2(4.9)	1.1	1.3(0.3)	19.5(1.0)
PRESSURE (BAR)	TEMP (°C)	INITIAL TOF (MIN ⁻¹)	ALDEHYDE (%)	L:B	HYDRO. (%)	ISO. (%)
30*	140	40.0(5.1)	73.7(1.5)	1.0	0.5(0.4)	21.8(1.7)
50	140	61.5(6.1)	84.7(1.2)	1.3	0	10.0(1.2)
70	140	36.7(3.5)	79.3(2.2)	1.6	0	10.7(0.9)
90	140	21.7(2.3)	82.5(2.6)	1.8	0	8.1(0.6)

Conditions: DEPBz = (Et₂P)₂-1,2-C₆H₄. All reactions run for 2 hrs with 1.0 M 1-hexene, 1.0 mM catalyst, 0.1 M heptane as internal standard, 1:1 H₂/CO in tetraethylene glycol dimethyl (t-glyme) solvent. TOF = initial turnover frequency based on a 5 min sample. Results are based on three or more consistent runs with standard deviations given in parentheses. * The reaction mixture was heated to 160°C for 5 mins to activate catalyst then cooled to operating temperature before the alkene was injected.

The DEPBz ligand was studied next to see the effects of a more electron-donating bisphosphine ligand on the cationic Co(II) catalyst 1-hexene hydroformylation. The pressure chosen for the variable temperature runs was 50 bar, which had shown consistent catalytic results

and was about in the middle of industrial medium-pressure conditions. The 140°C run ran the best overall at 2 hours converted 84.7% aldehydes with 10% isomers. Activation problems occurred at 120°C as this temp is too low to activate the catalyst. Overtime a long period of time (e.g., 24 hours) the catalyst can be activated at 120°C. Black cobalt metal deposits were observed at 160°C indicating some catalyst decomposition.

Using the optimal 140°C temperature we ran different pressures for the [Co(acac)(DEPBz)](BF₄) catalyst precursor. The best results were seen at 50 bar and it looked as if the catalyst was slowing down at 70 bar with a lower initial TOF and overall aldehyde conversion after 2 hours of reaction. This might be the point where CO pressure starts inhibiting the hydroformylation catalysis. The more electron-rich DEPBz phosphine ligand will promote stronger Co-CO bonding, which should slow down the catalysis as the CO pressure increases past a certain point. We did not observe this for the poorer donating DPPBz catalyst studies over the pressure range we studied. The initial TOF drops even more for the 90 bar run, but after 2 hours of reaction the overall aldehyde conversion is very similar to the 50 bar results.

As the pressure increased the aldehyde L:B increased slightly and the alkene isomerization decreased. One explanation for the high aldehyde conversion for the 90 bar study, despite the low initial turnover frequency is that there was less alkene isomerization. The cobalt catalyst does hydroformylate 1-alkenes faster than internal alkenes. The lower alkene isomerization at higher pressures provides the catalyst with more 1-hexene that it can convert more quickly to aldehyde product. This could allow the slower initial TOF 90 bar catalyst to “catch-up” to the 50 bar catalyst for the production of aldehyde product. The DEPBz ligand and cobalt catalyst are difficult to work with due to their reactivity. DEPBz is prepared in our lab and is a challenging synthesis with difficult purification that rarely removes all the impurities. Thus, the purity of the cobalt catalyst

precursor based on DEPbZ tends to vary somewhat. Because of this, most of our catalytic studies have shifted to using DPPbZ, depe, or dppe – all are commercially available in good purities and much easier to work with.

A great catalyst should have a long lifetime and be very robust. This has been a key problem for the dirhodium catalyst, however, the cationic cobalt catalyst has shown remarkable robustness. To showcase the lifetime of the cobalt catalyst a lifetime study was performed. We have never noticed any decomposition of the catalyst except with too high of a temperature or too low pressure (especially combining the two unfavorable conditions). We did a two million turnover hydroformylation experiment using 1-hexene to test the lifetime of the catalyst. The run used 3 μ M (0.24 ppm Co) of $[\text{Co}(\text{acac})(\text{DPPbZ})](\text{BF}_4)$ and 6 M 1-hexene, which equates to a 2 million possible turnovers. It was ran under 50 bar of 1:1 H_2/CO at 160°C for 14 days. After 14 days it produced 1.2 million turnovers of aldehyde with 1.2% hydrogenation and 42% alkene isomerization, and the catalyst did not show any signs of decomposition.

5.3 Characterization of the Cationic Cobalt Catalyst

The nature of the catalyst has been studied mainly by in situ FT-IR. Since the catalyst is Co(II) it is paramagnetic, which limits our use of NMR for characterization, although we have gained some important information using ^1H , ^{31}P , and ^{59}Co NMR spectroscopy. The ReactIR study used 10mM of $[\text{Co}(\text{acac})(\text{DPPbZ})](\text{BF}_4)$ in t-glyme at various pressures, temperatures, and over an extended 100 hour span. Showcasing the stability of the catalyst again there were many structures observed over time in the metal-carbonyl region.

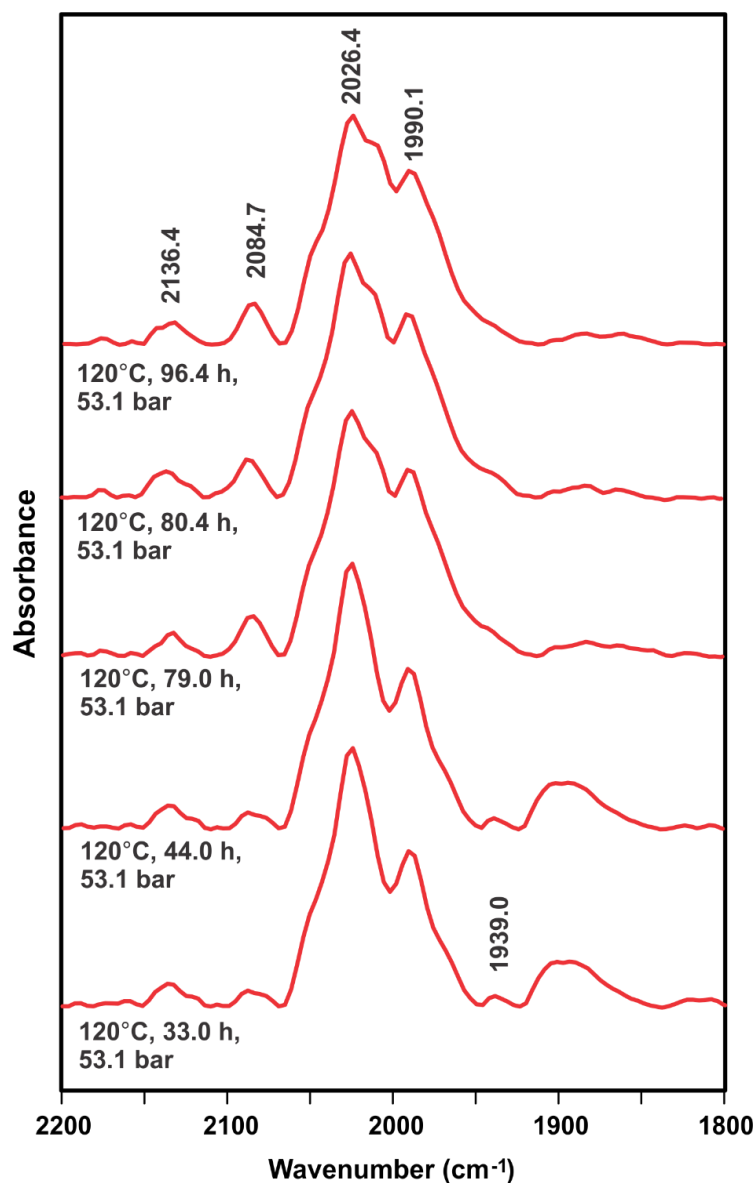


Figure 5.3. FT-IR study of $[\text{Co}(\text{acac})(\text{DPPBz})](\text{BF}_4)$ under H_2/CO from 33 hours to 96 hours

The catalyst precursor initially adds one CO ligand when exposed to carbon monoxide at low pressures and forms a low-intensity Co-carbonyl band at 1939 cm^{-1} . The catalyst starts reacting with H_2 around 120°C , which protonates off the acac ligand and forms the active catalyst, $[\text{HCo}(\text{CO})_x(\text{DPPBz})]^+$, which is believed to have 1 to 3 carbonyls depending on the pressure and temperature. The 2084 cm^{-1} peak is assigned to the tricarbonyl complex, along with several more bands in $2050\text{--}2000\text{ cm}^{-1}$ region. The dicarbonyl complex probably has bands

around 2026 cm^{-1} and 1990 cm^{-1} , while the monocarbonyl species should have the lowest CO stretching frequency, probably in the $1970\text{-}1990\text{ cm}^{-1}$ region. Temperature has a significant role in the catalyst system as these peaks do not appear rapidly until 120°C .

The remarkable stability of the $[\text{HCo}(\text{CO})_x(\text{DPPBz})]^+$, $x = 1\text{-}3$, catalyst is shown by the consistency of the IR spectra in Figure 5.3 between 33 and 96 hours. A simple industrial test for the stability of a Rh-phosphine catalyst that has P-arene, P-benzyl, or P-OR groups is to put it under H_2/CO and hydroformylation reaction conditions without any alkene substrate. Rhodium will quickly start reacting with the phosphine/phosphite ligands to do oxidative cleavage of the P-R bonds leading to complete catalyst deactivation within 24 hours (usually much sooner).¹⁰ The $[\text{HCo}(\text{CO})_x(\text{DPPBz})]^+$, $x = 1\text{-}3$, catalyst shows no sign of cobalt-induced phosphine ligand degradation reactions. After 100 hours the ReactIR cell was cooled and depressurized. The catalyst solution was carefully removed via syringe and transferred to one of our autoclaves where it hydroformylated 1-hexene with the same activity and selectivity as a fresh cobalt catalyst sample.

The catalyst is paramagnetic due to the d^7 cobalt(II) metal center. High pressure ^{31}P , ^1H , and ^{59}Co NMRs have been run on activated catalyst under H_2/CO pressure. No phosphorus resonances, hydride resonances, or ^{59}Co signals were seen indicating that all catalyst and related species are paramagnetic. This also indicates that we are not generating diamagnetic Co(I) catalysts like $\text{HCo}(\text{CO})_4$ or $\text{HCo}(\text{CO})_3(\text{PR}_3)$ that could be doing hydroformylation.

5.4 Proposed Catalytic Mechanism

The proposed hydroformylation mechanism is shown in Figure 5.4 and is consistent with previous monometallic cobalt and rhodium mechanisms. The 19e- tricarbonyl is in equilibrium with the 17e- dicarbonyl and 15e- monocarbonyl, which should be a very low concentration species under H₂/CO pressure. Key to our proposed mechanism is the 19e- tricarbonyl complex. The axial coordination sites are not open enough to coordinate sterically crowded internal alkenes. The least sterically hindered coordination site is the equatorial carbonyl, but that is the strongest bound carbonyl and the least likely to dissociate.

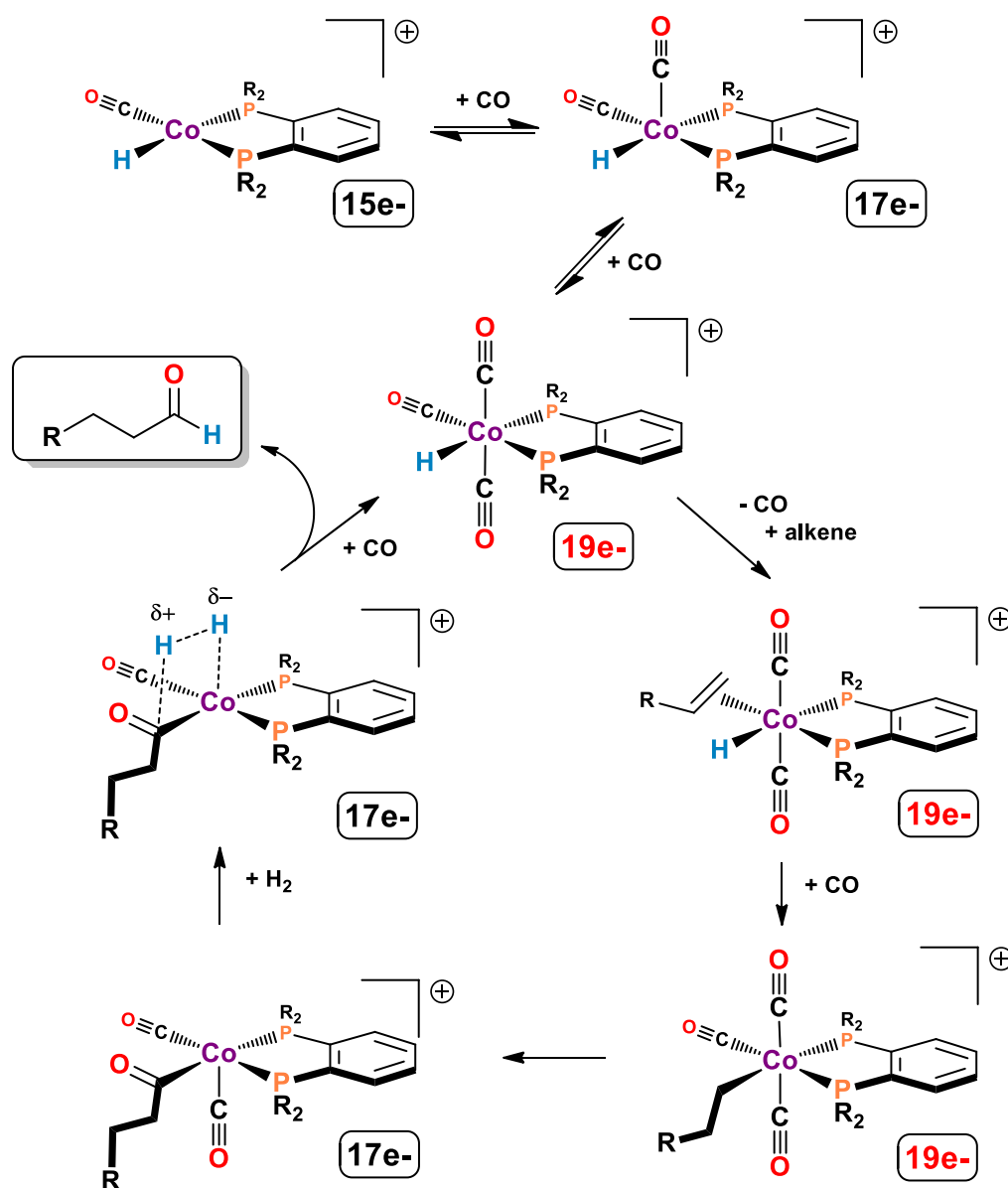


Figure 5.4. Proposed hydroformylation mechanism for the cationic cobalt catalyst

DFT calculations by Prof. Stanley show that as one adds more carbonyl ligands to the axial coordination sites, the equatorial Co-CO bond lengthens and weakens. The 19e- tricarbonyl complex, therefore, will have the weakest equatorial carbonyl that is now more likely to dissociate to allow alkene coordination. The next few steps are the same as any

hydroformylation catalyst: migratory insertion of the hydride and alkene to form the alkyl group. Another migratory insertion between the carbonyl and alkyl group to form the acyl group.

We now propose that H_2 reacts with the cobalt via a heterolytic cleavage to produce aldehyde and reform the active catalyst. Most hydroformylation mechanisms propose an oxidative addition of H_2 to the metal center, but that would make a cationic Co(IV) metal center, which is highly unusual for cobalt.

The ability to form a 19e⁻ complex, which further labilizes the carbonyl ligands, and the cationic charge on the metal center are a key factors that generates such an active cobalt catalyst system. Basolo demonstrated that there is a much lower activation barrier and energy cost in going from 17e⁻ to 19e⁻ compared to 18e⁻ to 20e⁻. V(CO)_6 is a 17e⁻ complex that can do an associative phosphine substitution of a carbonyl via a 19e⁻ complex at -70°C , while 18e⁻ $[\text{V(CO)}_6]^+$ does not react with molten PPh_3 at 150°C .¹¹ The cationic charge and Co(II) oxidation state work together to allow the coordination of a donating bisphosphine ligand, while still retaining good carbonyl ligand lability. The IR studies confirm this with fairly high energy carbonyl bands, which indicate limited π -backbonding from the cobalt center. Future research is still being conducted for a better understanding of the nature of the cationic cobalt catalyst.

5.5 References

1. Heck, R. F.; Breslow, D. S., The Reaction of Cobalt Hydrotetracarbonyl with Olefins. *J. Am. Chem. Soc.* 1961, 83, 4023-4027.
2. B. Cornils, "Hydroformylation. Oxo Synthesis, Roelen Reaction" in *New Syntheses with Carbon Monoxide*, J. Falbe, Ed. (Springer-Verlag, 1980)
3. L. H. Slaugh, R. D. Mullineaux, Novel hydroformylation catalysts. *J. Organomet. Chem.* **13**, 469-477 (1968)
4. L. H. Slaugh, R. D. Mullineaux, Hydroformylation of olefins. U.S. Patent 3,448,157 (1969).

5. D. Evans, J. A. Osborn, G. Wilkinson, Hydroformylation by use of rhodium complex catalysts. *J. Chem. Soc. (A)*, 3133-3142 (1968)
6. Hood, D. Cationic Cobalt (II) Hydroformylation. Ph.D. Dissertation, Louisiana State University, Baton Rouge, LA, 2019.
7. M. E. Broussard, B. Juma, S. G. Train, W.-J. Peng, S. A. Laneman, G. G. Stanley, A bimetallic hydroformylation catalyst: high regioselectivity and reactivity through homobimetallic cooperativity. *Science*, **260**, 1784-1787 (1993)
8. A. Borner, R. Franke, *Hydroformylation: Fundamentals, Processes, and Applications in Organic Synthesis*, Vol 1 & 2 (Wiley-VCH, 2016).
9. P. W. N. M. van Leeuwen, C. F. Roobeek, Hydroformylation of less reactive olefins with modified rhodium catalysts. *J. Organomet. Chem.* **258**, 343-350 (1983)
10. A. G. Abatjoglou, D. R. Bryant, Mechanism of rhodium-promoted triphenylphosphine reactions in hydroformylation processes. *Organometallics* **3**, 923-926 (1984)
11. Q.-Z. Shi, T. G. Richmond, W. C. Trogler, F. Basolo, Mechanism of carbon monoxide substitution in metal carbonyl radicals: vanadium hexacarbonyl and its phosphine-substitution derivatives. *J. Am. Chem. Soc.* **106**, 71-76 (1984)

Chapter 6: Experimental Procedures

6.1 General Considerations

All manipulations of air- and moisture-sensitive reagents were performed under an inert atmosphere of nitrogen in either a Vacuum Atmospheres or MBraun Glovebox or using standard Schlenk techniques. All solvents were reagent grade or higher. When dealing with air-sensitive reagents, the solvents were degassed with nitrogen prior to use. Chemicals used were the highest purity available from Aldrich or Strem Chemicals and used as received (degassed with nitrogen as needed).

^{31}P , ^{59}Co , and ^1H NMR spectra were recorded on either a Bruker AV-400 or AVIII-400 spectrometer. All ^1H NMR spectra were referenced internally to either added TMS (0.0 ppm) or to the residual solvent peak. All ^{31}P NMR spectra were referenced externally to 85% H_3PO_4 (0.0 ppm). ^{59}Co NMR were referenced to $\text{K}_3[\text{Co}(\text{CN})_6]$ (0.0 ppm). NMR data processing was done using Bruker Topspin 3.4 or MestReNova 11.0 software packages. Mass spectra were collected on an Agilent 6210 or 6230 Electrospray TOF instruments via direct injection of the sample dissolved in a 60:40 solvent system of acetonitrile and 0.1% formic acid/water.

FT-IR were collected on a Bruker Tensor 27 instrument equipped with a TDGS room-temperature detector. Bruker OPUS v8.0 software was used for data collection and processing. High-pressure/temperature FT-IR spectra were collected on a Mettler-Toledo ReactIR model 45m equipped with a liquid-nitrogen cooled MCT detector. This was connected with a fiber optic conduit to a Mettler-Toledo/Parr high pressure IR cell that used a SiComp (silicon ATR) probe. The high-pressure IR cell was modified with a Teflon gasket for the SiComp probe seal to the main cell body. This all-Teflon gasket makes a much better pressure seal compared to the original gasket that came with the IR cell. The head-piece of the IR cell was modified with

Swagelok quick-connects equipped with solvent-resistant Markez O-rings to facilitate assembly and cleaning. Mettler-Toledo iC IR v7.0 software was used for data collection. Bruker OPUS software was used to do baseline corrections on the data collected from the ReactIR system.

6.2 General Hydroformylation Procedures

Following the procedures from the literature, all reactions were carried out in modified Parr stainless steel autoclaves equipped with packless magnetic stirrers, thermocouples, and pressure transducers.⁴ The reactor is assembled and evacuated under a vacuum. Into a 125 mL Erlenmeyer flask, the catalyst is added with a solvent and internal standard. Through a column of Grade IV alumina, the alkene is passed and collected into a finger vial. While under negative pressure, the catalyst solution is added to the main reactor vessel and the alkene to the olefin reservoir arm. The main reactor is then allowed to heat up to the desired temperature while stirring at 1000 rpm. The pressure is used to inject the olefin at once into the reactor. The reaction's progress is monitored by SpecView (v 2.5) for gas consumption along with sampling analyzed by GC-MS.

6.3 Synthesis of Phenylphosphine

Day 1

In a 500 mL Schlenk flask 40 g dichlorophenylphosphine are mixed with 154 mL t-glyme (1 eq.). A 1000 mL Schlenk flask containing a stir-bar has 9.9 g LAH (or up to 10.1 g to make up for potential loss) mixed with 285 mL t-glyme (1.1 eq.). Each flask is cooled to 0° C with ice-baths for 30 minutes. The dichlorophenylphosphine is then added dropwise to the LAH via cannula (~2.5-4 hours).

Day 2

The resulting phenyl phosphine is transferred to a 250 mL Schlenk flask that is pre-massed via trap-to-trap distillation.

6.4 Synthesis of Bridge (H-Bridge)

Day 1

The phenyl phosphine previously made is moved into a 500 mL Schlenk flask with a stir-bar using DMF as the solvent (10 mL/g) (1 eq.). DCM is added to the same flask (0.5 eq. + 20 % or 0.6 eq.). This flask is cooled to 0° C with an ice-bath for 30 minutes. KOH (3.51 eq.) is added to a 100 mL Erlenmeyer flask along with H₂O using the following formula:

KOH or x = 58%, H₂O or y = 42%

$$y = \frac{100x}{58} - x$$

Note: The mixture of H₂O and KOH is exothermic. Once cool, degas the solution for 20 minutes. The KOH solution is the added to the phosphine over a 30 minute period with occasional shaking. Some Na₂SO₄ is put into a 1000 mL Schlenk flask and evacuated overnight.

Day 2

25-50 mL H₂O and 250 mL hexane are degassed separately for 30 minutes. The H₂O is added to the bridge solution. Following this, the degassed hexane is used to extract the bridge 3-5 times into the Na₂SO₄. The solution is filtered in the glovebox using a vacuum and then the hexanes (with impurities) are boiled off. Note: H₂O may still be on the bridge, so extra heating will be needed (heat-gun optional).

6.5 Synthesis of Cl-Bridge

Toluene is added to the previously made bridge as follows:

$$x \text{ g Bridge} \times \frac{1 \text{ mol}}{232.197784 \text{ g}} \times \frac{1000 \text{ mL}}{10 \text{ M}} = y \text{ mL Toluene}$$

A two-necked Schlenk flask charged with C₂Cl₆ (2.1 eq.) and Toluene as follows:

$$a \text{ g C}_2\text{Cl}_6 \times \frac{1 \text{ mol}}{236.7394 \text{ g}} \times \frac{1000 \text{ mL}}{2 \text{ M}} = b \text{ mL Toluene}$$

The two-necked flask is heated to ~80° C (up to 90° C) using an oil-bath while the upper neck is attached to a condenser. The bridge is added over 30 minutes to the C₂Cl₆ with periods of N₂ flowing into the two flask to help remove the HCl being produced. Once added, the solution reacts for 2-3 hours. If shown to be done via NMR, the toluene is boiled off leaving behind Cl-bridge. Note: The Cl-bridge will need to be moved to a second flask for weighing; this process helps to remove excess C₂Cl₆ and H₂O if carefully transferred (heat-gun optional). Also in boiling off the toluene, do not heat the Cl-bridge above 85° C. Removal of toluene must be done promptly after the reaction is complete.

6.6 Synthesis of Diethylchlorophosphine

Day 1

To a 250 mL Schlenk flask, 30 g PCl₃ are added along with a stir-bar and 40 mL t-glyme (1 eq.). A second 250 mL Schlenk flask is charged with 30 mL t-glyme followed by 29.6 g Et₂Zn and finally a second 30 mL t-glyme (1.1 eq.). Both flasks are cooled to 0° C via ice-baths for 30 minutes. The Et₂Zn solution is added dropwise to the PCl₃ via cannula (~1.5-3 hours). Note: Et₂Zn is highly reactive and may produce smoke during the addition. If this were to happen, stop the addition and purge the flasks with N₂.

Day 2

The resulting PEt₂Cl is transferred to a pre-massed 250 mL Schlenk flask via trap-to-trap distillation.

6.7 Synthesis of Small Arm (I-Small Arm)

Day 1

THF is added to PEt_2Cl as a solvent (9.25 mL/g) and the flask is put into the freezer until needed (1 eq.). A 500 mL (or 1000 mL) Schlenk flask containing a stir-bar that is covered in foil and is charged with I_2Bz and THF as the solvent (3.2 mL/g) (0.97 eq.). A round bottom flask is filled with $^i\text{PrMgBr}$ (0.97 eq.) in THF as follows:

$$x \text{ mol} \times \frac{1000 \text{ mL}}{2.9 \text{ mol}} = y \text{ mL } ^i\text{PrMgBr}$$

Extra THF (1-2 mL) is used to wash all $^i\text{PrMgBr}$ into the flask. The I_2Bz solution is cooled to 0°C with an ice-bath for 30 minutes. The $^i\text{PrMgBr}$ is then added to the I_2Bz (slowly based on viscosity). The resulting Grignard solution is allowed to stir at 0°C for 4-6 hours. After the wait, PEt_2Cl is added to the Grignard over the course of 30 minutes at -25°C . Then the solution slowly warms to room temperature overnight while still stirring. Some Na_2SO_4 is put into a 1000 mL Schlenk Flask and evacuated overnight.

Day 2

75 mL H_2O are degassed and added to the Grignard to quench the reaction. The flask is shaken and allowed to rest forming two layers in the solution. The organic layer is extracted into the Na_2SO_4 and further extracted with 150 mL diethyl ether (3-5 times). This solution is filtered in the glovebox, and the solvent is boiled off under vacuum. Note: The compounds produced are light sensitive. The small arm is then purified via short-path distillation. For this an oil-bath is heated to $130^\circ - 135^\circ\text{C}$.

6.8 Synthesis of Br-Small Arm

The same method previously described is used here only using I-Br-Bz instead of I₂Bz. The Grignard from the I-Br-Bz and ¹PrMgBr can be tested via GCMS to shorten the 4-6 hour period. Take a sample of the Grignard, add H₂O, and run it on GCMS after 1.5 hours (instead of 4-6 hours). Short-path distillation can be done at a lower temperature, but may not work at that lower one. The prescribed temperature for this is 84° – 86° C.

6.9 Synthesis of “New Ligand” et,ph-P4-Ph via I-Small Arm

Day 1

Cl-Bridge are added to a Schlenk Flask with THF as the solvent and stored in the freezer until needed (2.43 mL/g) (1 eq.). A 500 mL pear-shaped Schlenk Flask that is covered in foil and containing a stirbar has small arm added to it with THF as the solvent (2.5 mL/g) (2 eq.). A round bottom flask is charged with ¹PrMgBr (2 eq) in THF as with the Small Arm using extra THF as a wash. The small arm is cooled to 0° C in an ice-bath for 30 min. The ¹PrMgBr is then added to the flask and the two mix overnight at a continuous 0° C.

Day 2

The Grignard is cooled further to -25° C using an acetone/dry ice-bath. The Cl-bridge is then added to the Grignard over a 30 min period. The solution then reacts overnight while warming back to room temperature. Some Na₂SO₄ is put into a 1000 mL Schlenk Flask and evacuated overnight.

Day 3

10 mL H₂O are degassed and added to the NL to quench the reaction. The flask is shaken and allowed to rest to form two layers in the solution. The organic layer is extracted into the Na₂SO₄ and further extracted with 150 mL diethyl ether (3-5 times). The solution is filtered in the glovebox and the solvent boiled off via vacuum. The ligand is epimerized by heating it for 3 hours on an oil bath at 130° C.

6.10 Synthesis of “New Ligand” et,ph-P4-Ph via Br-Small Arm

Day 1

Mg turnings are added to a two-necked Schlenk Flasks with a balloon wrapped to the top neck (2 eq. + 30 % or 2.6 eq.). The flask is purged and the balloon filled with Ar. The flask is then set on a stir-plate overnight.

Day 2

The balloon is removed and a refluxing condenser is attached to the top of the flask. The whole apparatus is then flame-dried to remove any water. The flask is set in an oil bath heated to 70° C. Once hot Br-small arm in THF (4 mL/g) (2 eq.) is added to the Mg and allowed to react for 60 min. Cl-bridge in THF (3.3 mL/g) (1 eq.) is cooled to -35° C via an acetone/dry ice-bath. The Grignard solution is added to the Cl-bridge slowly while still hot leaving any excess Mg behind. Note: The Grignard may clog the cannula if too cold or added too slowly, but it should not all be added at once. The solution then reacts overnight while warming back to room temperature. Some Na₂SO₄ is put into a 1000 mL Schlenk Flask and evacuated overnight.

Day 3

10 mL H₂O are degassed and added to the NL to quench the reaction. The flask is shaken and allowed to rest to form two layers in the solution. The organic layer is extracted into the Na₂SO₄

and further extracted with 150 mL diethyl ether (3-5 times). The solution is filtered in the glovebox and the solvent boiled off via vacuum. The ligand is epimerized by heating it for 3 hours on an oil bath at 130° C.

6.11 Synthesis of Vinyldiethylphosphine

Day 1

The PEt_2Cl is added to a 250 mL Schlenk flask with t-glyme as a solvent (8.9 mL/g). In a 500 mL Schlenk flask fitted with a stir-bar equal volumes of Vinyl-MgBr in THF (1 M solution) (1.1 eq.) and t-glyme are added. The following is used to determine the amount of Vinyl-MgBr:

$$x \text{ g } \text{PEt}_2\text{Cl} \times \frac{1 \text{ mol}}{124.548962 \text{ g}} \times \frac{1.1}{1} \times \frac{1000 \text{ mL}}{1 \text{ mol}} \times \frac{0.981 \text{ g}}{1 \text{ mL}} = y \text{ g } \text{Vinyl} - \text{MgBr}$$

The majority of the THF in the Vinyl-MgBr solution is boiled off under vacuum leaving t-glyme as the solvent. The Vinyl-MgBr is allowed to cool to room temperature, and then it and the PEt_2Cl are cooled further using ice-baths for 30 minutes. Once at 0 °C, the PEt_2Cl is added via cannula to the Vinyl-MgBr in a dropwise addition. The mixture is allowed to react overnight.

Day 2

The newly formed Vinyl- PEt_2 is transferred to a pre-massed 250 mL Schlenk flask via trap-to-trap distillation.

6.12 Synthesis of “Old Ligand” et,ph-P4

In a neat reaction, a small Schlenk flask is charged with Bridge (1 eq.) and Vinyldiethylphosphine (2.2 eq.). The flask is placed under UV-light for 8 hours. Excess vinyl can be boiled off via vacuum at 90° C. The OL is then put into a 250 mL Schlenk Flask with hexane. This is placed into the freezer. The ligand that crystalizes with the hexane is the *meso*-form, while the ligand that remains in solution is the *rac*-form.

6.13 Column Chromatography for the Removal of Impurities from *et,ph*-P4-Ph

Into a 400 mL beaker, ~200 mL of alumina are poured. DCM is slowly added to the alumina until fully absorbed and about 1 mm of DCM rest atop the surface. The alumina is agitated and poured into a glass column with a diameter of 4 cm. Sand is added to the top of the alumina and the ligand is added to the sand. DCM is used to elute the ligand from the column; the impurities do not travel in DCM. The solvent is boiled off under vacuum.

6.14 Column Chromatography for the Separation of *meso*- and *rac-et,ph*-P4-Ph

Into a 500 mL Erlenmeyer flask, 210 – 240 g of dry (Grade I) alumina are added. A volume of H₂O equaling 10 % of the mass of the alumina is added to the same flask and allowed agitated until the H₂O is evenly mixed. 40 mL of DCM and 160 mL of hexane are added to a second Erlenmeyer and shaken. The solvent mixture is added to the alumina, and once mixed, the alumina is poured into a glass column with a diameter of 4 cm fitted with glass wool and sand. Sand is added to the top of the alumina and the ligand is added to the sand. The same solvent mixture of DCM/Hexane in a 1:4 are used to elute the ligand from the column. Once the ligand comes off the column, fractions are collected 10 mL at a time. Sampling of the fractions by TLC is done to pull the appropriate fractions together. The solvent is boiled off under vacuum. Note: DCM can degrade the ligand if left to interact with it for extended periods. The solvent must be boiled off as soon as possible.

6.15 Synthesis of Rh(nbd)₂BF₄

THF is added to the powder Rh(nbd)acac (15 mL/g). The solution is put in a recrystallization dish with acetone and allowed to stir to better dissolve. The acetone is then cooled to -20 °C using dry ice. While cooling, into a tubular Schlenk flask HBF₄·OEt₂ (2 eq.) [Or HPF₆] is added. Into a second tubular Schlenk flask nbd (4.5 eq.) is added. Using a cannula, the contents of both

flasks are added dropwise to the cooled Rh(nbd)acac beginning with the acid. Once the second addition is finished, the mixture is brought into the glovebox and placed in the freezer for exactly 2 hours. Note: If the time period is exceeded, the acid will begin to “polymerize” making a mess, causing subsequent steps to be challenging. After the 2 hours, the solid that precipitates out of solution is filtered in the glovebox using vacuum filtration. The solid is then put into a vial and dried overnight.

Later Rh(nbd)₂BF₄ material was purchased from Umicore, Precious Metals Chemistry.

6.16 Synthesis of *rac/meso/mix*-Rh(OL)(nbd)₂BF₄ or *rac/meso/mix*-Rh(NL)(nbd)₂BF₄

DCM is added to both Rh(nbd)₂BF₄ (20 mL/g) (2 eq.) and new ligand (NL or et,ph-P4-ph) (10 mL/g) (1 eq.). The Rh(nbd)₂BF₄ is set to stir while the new ligand is added dropwise via cannula to the Rh(nbd)₂BF₄. Note: The reaction is complete once the ligand is added, but it is best to let the solution mix for an extra 30 min. Remove the solvent from the mixture under vacuum pressure. The *rac/meso/mix*-Rh(OL)(nbd)₂BF₄ catalyst is then recrystallize the material using acetone and hexane in the freezer for a few days in a 500 mL Schlenk flask.

6.17 Synthesis of Small Arm (Phenyl substituted and Methyl external arms)

Day 1

THF is added to PPh₂Cl or P(CH₃)₂Cl as a solvent (9.25 mL/g) and the flask is put into the freezer until needed (1 eq.). A 500 mL (or 1000 mL) Schlenk flask containing a stir-bar that is covered in foil and is charged with I₂Bz and THF as the solvent (3.2 mL/g) (0.97 eq.). A round bottom flask is filled with ⁱPrMgBr (0.97 eq.) in THF as follows:

$$x \text{ mol} \times \frac{1000 \text{ mL}}{2.9 \text{ mol}} = y \text{ mL } i\text{PrMgBr}$$

Extra THF (1-2 mL) is used to wash all $i\text{PrMgBr}$ into the flask. The I_2Bz solution is cooled to 0°C with an ice-bath for 30 minutes. The $i\text{PrMgBr}$ is then added to the I_2Bz (slowly based on viscosity). The resulting Grignard solution is allowed to stir at 0°C for 4-6 hours. After the wait, PPh_2Cl is added to the Grignard over the course of 30 minutes at -25°C . Then the solution slowly warms to room temperature overnight while still stirring. Some Na_2SO_4 is put into a 1000 mL Schlenk Flask and evacuated overnight.

Day 2

75 mL H_2O are degassed and added to the Grignard to quench the reaction. The flask is shaken and allowed to rest forming two layers in the solution. The organic layer is extracted into the Na_2SO_4 and further extracted with 150 mL diethyl ether (3-5 times). This solution is filtered in the glovebox, and the solvent is boiled off under vacuum. Note: The compounds produced are light sensitive.

6.18 Synthesis of $\text{Rh}(\text{cod})_2\text{BF}_4$

The same method used to describe 4.15 is used here only switching norbornadiene for 1,5-Cyclooctadiene.

6.19 Synthesis of *meso/rac*- $[\text{Rh}_2(\text{CO})_4(\text{et,ph-P4-ph})]\text{BF}_4$

DCM is added to $\text{Rh}(\text{CO})_2(\text{acac})$ in a 250 schlenk flask containing a stir bar (25mL/g). As the solution stirs $\text{HBF}_4\cdot\text{OEt}_2$ (2 eq.) is added to the solution and it continues to stir for an additional 10 minutes. The et,ph-P4-ph ligand is dissolved in DCM (10ml/g) and added dropwise to the solution. Once the dropwise addition is finished the solution stirs for an additional 30 minutes. The solution is reduced to 10 mL via vacuum pressure, and CO gas is flowed through the solution for an additional 10 minutes. The concentrated solution is added dropwise to 100 mL of

diethyl ether while stirring. After the addition is finished the solution was placed in the freezer. ,
The solid that precipitates out of solution is filtered in the glovebox using vacuum filtration.

6.20 Synthesis of Rh(nbd)₂ BARF and Rh(nbd) BF₂₀

Acetonitrile is added to Rh(nbd)₂BF₄ (20 mL/g). The solution stirs for 5 minutes, and the anion (BARF or BF₂₀) is dissolved in acetonitrile (10 mL/g). The anion solution is added dropwise to the stirring rhodium solution. After the addition is completed the solution stirred for an additional 30 minutes. The solution is boiled off under vacuum pressure. The solid is dissolved in diethyl ether and filtered and a white powder will remain in the old flask. The solution is boiled off under vacuum pressure.

6.21 Synthesis of [Rh₂(acetonitrile)₄ (et,ph-P4-ph)]BF₄

70 mL of acetonitrile is added to Rh(nbd)₂BF₄. The solution is refluxed overnight at 90°C. The solvent is boiled off under vacuum pressure. The new ligand and the yellow powder Rh(acetonitrile)₃BF₄ is dissolved in 10 mL of DCM, and the ligand solution is added dropwise to the Rh(acetonitrile)₃BF₄ solution and is allowed to stir for an additional 10 minutes. The solution is boiled off under vacuum. The solid is further dried by vacuum pressure overnight.

6.22 Synthesis of [Rh₂(solvent)_x (et,ph-P4-ph)]BF₄ / Solvent = dioxane, pyridine

The same method used to describe 4.21 is used here only switching acetonitrile for dioxane or pyridine. Instead of refluxing at 90°C it was 110°C.

6.23 Synthesis of [Co(acac)(dioxane)₄](BF₄)•(dioxane)_x (x ≈ 2-6)

10 g of cobalt (II) acetylacetonate along with 150 ml of dioxane is added to a 500 ml two neck schlenk flask equipped with a condenser. The solution is heated to 60°C while stirring until all cobalt (II) acetylacetonate has dissolved. Then the solution is allowed to cool to 50-45°C before 6.61 g (1.05 equivalents) of tetrafluoroboric acid in ether is added to the solution via cannula.

Important Note: the tetrafluoroboric acid ether complex has to be relatively fresh. We have observed that if the acid is more than a month or two old the acid does not yield clean enough product.

The resulting solution is allowed to stir overnight while returning to room temperature. The pink precipitate is collected on a glass frit and washed with ether. The pink powder is then dried under vacuum overnight to remove excess dioxane. Based on the pink color the complex is assigned as octahedral $[\text{Co}(\text{acac})(\text{dioxane})_4]^+$, but there are clearly extra dioxanes present as solvates, the exact number of dioxane solvates varies considerably. In order to obtain a final molecular weight for synthesis applications an NMR has to be done using D_2O as a solvent. The dioxane and acetylacetonate ^1H NMR resonances are integrated and their respected areas correlated as shown below. The molecular weight of the $[\text{Co}(\text{acac})(\text{dioxane})_4](\text{BF}_4) \cdot (\text{dioxane})_x$ ($x \approx 2-6$) complex is then calculated and used for further syntheses.

$$\# \text{ of Dioxanes} = \frac{6(\text{area of Dioxane NMR peaks})}{8(\text{area of Acetylacetonate NMR peaks})}$$

Note that the solvated dioxane is slowly lost by the solid so the calculated molecular weight does not stay constant over long periods of time. The molecular weight should be recalculated if more than a day or two has passed since the last calculation.

6.24 Synthesis of $[\text{Co}(\text{acac})(\text{bisphosphine})](\text{BF}_4)$

The catalyst precursor of a desired bisphosphine ligand is made by adding one equivalent of ligand dissolved in CH_2Cl_2 to the $[\text{Co}(\text{acac})(\text{dioxane})_4]\text{BF}_4$ complex dissolved in acetone. The resulting solution is stirred for 30 mins and the solvent is then removed under vacuum. If the resulting solid is sticky (this occurs when considerable amounts of dioxane are not removed) then dissolve the material in CH_2Cl_2 before removing the solvent under vacuum again. The resulting powder should be red to brown depending on the ligand bound. Reaction yields are

typically quantitative. Due to the paramagnetism of the Co(II) complex some ^1H NMR data can be collected, but ligand resonances are considerably broadened. No ^{31}P NMR data could be collected. High resolution mass spectral data on some catalyst precursor species was collected and supports their formulation. Due to some variable solvent incorporation in the samples, elemental analyses were not attempted.

6.25 References

1. Broussard, M. E.; Juma, B.; Train, S. G.; Peng, W.-J.; Laneman, S. A.; Stanley, G. G., A Bimetallic Hydroformylation Catalyst: High Regioselectivity and Reactivity Through Homobimetallic Cooperativity. *Science* 1993, 260 (5115), 1784-1788.
2. Barnum, A. R. Studies of a Dirhodium Tetrphosphine Catalyst for Hydroformylation and Aldehyde-Water Shift Catalysis. Ph.D. Dissertation, Louisiana State University, Baton Rouge, LA, 2012.

Vita

Ryan Alexander Johnson was born in Oklahoma City, Oklahoma to Leonard and Francine Johnson. He received his Bachelor of Science in Chemistry from Langston University in May 2015. In Fall 2015, he joined the chemistry graduate program at Louisiana State University working under Professor Stanley. Ryan is expecting to graduate with a Doctor of Philosophy in Chemistry in May of 2019.